NTNU
Norwegian University of
Science and Technology

Experiments and Numeric Simulation on Displacement and Flushing of Hydrocarbon Fluid in Subsea Systems

Jon Arne Karstad Opstvedt

Subsea Technology
Submission date: May 2016
Supervisor: Milan Stanko, IPT

Norwegian University of Science and Technology
Department of Petroleum Engineering and Applied Geophysics

Summary

With the increasing number of subsea developments in the oil and gas industry, there is a need for more, and reliable, information on how to conduct safe and well informed subsea operations. One of the hot topics today is displacement of hydrocarbons during shut-in situations and interventions. This is done by injecting a displacement liquid, typically MEG or methanol, to lower the content of hydrocarbons in the domain, aiming to prevent formation of hydrates or release of chemicals that pose a risk to the environment.

This report presents results obtained from experimental work and numerical simulations conducted on a U-shaped subsea jumper like pipe setup, performed to analyze how the shape of the displacement front, flow pattern and phase hold up evolves with varying displacement velocity. To examine the accuracy of the numerical model and provide more details about the multiphase flow dynamics, experimental and simulated results were compared.

A pipe geometry was designed and constructed to mimic a U-shaped subsea jumper, using 153.6mm inner diameter (ID) transparent PVC pipes. Displacement was done through two different inlets, located at the bottom left and top of the U. When displacing trough the bottom inlet, parts of the closest vertical section were blocked to mimic a dead-leg. In total eight experiments were conducted through each inlet, with water-oil displacement and oil-water displacement with four different velocities. Liquid hold-up was measured after displacing one, two and tree jumper volumes. A high-speed camera was used to capture the flow for further analysis.

The experimental cases were recreated and simulated using ANSYS CFX, a computational fluid dynamics simulation (CFD) tool, to check the accuracy of the solver and models used. Two different multiphase models were tested, inhomogeneous mixture model and homogenous standard free-surface model. Shear Stress Transport model was used to model turbulence for both models. Results are reported numerically and visually before being compare to experimental results.

Experimental results show that the displacement efficiency is dependent on the establishment of a displacement front. A clear displacement front was only observed for rates higher than 20 m^3/h with water-oil and oil-water displacement. Water-oil displacement had the highest displacement efficiency, although it was severely reduced after one displacement volume. Oil-water displacement shows a better displacement efficiency after one displacement volume, but has a lower sweep efficiency due to a

reduced front height. Overall the numerical simulations results has problems predicting displacement with low velocities, for oil-water and water-oil displacement. The inhomogeneous mixture model has a better prediction of hold-up for oil-water displacement when there is mixing of the liquids. The homogenous free-surface model predicts best for water-oil displacement, when there are clear interfaces between the liquids.

Sammendrag

Med økende antall undervannsutbygginger i olje- og gassindustrien, er det behov for mer og pålitelig informasjon om hvordan trygge og velinformerte undervannsoperasjoner skal gjennomføres. Et hett tema i dag er fortrengning av hydrokarboner ved nedstengninger og intervensjoner av undervanns utstyr. Dette gjøres ved å injisere en fortrengningsvæske, typisk MEG eller metanol, for å senke innholdet av hydrokarboner i domenet. Målet er å hindre dannelse av hydrater eller utslipp av kjemikalier som utgjør en risiko for miljøet.

Denne rapporten presenterer resultatene fra eksperimentelt arbeid og numeriske simuleringer utført på U-formet rørstruktur som typisk brukes for å koble samme undervanns utstyr. Det eksperimentelle arbeidet er gjort for å analysere strømningsfront, strømningsmønster og hvordan innholdet av de ulike væskene variere med ulike fortrengningshastigheter. Eksperimentelle og simulerte resultater ble sammenlignet, for å undersøke nøyaktigheten av de numeriske modeller og for å kunne gi flere detaljer om flerfase dynamikken.

En rør-geometri ble designet og konstruert med 153.6mm ID gjennomsiktig PVC-rør. Fortrengning av innestengt væske ble utført gjennom to forskjellige innløp, det første ligger nede til venstre på U'en og det andre på toppen av U'en. Ved fortrengning gjennom nedre innløpet, ble deler av den hosliggende vertikale delen blokkert for å etterligne et død-punkt. I alt ble åtte eksperimenter utført via hvert av innløpene, med vann-olje fortrengning og olje-vann-fortrengning med fire forskjellige hastigheter. Et høyhastighets kamera ble brukt til å filme fortrengningen for videre analyse.

Eksperimentelle resultater ble gjenskapt og simulert ved hjelp av ANSYS CFX, for å sjekke nøyaktigheten til programmet og de ulike flerfasemodellene. To forskjellige flerfasemodeller ble testet, inhomogen blandingsmodell og homogen standard fri-overflatemodell. Skjære Stress Transport modellen ble brukt til å modellere turbulens for begge modellene. Resultatene ble presentert numerisk og visuelt, før de ble sammenlignet med de eksperimentelle resultatene.

Eksperimentelle resultater viser at fortrengningseffektiviteten er avhengig av etableringen av en fortrengningsfront. En klar forskyvningsfront ble bare observert for hastigheter høyere enn 20 m^3/h med vann-olje og olje-vann fortrengning. Olje-vann fortrengning hadde den høyest fortrengningseffektiviteten, selv om det ble sterkt redusert etter et fortrengningsvolum. Olje-vann fortrengning viser en bedre fortrengningseffektivitet etter et fortrengningsvolum, men har en lavere sveipeeffektivitet på grunn av en lavere fortrengningsfront høyde. Numeriske simulerings resultater hadde i dette prosjektet

problemer med å kalkulere fortrengning med lave hastigheter, for både olje-vann og vann-olje fortrengning. Den inhomogene miksingsmodellen hadde en bedre prediksjon av gjenværende væske for olje-vann forskyvning ved stor miksing av væskene. Homogen fri-overflatemodellen er nærmest for vann-olje forskyvning, når det er klare grensesnitt mellom væsker.

Acknowledgment

The master thesis presented in this paper was prepared during the spring of 2016 at the Norwegian University of Science and Technology (NTNU) located in Trondheim, Norway. The thesis is a part of the "TPG4910 PETTEKN BORETEKN VÅR 2016" course at the Department of Petroleum Engineering and Applied Geophysics (IPT). The objective of this thesis is to highlight current research done in the field of liquid-liquid displacement in subsea systems and present the work conducted by the author this semester.

The author would like to thank Associate Professor Milan Stanko for agreeing to supervise this thesis and for all his help and input on the work. The author would also like to thank PhD candidate Gilberto Nunez and Dr. Anna Elisabet Borglund for input on the experimental design. Ted Oerjan Kjellevik Gundersen also came with useful input on the numerical simulation. The author is grateful for the financial help from NTNU that made this project possible.

In addition, the author would like to thank Terje Bjerkan and Håkon Myhren for fabricating custom parts used to build the experimental rig, based on drawings from the author. Lastly, Henrik Nikolai Gussiås Kulseth and Erik Hjertholm also deserves a thanks for their cooperation and good mood at the lab.

Regards,
Jon Arne Opstvedt

June 2016

Table of Content

List of Figures

List of tables

List of Equations

1 Introduction

1.1 Background

Recently, the world have seen a large drop in the oil price, which forced field operators and service providers to cut costs in order to keep up their profit margins. New and marginal offshore fields are often tied back to existing infrastructure with a subsea development instead of being developed separately, possibly due to the additional price drop (Thomas, 2010).

This has led to an increased demand for complex and reliable subsea equipment. Installation and intervention of the equipment can often be a challenge, due to large water depths, rough seabed and harsh weather conditions. When doing interventions, due to abandonment, replacement, corrective- or preventative-maintenance, fluids that pose a threat to the surrounding environment needs to be displaced. Displacement has to be done before disconnecting and lifting up the equipment.

Due to accidents and increased environment focus, the rules and regulations regarding amounts of harmful liquids that can be released are getting stricter. Subsequently, the focus on determining the required flowrate and flushing time to displace all the liquids that pose a risk has increased. Suppliers of subsea equipment are therefore looking for alternative solutions during the development-phase, in an inexpensive manner.

1.2 Existing work

The field of liquid-liquid flow is not a new one, and there has been extensive work done to analyze different flow patterns in horizontal and vertical pipes. Brauner summarizes much of this work and generated a database for experimental-research conducted on liquid-liquid flow in pipes (Brauner, 2003).

Although there has been extensive work within the liquid-liquid flow field, most of the research is pointed towards steady-state flow conditions in long pipelines. However, when it comes to one liquid displacing another liquid, the amount of research is limited. Some research has been conducted with hydrate inhibition and oil displacement at NTNU and SINTEF. Kazemihatami did water-oil, oil-water displacement experiments and numerical simulations on an M-jumper and horizontal/inclined pipe (Kazemihatami, 2013). Mo ran Quasi-3D simulations on liquid-liquid and gas-liquid displacement in a horizontal/inclined pipe (Mo, et al., 2013). Schumann did water-oil and oil-water experiments on a horizontal/declined pipe section (Schumann, et al., 2014). External researchers include

Dellecase and Cagney. Dellecase et al examined MEG-water and methanol-water mixing on an m-shaped jumper through experimental work (Dellecase, et al., 2013). Cagney et al researched methanol-water and gas-oil/water mixing and displacement in an m-shaped jumper (Cagney, et al., 2006). In chapter 2 the most important results published by these researchers is presented.

As the subject is still fairly unexplored, reliable experimental data in order to gain further understanding of how the liquids propagate in different pipe structures during displacement or restarts, seems necessary. Experimental data will be needed to increase trust in commercial simulation tools and determine their capabilities, un-certainties and limitations to model fluid displacement in pipe conduits. Using a simulator to estimate the optimal displacement rate and time with a certain range of accuracy would be the ultimate goal.

1.3 Aims

The aims of the project can be summarized in the following manner:

- Produce reliable experimental data on liquid-liquid displaced in a pipe structure
- Compare experimental data with simulated data
- If results are promising, develop guidelines for liquid-liquid displacement in a u-shaped pipe geometry

1.4 Approach

A stepwise approach was used in order to achieve the aims set. The steps of approach are listed below:

1. Conduct extensive literature search, in order to determine research gaps needed to be filled
2. Contact experts from the industry, to get input on current problems and solutions.
3. Based on expert input and research, design and build an experimental rig.
4. Conduct experiments and simulations in parallel, to use learnings from both in order to unveil problems, missing parameters and improve setups.
5. Compare final results, discuss them and draw conclusions.

2 Liquid displacement

In relation to subsea equipment, liquid displacement is the process of replacing a liquid that pose a threat to the equipment or surrounding environment with a liquid that poses little or no threat. However, there are several aspects to consider, such as government regulations, fluid to displace, pipe geometry and available displacement flow capacity.

2.1 Pollution regulations

During offshore operations, the allowable amount of polluting substances to be released into the sea is governed by local laws and regulations. On the Norwegian Continental Shelf it is regulated by Miljødirektoratet. In Norway, when field operators are doing a marine operation, with a risk of chemical spill, they are obliged by law to apply for a permit (pollution act § 11).

Chemicals are categorized into four categories, black, red, yellow and green, depending on the threat they pose to the environment. A description of how they are classification can be found in (M-107 Retningslinjer for rapportering fra petroliumsvirksomhet til havs, 2014). The most important information is highlighted in Table 1 below.

Table 1 – Categorization of chemicals

Category	Description
Black	Chemicals that are persistent and simultaneously show high potential for bioaccumulation or have high acute toxicity (Miljødirektoratet, 2015). These chemicals should generally not be released, exceptions can be given in special cases when there are safety concerns.
Red	Chemicals that are slow to degrade in the marine environment, with potential for bioaccumulation and / or acute toxicity (Miljødirektoratet, 2015). These chemicals should generally not be released, exception usually given for a limited volume.
Yellow	Chemicals that are broken down relatively quickly in the marine environment, and / or shows low potential for bioaccumulation and / or acute toxicity (Miljødirektoratet, 2015). These chemicals are usually allowed to be release into the marine environment.
Green	Chemicals that pose low or no negative effect to the environment (Petoro, 2012). Release of these chemicals are usually allowed, without any special terms.

2.2 Design considerations

When designing subsea equipment, such as jumpers, there are several parameters to consider. These include; how to deal with shut-in situations, equipment failure, installation and interventions, structural integrity, fatigue and erosion. Since the chemicals the equipment will be exposed to and surrounding environment varies from location to location, these variables needs to be highlighted early in the design process. Deepwater will offer issues such as low temperatures and high pressure, which again introduces problems such as hydrate formation and installation and intervention difficulties.

There has been several studies on how to deal with hydrate formation in subsea jumpers, such as electric heating or using inhibition liquids or gases. Solheim and Nysveen found that hydrates could be effectively inhibited by utilizing direct electric heating alone (Solheim & Nysveen, 2014). Furthermore, Bardon colleagues combined electric heating with methanol injection and showed that the required methanol rate could be reduced, which again decreased the required pumping capacity and umbilical size (Bardon, et al., 2007). Although these studies offer solutions for hydrate inhibitions, they do not tackle the issue of displacing harmful chemicals during an intervention.

2.3 Displacement of subsea jumpers

Before conducting liquid-liquid displacement, several variables needs to be outlined. This includes the properties of the trapped liquid, geometry to be displaced and available displacement flow capacity. Displacement of liquid trapped in a pipe section is usually done in two different manners; using hydrate inhibition lines or with a dedicated displacement line (Figure 1). The inhibition lines are designed and dimensioned for hydrate inhibition and therefore usually has a low maximum flow capacity. Using a dedicated displacement line will require an remotely operated vehicle (ROV) connecting a liquid feed-hose from an intervention vessel, which provides displacement liquid. The optimal solution will depend on equipment and liquid to displace.

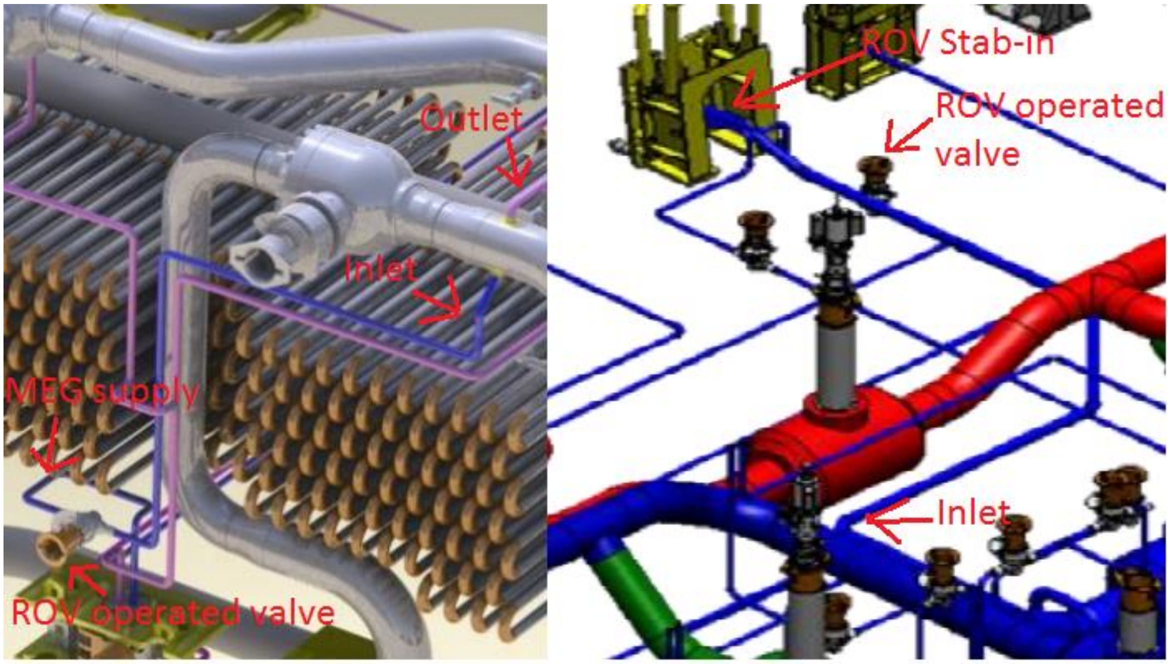

Figure 1 - Hydrate inhibition line (left) and dedicated line (right) (Statoil/Aker Solution)

If the trapped liquid has a high density, it will sink down and occupy low sections of the pipe. Displacing these sections will either require a continuously liquid flow or a more dense displacement liquid. If a denser liquid is used, it will displace the trapped liquid by natural buoyance. A less dense fluid will require a high and continuous flow to displace the trapped liquid. Utilizing the interfacial tension between the liquids causes further displacement of the liquids. Findings by Schumann et al. indicates that the displacement efficiency increased in combination a high viscous displacement liquid, due to the subsequently increased interface tension (Schumann, et al., 2014). On the contrary, a low viscosity liquid will flow easier than a high viscosity liquid, that tends to stick to the pipe wall. According to Reynolds equation, low viscosity liquids will become turbulent at lower velocity than high viscosity liquids. Turbulent flows tend to increase the wall cleaning due to vortexes in the boundary layer close to the wall.

Dellecase et al suggest that high displacement velocity causes a more piston like displacement front (Dellecase, et al., 2013), and several studies has verified these findings (Schumann, et al., 2014) (Coletta, et al., 2011). Schumann et al found that with a low displacement velocity, the flow pattern is stratified (Schumann, et al., 2014). As the displacement velocity increases the displacement front becomes plug like, meaning that it moves towards the superficial velocity of the displacement liquid. Coletta et al vertified this by being able to displace 70% of the oil in a jumper-structure with one jumper volume of water, thereafter only 5% was removed for each volume (Coletta, et al., 2011). They further suggest that low velocities will lead to better mixing, which is beneficial for hydrate inhibition. Through simulations it was found that a too high displacement velocity in a pipe structure with sharp bends causes accumulation of trapped liquid in low pressure zones of the pipe (Opstvedt, 2015).

A limiting factor related to the utilizing a high displacement velocity is the required pumping capacity, due to high backpressure for subsea equipment placed at large water depths. Trough design changes of a u-shaped subsea jumper, it has been shown that displacement efficiency may be increases, by moving from a horizontal bottom section to an angled bottom section of just minus one degree, the displacement efficiency was increased dramatically (Cagney & Hare, 2006) (Herrmann, et al., 2004).

2.4 Accuracy of numerical simulations

There are several options for analyzing multiphase flows with numerical computer tools including, the computational fluid dynamic (CFD) tool CFX by Ansys, LedaFlow by Kongsberg and OLGA by Schlumberger. CFD software are governed by physical laws, and applied through averaged Navier-Stokes equations along with models for phase interaction and turbulence. Other multiphase flow simulators such as OLGA, tune the model with experimental data. When using purpose built tools, such as OLGA and LedaFLow, the user have to keep in mind that these softwares are developed for large scale problems such as pipelines, risers and wellbores. The accuracy of the multiphase flow simulators will depend on how accurate the user is able to analyze and model the problem at hand.

There has been several studies comparing experimental data and simulation tools, they often conclude that it is hard to capture and model all physical phenomena in an experiment. Coletta et al ran simulations on a wellhead jumper using OLGA, and concluded that “Simulations over predict carry over; more liquid is left in the experiments. Explanations to this phenomenon include: 1) a possible wall wettability effect, 2) the length of the pipe may be too small and 3) the use of pressure below 100 psia.” (Coletta, et al., 2011). Schümann et al compared experimental data with LedaFlow on a jumper geometry, the results point to “…good agreement in general. The low behavior and general tendencies were predicted in the right way. However, further improvement is needed as shown by for instance the results for low rates.” (Schümann, et al., 2013). Lybeena et al used the CFD software by Ansys to simulate experimental results from an inhibition study performed by Cagnay et al, their conclusion was “The numerical results are in good agreement with the experimental results” (Lubeena, et al., 2011) (Cagney, et al., 2006).

3 Experiment Setup

The experimental setup was designed and built to analyze the process of liquid-liquid displacement and generate verification data for numerical simulations. The test-rig was built exclusively for this experiment in the test hall at the Department of Petroleum Engineering and Applied Geophysics, Norwegian University of Science and Technology, by the author. The test-rig was built to scale and mimics a U-shaped subsea jumper.

Before building the test-rig, a list of requirements for the hardware, data-acquisition system and liquids were developed. Based on the derived requirements, a detail design of the experiment and stepwise procedure for operating the-test rig was developed. Each step of the design process are described in chapter 3.1 and the operation procedure in chapter 3.2.

3.1 Experimental design

The experimental setup was designed to fit the reality as accurately as possible. To minimize the uncertainties and errors during the experiment, it was decided to use standardized equipment from well-known vendors. The design part of the experiment was divided into three parts, hardware design, data-acquisition design and liquid selection.

Before the design process started, the design requirements were developed in cooperation with Dr Anna Elisabet Borgund at Onesubsea and Proffesor Milan Stanko at NTNU.

- Hardware requirements
    - Jumper shall provide for visual inspection of flow
    - Jumper shall mimic a u-shaped subsea jumper, where the first riser has a length of 1.5m, bottom section 3m and second riser 2m.
    - The jumper shall have the ability to isolate the bottom 0.4m of the first riser
    - The displacement liquid volumetric flow shall be adjustable between 4 m^3/h and 30 m^3/h
    - The jumper shall have valves for venting trapped air.
    - The jumper shall have two independent inlets, one at the low-point and the other normal to the entrance of the U.
    - The setup shall have a solution for establishing initial conditions.
    - The setup shall contain a separator for storing liquids in-between experiments, with a ventilation system for gases.
    - The entrance length of the U shall be designed so that turbulent flows will stabilize before reaching the U-shape.
    - Drainage valve shall be located at each low-point of the setup

    - Isolation valves shall be used, to isolate potential leaks
- Acquisition requirements
    - Pressure and temperature at the inlet and outlet shall be read and displayed in real time during displacement
    - Flowrate from pumps shall be read and displayed in real time
    - Displacement liquid volume fraction shall be monitored at the outlet
    - Data acquisition solution shall offer the possibility of data logging
    - Flow shall be visually recorded
- Liquid requirements
    - Two different liquids shall be used
    - Both liquids shall have known specifications
    - Both liquids shall be rapidly available around the world.
    - The liquids shall be allowed in the experimental facility
    - The liquids shall be immiscible

Based on the initial requirement of the experimental rig, a P&ID (Figure 2) and Isometric CAD model (Figure 3) of the setup was develop before moving on to the detail design. This was done to gain a better understanding of the requirement and provide a visual overview of the experimental setup.

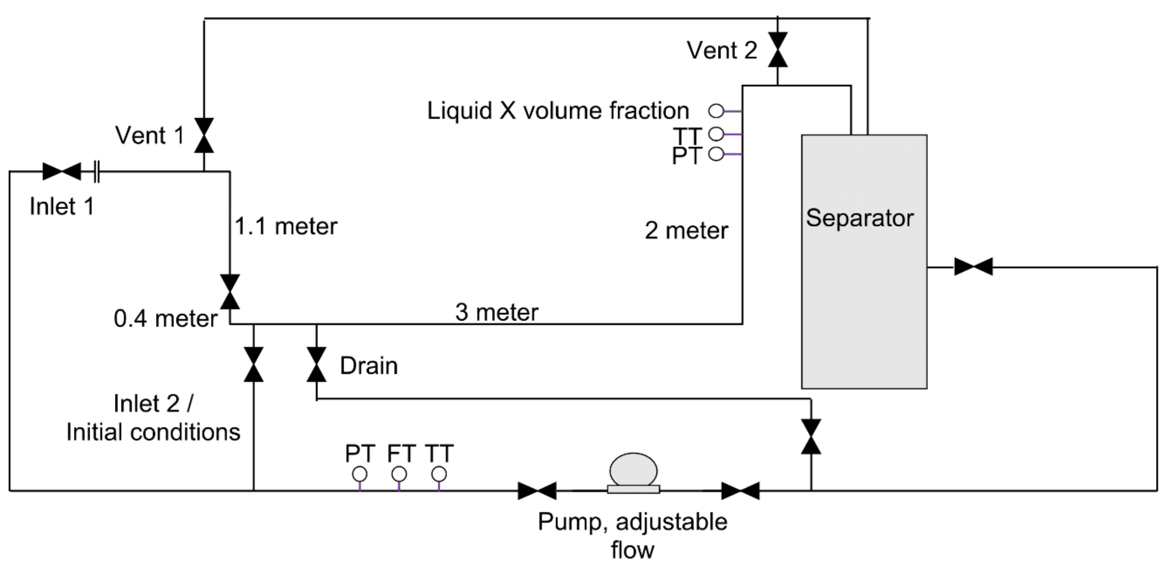

Figure 2 - P&ID based on initial requirements

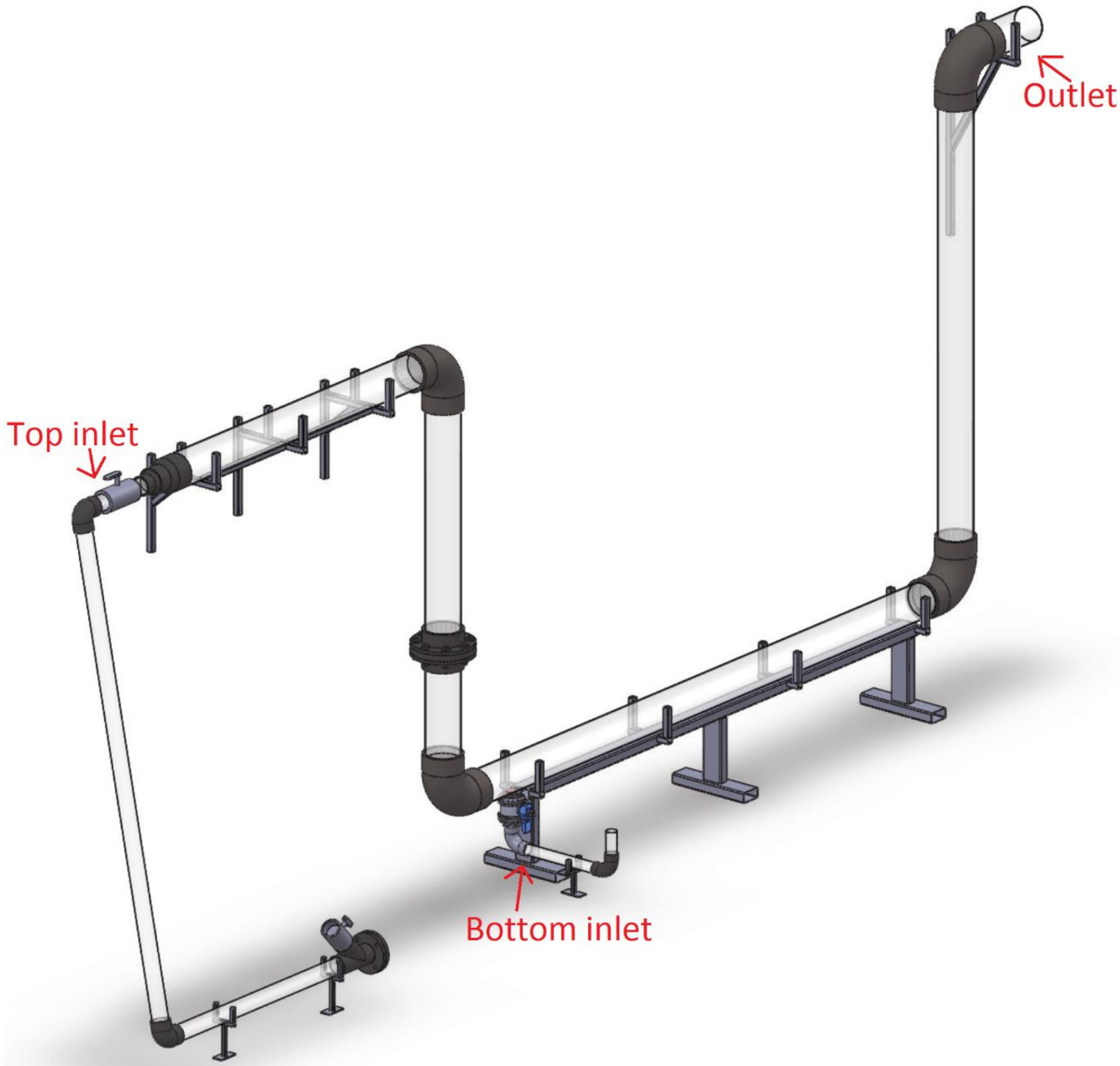

Figure 3 - Isometric view of jumper based on requirements

3.1.1 Data Acquisition

As one of the main objectives of the experiment was to generate reliable data intended to verify numerical simulations, the sensor setup would directly influence the hardware design. The requirements specify that the pressure, temperature and flow rate will be logged at the inlet and the pressure, temperature and volume fraction logged at the outlet. The data acquisition system shall also have the possibility to log sensor values and visualization of the flow throughout the experiment.

Although the requirements state that the volume fractions shall be logged, the author was unable to acquire a in the limited period of time. The data acquisition setup was developed to function in combination with a volume fraction sensor that outputs 4-20mA, so that an additional sensor can be added in the future. Instead of using a volume fraction sensor, the volume fraction was measured by draining the jumper and measuring the liquid hold-up with a measuring cup. The circuit design for the electronics was done using NI Multisim and built by the author.

3.1.1.1 Sensor selection

The requirements state that standard components must be used and that flow, pressure and temperature is obligated to be measured. The temperature is not likely to increase much during the displacement, and therefore the selected sensor should be accurate for temperatures around 20 +- 10 degrees Celsius. It is unlikely that the pressure in the loop will reach high levels due to the large pipe dimensions and low flowrates, accordingly a measurement range between 0 and 8 bar should be sufficient. The flowrate is given in the requirement, and selected flowmeter should therefore meet this range.

For temperature measurements, a standard PT100 elements was selected, as they are simple in use and field proven. To measure pressure, a UNIK 5000 pressure transducer from GM electronics was selected, with a measurement range from 0 to 16 BAR. For the flow measurements, a single sensor that met the requirements was not available. Two different turbine-based flow sensors were selected, a 1” with a range between 27-270 l/min and a 3” with a range of 270-2700 l/min. All the selected sensors were available at IPT, more detailed description and a link to the datasheets is listed in Table 2.

For visual documentation of the displacement, a high-speed GoPro HERO4 Black video camera was used, with the capability of filming with a resolution of 1280x720 pixels at a rate of 120 frames per second. Meaning that with a flowrate of 30 m^3/h, the displacement front will move 0.37 cm each time a frame is captured with a resolution of 1280x720.

Table 2 – Sensors used in the experiment

Part	Type	Vendor	Quantity	Datasheet link
Temperature Transmitter	PT100	RS Pro	3	http://docs-europe.electrocomponents.com/webdocs/1122/0900766b81122208.pdf
Pressure transducer	UNIK 5000	GM Electronics	3	http://www.ge-mcs.com/download/pressure-level/920-483F-LR.pdf
1" Flowmeter	FT100	Fluidwell	1	http://www.fluidwell.com/statisch/download/F110-DATA-EN-V1540.pdf
3" Flowmeter	Liquid Turbine Flow Meter	Halliburton	1	http://www.rental.no/content/mma/publish/00/09/989/Halliburton%20FlowMeters%20Brochure.pdf

3.1.1.2 PCB Design

As all of the selected sensors produce an analog output signal, an external acquisition system with interface towards a PC was required. The simplest solution for this was using LabVIEW from National Instruments in combination with National Instruments USB based data acquisition system USB-6009 (http://www.ni.com/pdf/manuals/375296a.pdf). From Table 2, it can be seen that at least eight analog inputs would be required. Although the NI USB-6009 has eight analog inputs, accommodation for volume fraction sensors will require nine and differential sampling requires two analog inputs for one sensor. To overcome this issue, it was decided to only connect sensors from one inlet at the time, as this would free up three analog inputs and make the selected data acquisition system feasible. Although the sensors selected will generate an analog signal, they cannot be connected directly to the NI USB-6009. An external circuit was required to power the sensors and improve the signal quality.

The PT-100 element is a resistance thermometer, so that the measured sensor resistance will change with temperature. It has a resistance of 100 ohm at 0 °C, which will change with a rate of 0.003925 ohm/ohm°C. To measure the sensor resistance, the PT100 element was connected to a Wheatstone bridge with a two wire configuration. The input voltage for the bridge was set to 5V and the bridge voltage, Ub, measured with differential sampeling on the NI USB-6009. In order to make the sensor accurate for temperatures around 20 °C, R1 was set to 120 ohm and R2=R4= 10k ohm. The circuit design for the PT100 element can be seen to the left in Figure 4. The resistance of the sensor, with wiring resistance between sensor and bridge circuit, can be calculated using Equation 1. To convert the resistance into temperature, Equation 2 is used with A = 3.9083E-3, B = -5.775E-07, C = -4.183E-12 and D as a calibration coefficient to compensate for wiring resistance.

Equation 1 – Calculation of PT100 resistance with Wheatstone bridge

$$R_{PT100} = \frac{R4}{\frac{R2}{R1+R2} - \frac{Ub}{Us}} - R4$$

Equation 2 - Converting resistance to temperature with PT100 element

$$T = \frac{-A + \sqrt{A^2 - 4B(1 - \frac{R_{PT100}}{R0})}}{2B} + D$$

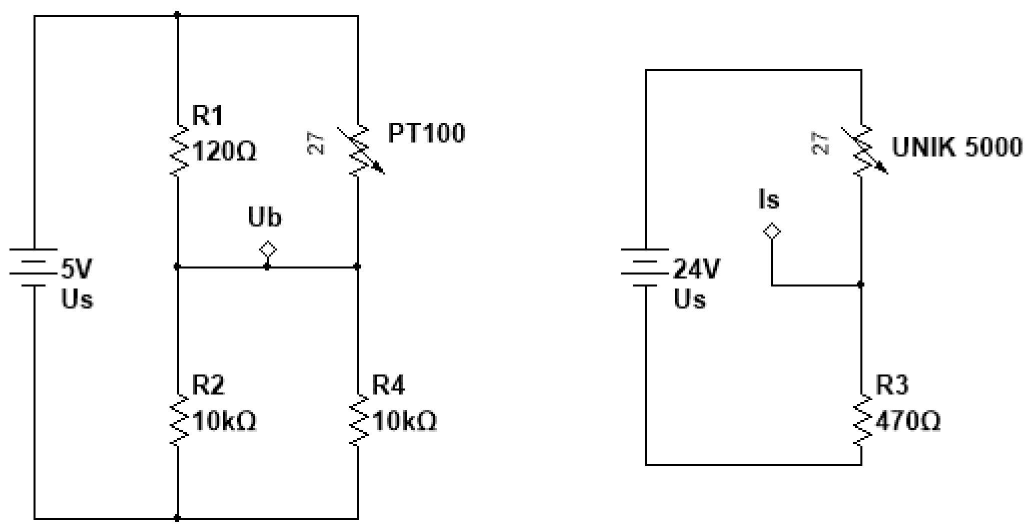

Figure 4 - Voltage and current measurement circuits

The pressure transducer and flowmeter will output a linear current signal between 4 and 20 mA, with regards to the pressure and flow read. The pressure transducer requires a voltage input between 7 and 32 VDC and the flowmeter between 8 and 32 VDC, an external power supply was therefore required. To measure the output current signal, a resistor is series with the sensor was required. As the NI USB-6009 has a max input of 10V for the Analog to Digital Converter, the resistor had to be kept bellow 500 ohm to limit the input voltage. A standard 470 ohm resistor was therefore put in series with the sensor. The physical value of the sensor can be calculated using Equation 3, based on the measured current. The input circuit for the current based sensors can be seen to the right in Figure 4.

Equation 3 – Calculation of physical value from measured current

$$P = P_{min} + \frac{P_{max} - P_{min}}{I_{max} - P_{min}} * (I - I_{min})$$

To accommodate for the requirements of the sensors, a PCB was made with two 5 volt Wheatstone bridges and four current sensing circuits. As a power supply for the PCB, an external 12 volt differential DC power supply was used. Due to the fact that the 5 volt analog output of the NI USB-6009 is known to be unstable, and to limit the size of the PCB - NI USB-6009 wiring harness, a voltage regulator was added to supply 5 volts to the Wheatstone bridges. As a safety measure, to turn on and off the 5 volt and 24 volt supply, switches was added. An additional button was required to start and stopping the data logging. Furthermore, LEDs were added to show the status of each switch. The complete PCB design can be seen in Figure 5, data communication wiring harness between PCB and NI USB-6009 in Figure 6 and sensor wiring harness and sensors in Figure 7. The PCB was built using a standard circuit test board and soldered together by the author. The finished PCB was placed inside a closed box to protect it from the environment; the external circuit box can be seen in Figure 8.

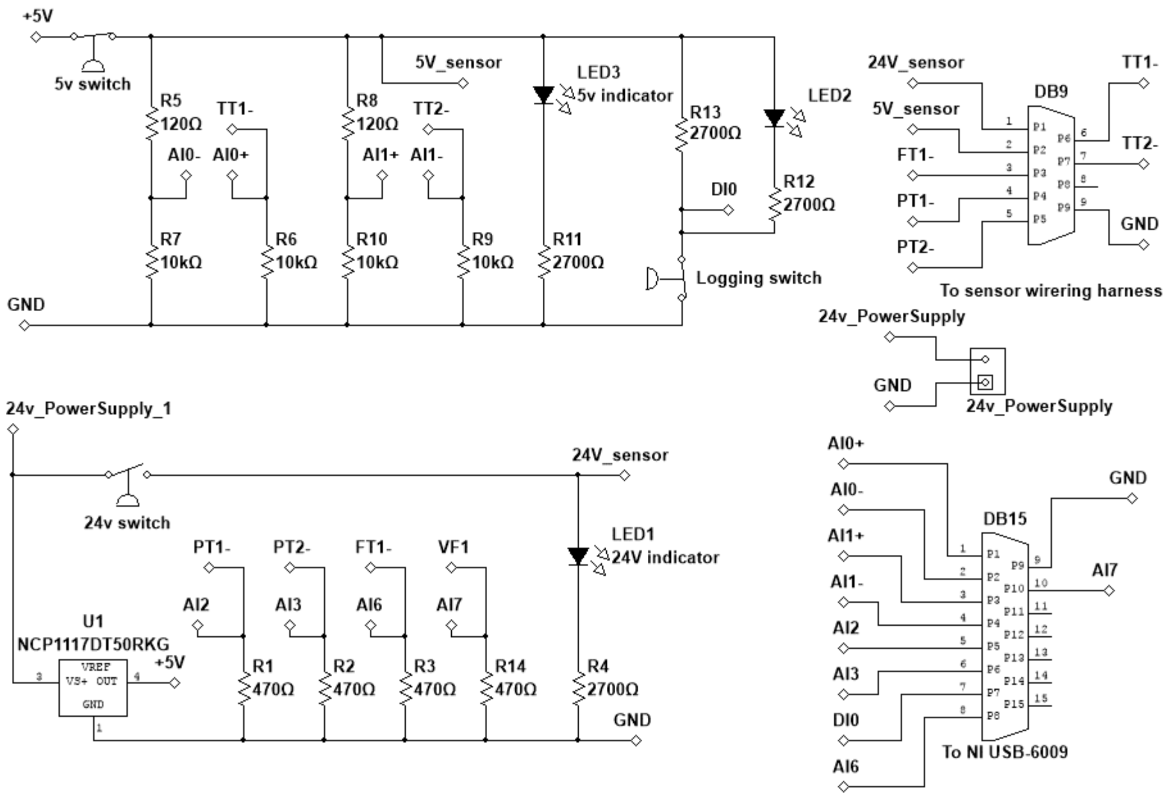

Figure 5 - PCB design and interfaces towards wiring harnesses

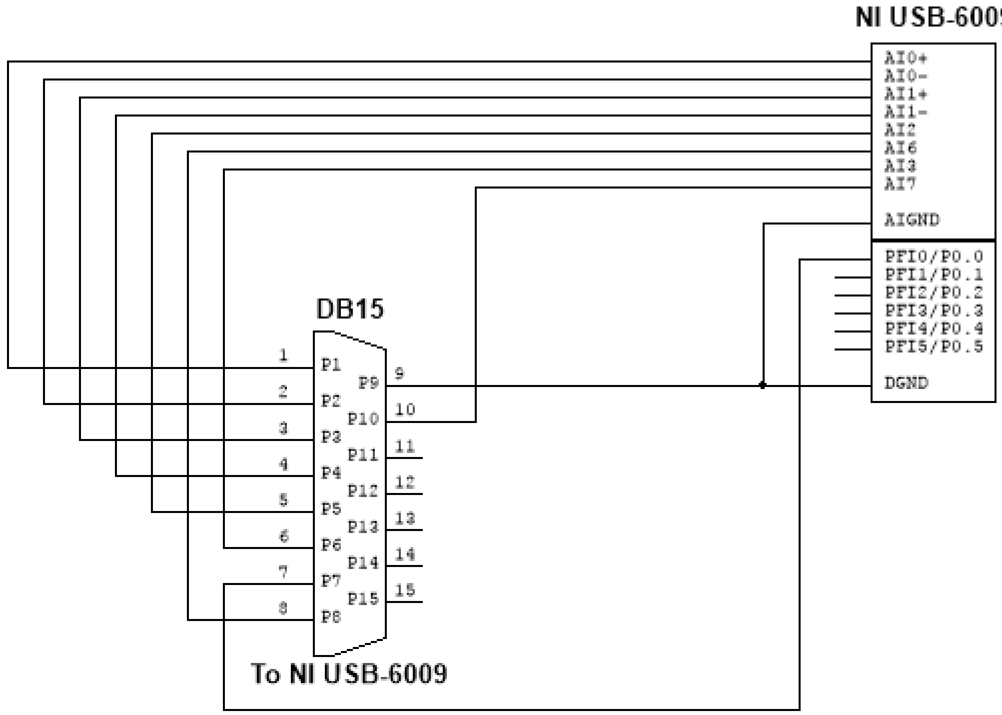

Figure 6 - shows the interface between wiring harness and NI USB-6009

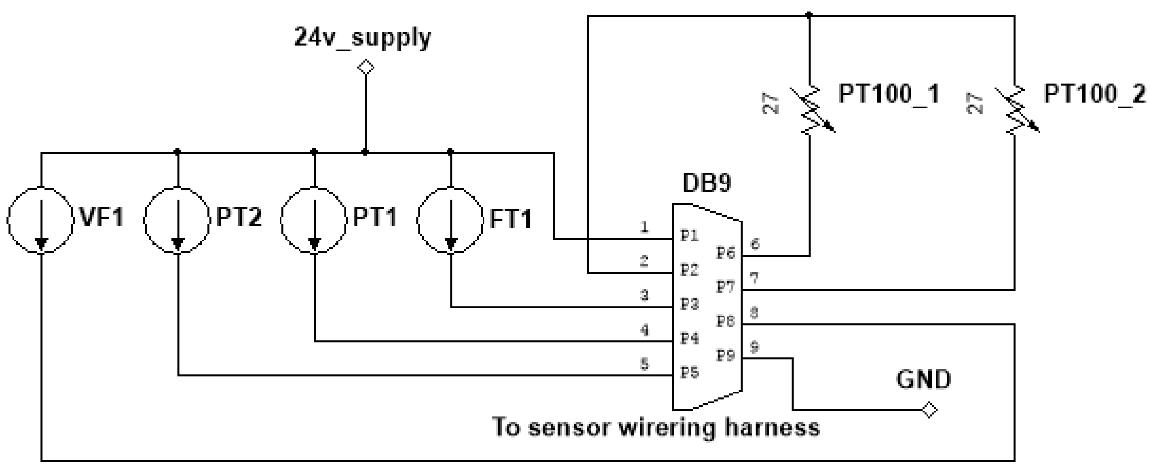

Figure 7 - Interface between the wiring harness and sensors

Figure 8 - External logging box

3.1.1.3 Software development

For reading sensor values in real time and logging the data, a simple LabVIEW Virtual Instrumentation application was developed. The application reads data from the NI USB-6009 data acquisition card at an adjustable rate dt. The read signal is then converted into the correct measurement unit and displayed in the frontpanel. The pressure, temperature and flowrate was plotted in separate graphs against time and real-time values shown in separate numerical indicators. In addition to the external logging control button on the PCB, an additional button was added to the frontpanel to start and stop the data logging directly from the computer. Once the logging was stopped, the sensor data is automatically saved to a comma separated values (CSV) file. The complete frontpanel can be seen in Figure 9 and the block diagram in Figure 10.

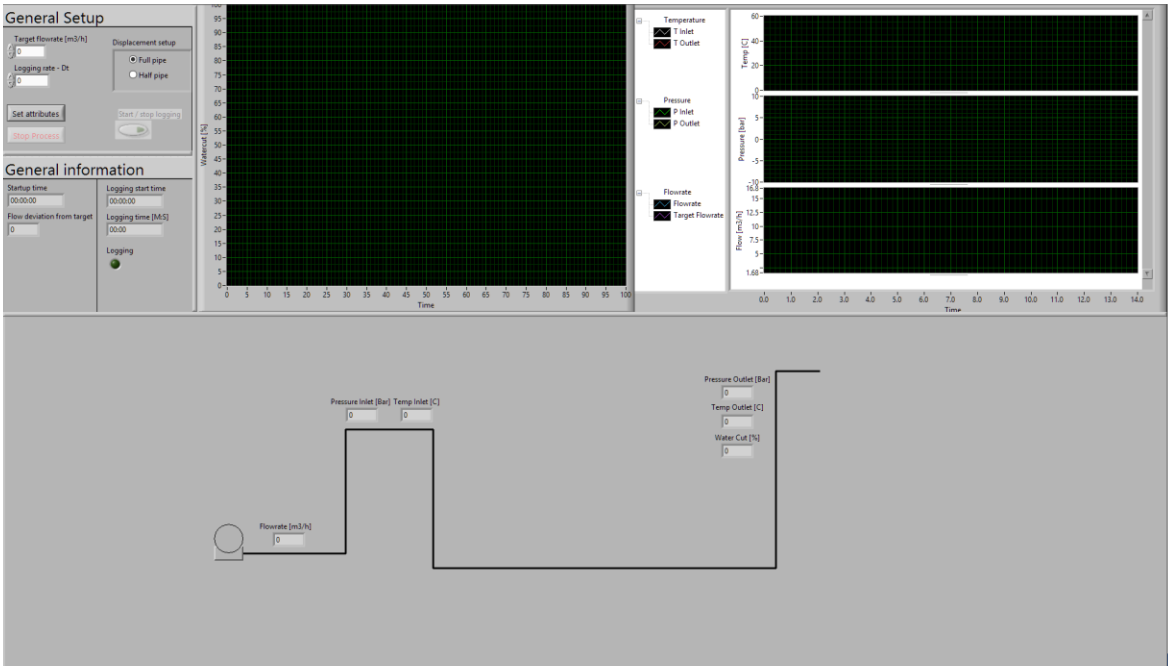

Figure 9 - LabVIEW Virtual Instrumentation frontpanel

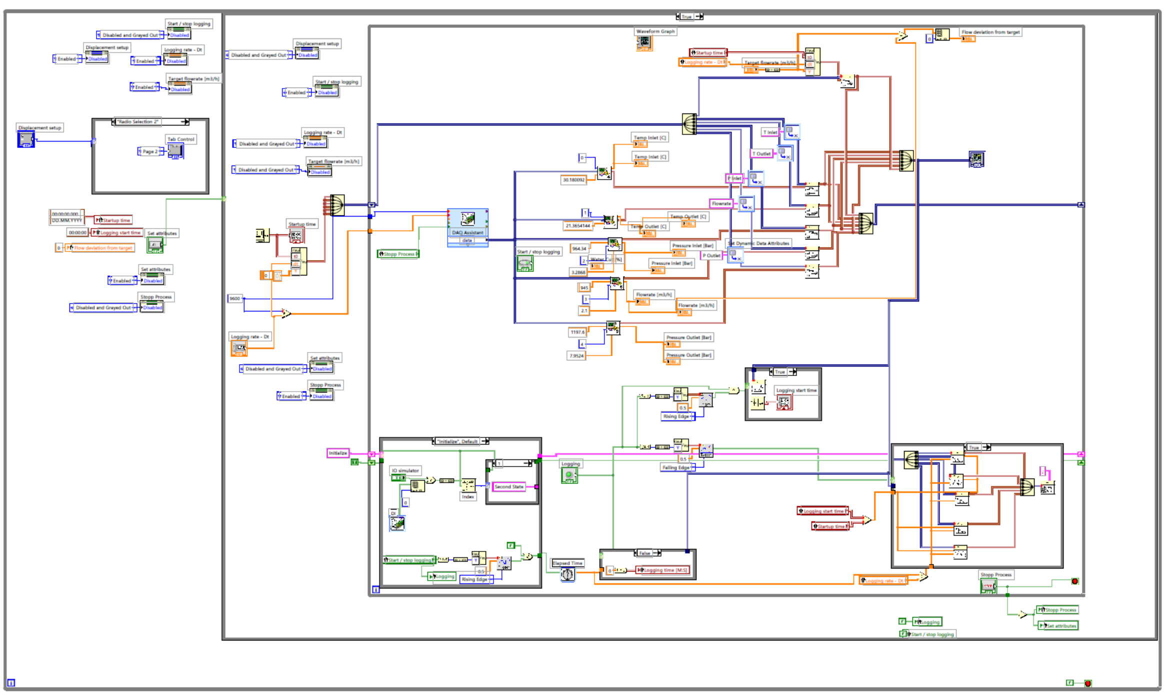

Figure 10 - LabVIEW Virtual Instrumentation block diagram

3.1.2 Hardware design

For the hardware design, it was decided to reuse as much as possible of the equipment available at IPT. The hardware design was divided into five steps, first the jumper was detailed designed and thereafter the pump and separator selection was made. Afterwards, the interfaces between the equipment was designed. Finally the support and mounting equipment was designed. The detail design was made using computer aided design tool Solidworks, Figure 11 below shows a complete drawing of the setup and Figure 12 the finished product.

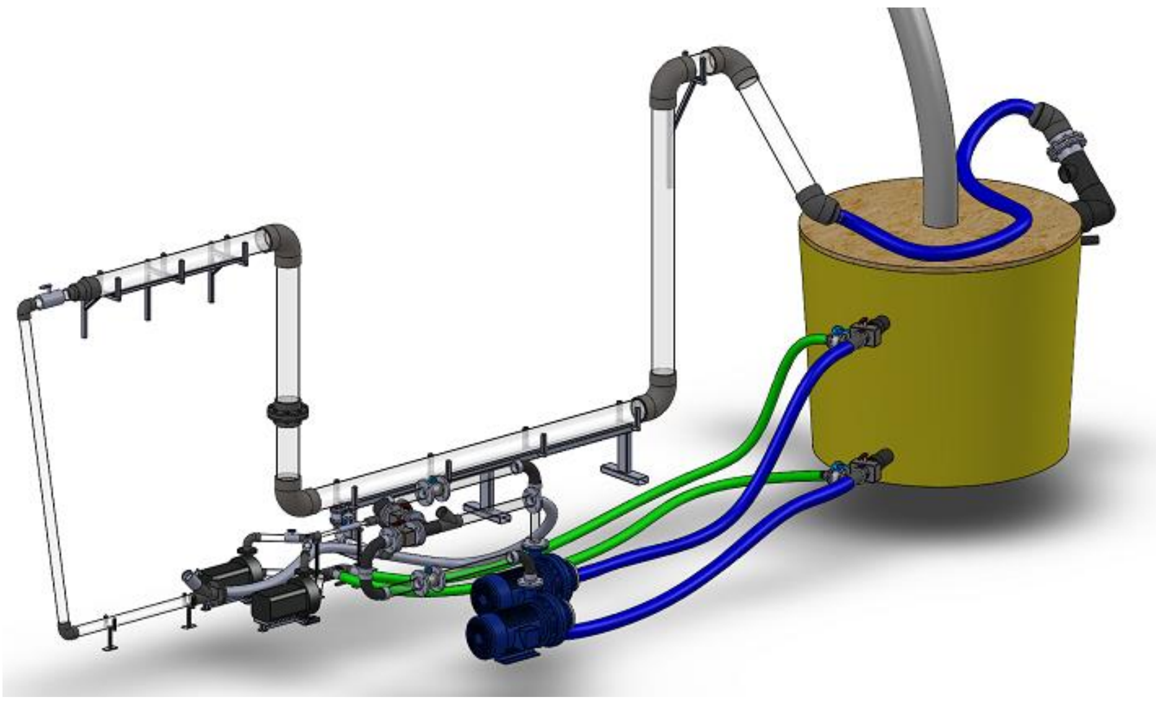

Figure 11 - Complete CAD model of the experimental setup

Figure 12 - Finished experimental setup

3.1.2.1 Jumper design

For the jumper pipes, 4 meters of acryl pipe with an OD of 160 mm and wall thickness of 3.2 mm was available at IPT and this size was therefore used for the whole jumper. To satisfy the requirement of stable flow at the inlet, the entrance length of the U was set to 1.536 meters (10x hydraulic diameter of pipe). To avoid a valve disturbing the flow in the first riser, it was decided to use two pipe sleeves with flanges to split it. A blind flange, with venting valve, was used to isolate a section of the pipe. To keep the setup as compact as possible, the outlet was kept as short as possible. The detail design of the jumper can be seen in Figure 13 with the parts list in Table 3

Table 3 - Parts list for the jumper

Part	Location	Description	Quantity
Pipe	Inlet section	160x3.2mm	1.536 m
	Top of first riser	160x3.2mm	1.1 m
	Bottom of first riser	160x3.2mm	0.4 m
	Bottom section	160x3.2mm	3 m
	Second riser	160x3.2mm	2 m
	Outlet section	160x3.2mm	0.3 m
Bend	Inlet - First riser	160mmx90 degree	1
	First riser - bottom section	160mmx90 degree	1
	Bottom section - second riser	160mmx90 degree	1
	Second riser - Outlet	160mmx90 degree	1
Sleeve	First riser	ID 160 mm	2
Flange	First riser	ID 160mm	2
Blind flange	First riser	OD 220 mm	1
Bolts	Flange	M16x120	4
Nuts	Flange	M16x10	4
Disc	Flange	M16	8

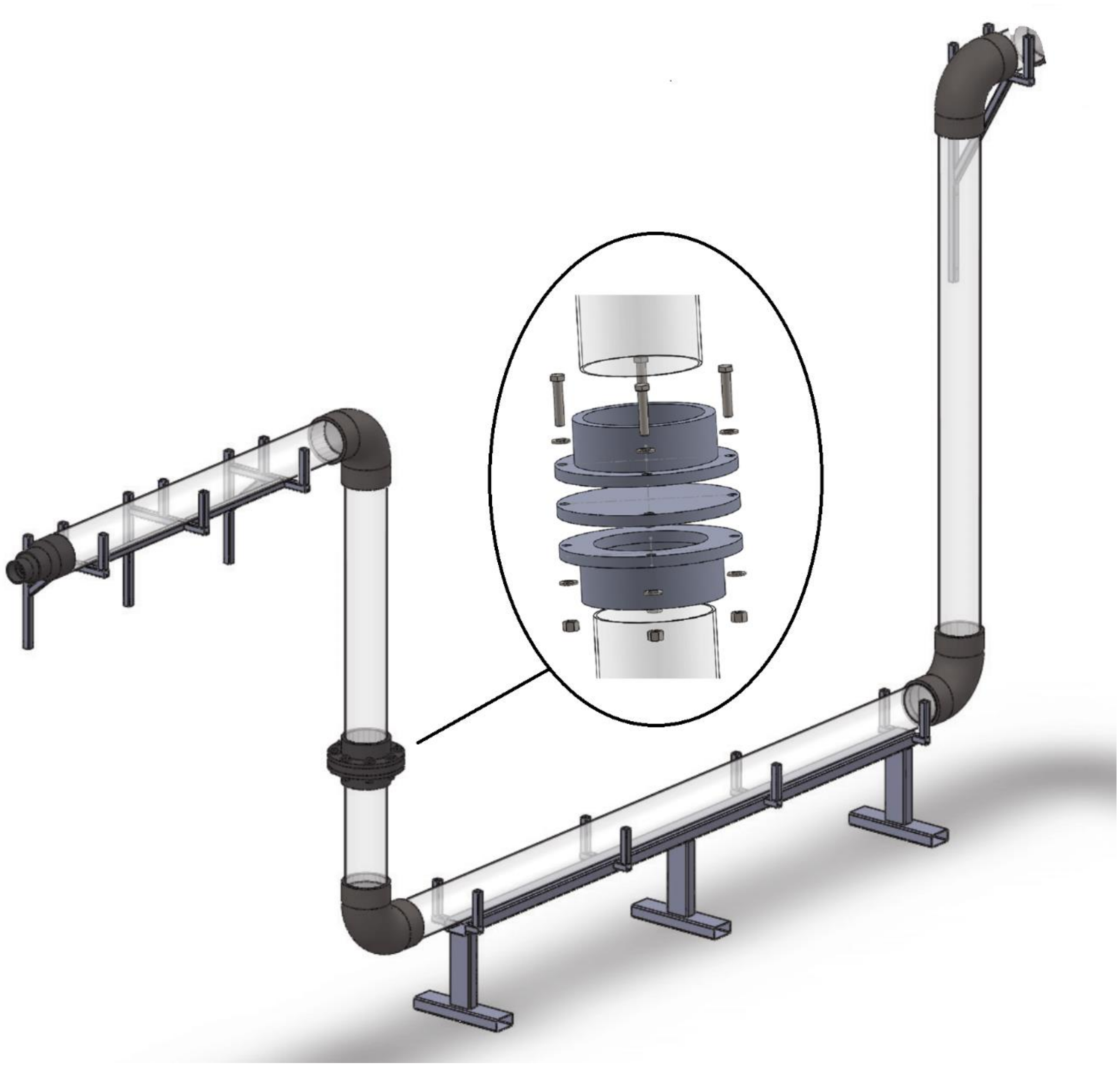

Figure 13 – Jumper design with highlight of split section

3.1.2.2 Inlet design

Two inlets were added to the pipe, one at the bottom section and one normal to the U. To limit the size of the structure and costs, it was decided to reduce the diameter at the inlet of the U to a 75mm OD pipe. For the inlet at the bottom section, it was decided to use 50mm OD piping to have realistic scaling between the inlet and the jumper. In addition, the bottom inlet will function as a filling point for establishing initial conditions. Detail design for both inlets can be seen in Figure 14 and Figure 15, a parts list can be seen in Table 4 and Table 5.

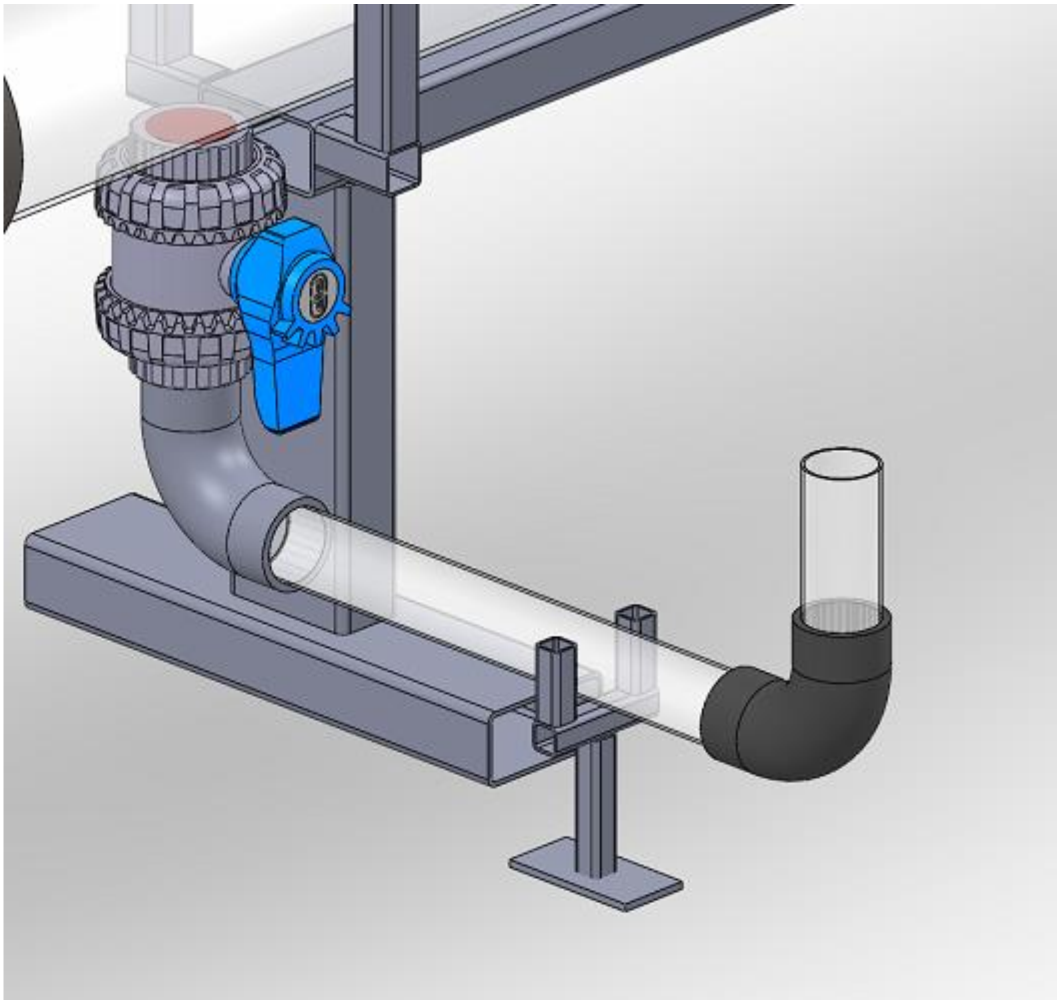

Figure 14 - Lower inlet

Table 4 - Parts list for the lower inlet

Part	Description	Quantity
Bend	50mm - 90 degree	2
Connector	50 mm - Threaded straight connector	1
Pipe	50mm	0.7 m
Valve	50mm - ball	1

Figure 15 - Top inlet

Table 5 - Parts list for the top inlet

Part	Description	Quantity
Bend	75mm - 90 degree	2
Connector	160mm ID to 110 mm ID - straight transfer	1
	110mm OD to 75 ID - straight transfer	1
	75mm – Y	1
Valve	75mm - ball valve	2
Flange	75mm	2
Fittings	3” hose adapter	1
	4” hose adapter	1

3.1.2.3 Pump selection

Due to cost, it was decided to use pups available at IPT. However, none of the pumps available at IPT met the flow requirements and two different pump setups was therefore used. One high-flow setup and a low-flow setup. The high-flow setup have an individual pump for each liquid and the low-flow setup two pumps in parallel pumping the same liquid. The specifications and make of the pumps can be seen in Table 6 below.

Table 6 – Pump specifications

Make	Specification				Quantity	Datasheet
	Q [m^3/h]	H [m]	n [min^{-1}]	p/t [bar/◦C max]		
Grundfos NB32-200/194 A-F-A-BAQE	6	11	1430	16/120	2	http://www.pumppower.com.au/wp-content/uploads/2013/07/NB_NBE-Data-Booklet.pdf
Pedrollo F50/200B	102	38	2900	10/90	1	http://www.pedrollo.co.uk/pdf/Product%20Pages/Centrifugal/Standardized/F/F.pdf
Pedrollo F65/200AR	126	46	2900	10/90	1	

3.1.2.3.1 Low flow pump setup

The low-flow pump-setup consists of two centrifugal pumps with a max flowrate of 6 m^3/h. The small pump setup was controllable with flow control valves and a frequency converter, adjusting the head pressure of the system and pump RPM. This gives the pump-setup a flow range between 0 m^3/h - 12 m^3/h, for the low-flow setup.

To supply liquid to the pumps, two separate 50mm ID hoses were used from the separator outlets, one for oil and one for water. The hoses has an isolation valve at each end and are combined into one 46.4mm ID pipe using a T-connector and rerouted to the individual pumps using a symmetric Y-connector. The pump outlets are connected using a 46.4mm ID symmetric Y-connector, before being routed to the flowmeter. The 1" flowmeter requires an entrance length of 10x the hydraulic diameter and 5x the hydraulic diameter for the outlet. After the flowmeter, the flow was split with a straight Y-connector, with one flow going to the top inlet via a 75mm ID hose and the other to the bottom inlet via 46.4mm ID piping. In the symmetric Y splitting the flow, the pressure- and temperature-transmitter were connected. A detail design of the low flow pump setup can be seen in Figure 16, with parts listed in Table 7.

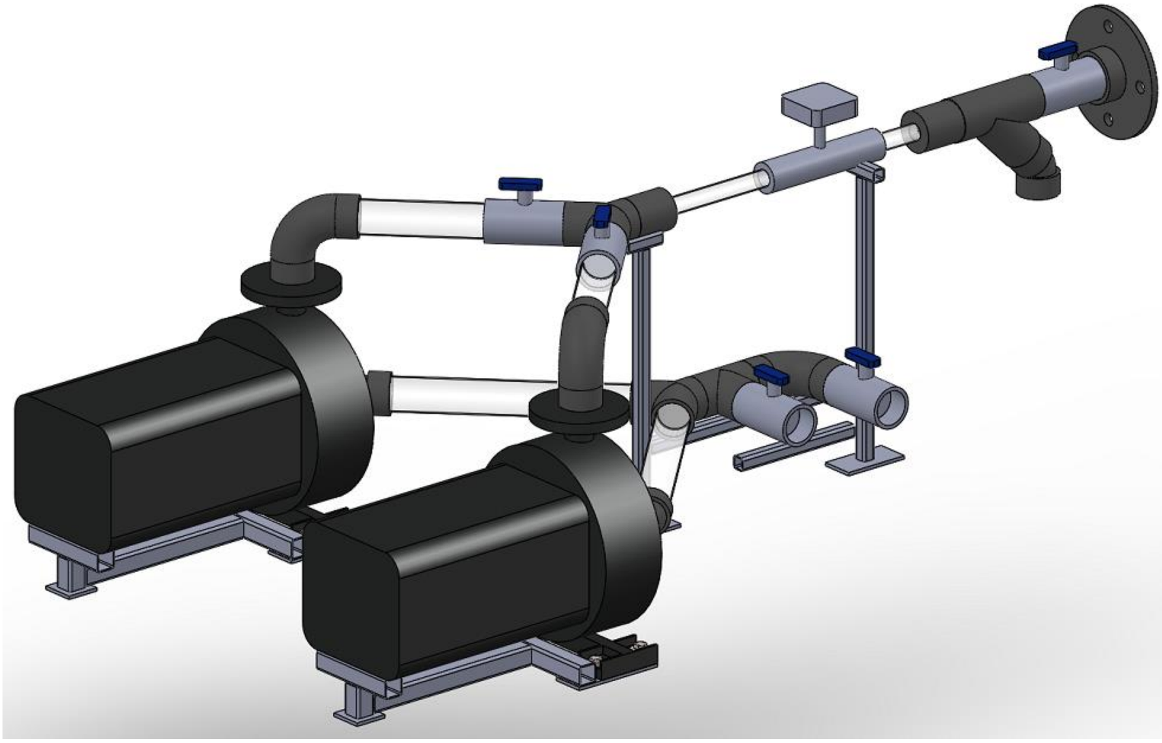

Figure 16 - Low-flow pump setup

Table 7 - Low-flow pump setup parts list

Part	Description	Quantity
Bend	50mm - 90 degree	3
	50mm - 45 degree	2
Connector	50mm - symmetric Y	2
	50mm - straight Y	1
	50mm to 25mm - Reducer	2
	50mm - T	1
Pipe	50x1.8mm	1.222m
	25x1.8mm	0.375m
Valve	50mm ID - ball	3
	50mm ID - flow control	2
Fittings	50mm hose adapter	2

3.1.2.3.2 High Flow Pump Setup

The high-flow pump-setup consist of two different centrifugal pumps, and was designed and built by Henrik Nikolai Gussiås Kulseth and Erik Hjertholm. The pumps has a max flow of 102 m^3/h and 126 m^3/h, the flow can be adjusted using a 0 to 50 Hz 400v frequency converters. A 3” flow transmitter was connected to each pump outlet, with a range from 270 to 2700 l/min.

The high-flow pumps will be exclusively used for displacement through the top inlet, as the bottom inlet has an inner diameter of just 46.4mm, which would result in an extremely high flow velocity. The pumps are connected to the separator with individual 75mm ID suction hoses, so that the first pump will provide oil and the second water. Further, the flow from the pumps are gathered in a T-connector, with isolation valves for each flow. After the T- connector, a straight pipe with temperature and pressure sensors, was used to stabilize the flow before it was re-routed to the top inlet via a 75mm ID hose. The high flow pump setup can be seen in Figure 17, with the parts listed in Table 8.

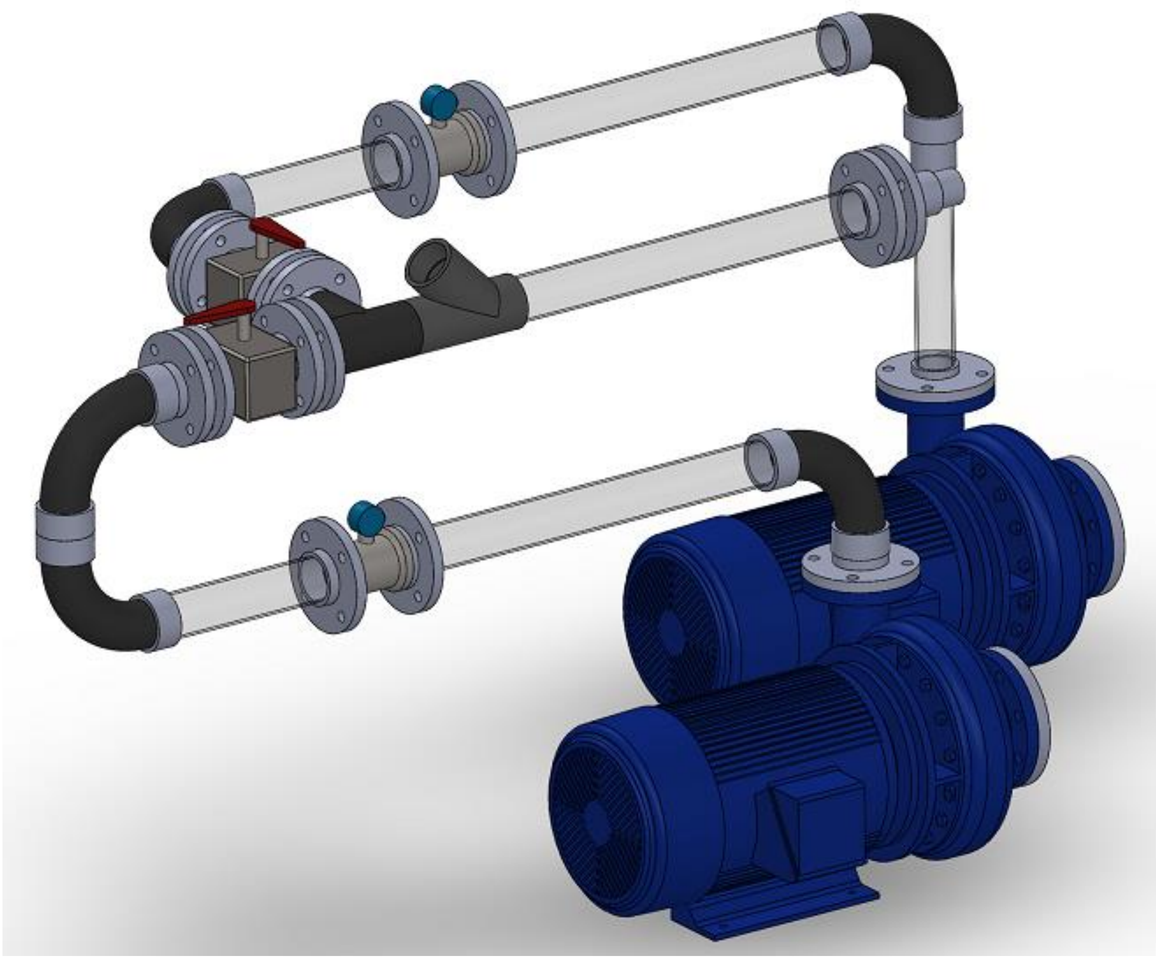

Figure 17 - High flow pump setup (Drawing by Henrik Nikolai Gussiås Kulseth)

Table 8 - High flow station parts list

Part	Description	Quantity
Bend	75mm - 90 degree	5
Connector	75mm - straight Y	1
	75mm - T	1
Pipe	50mm	3.190
Valve	75mm - ball	2
Flange	3”, 4 bolt	18
Fittings	3” hose adapter	3

3.1.2.4 Separator selection and interface design

A closed circular vertical two-phase separator was selected for separation of the liquids after the displacement and storage in-between experiments. The separator has a bottom diameter of 1.82 meter, top diameter of 2.02 and a total height of 1.64 meters, giving it a capacity of 5 m3. The separator has one 6.5 inches inlet, located at 6 o'clock, and two 4" outlets located at 10 o'clock with a height of 0.2 meters and 1.4 meters. In order to reduce the settling time of the liquids, the inlet enters the separator at 1.4 meters and is routed to the bottom of the separator trough a perforated pipe. Furthermore, a full separator will provide the displacement pumps with a hydrostatic suction pressure of 0.16 bar. The top of the separator was connected to an ATEX-approved EX safe fan, for ventilation of gases emitted from the oil.

The separator has interfaces toward the jumper, recycling loop and displacement pumps, with hoses and pipes. Each of the outlets has a 4" isolation ball valve, with a T-connector splitting the flow and providing liquid to each of the pump stations. The separator inlet is 6.5" and is directly connected to a 90 degree 160mm ID reduction bend. The bend is connected to a T-connector with one interface towards the jumper and the other to the recirculation loop. A drawing of the separator with interfaces can be found in Figure 18 and a list of parts in Table 9.

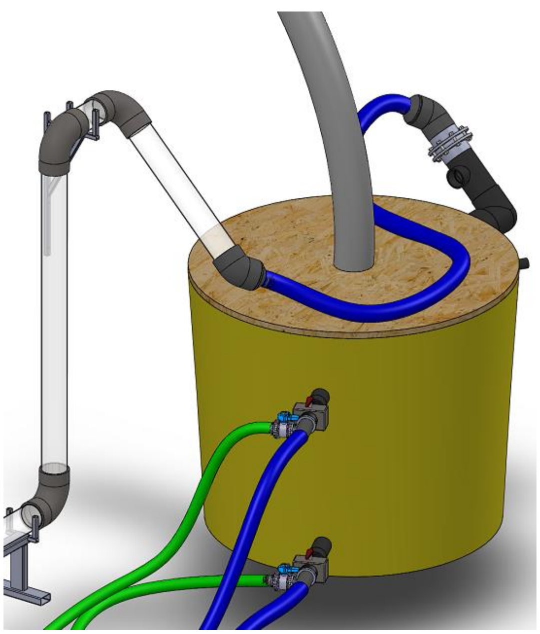

Figure 18 - Separator with surrounding equipment

Table 9 - Separator parts list

Part	Description	Quantity
Separator	2x1.8m	1
Bend	160mm ID, 90 degree	2
	160mm ID, 45 degree	2
Connector	T – 75mm ID	2
	T – 160mm/110mm ID	1
Fittings	2” hose adapter	2
	3” hose adapter	2
Pipe	160x3.2mm	1m
Hose	2” - suction	15m
	3” – suction	6m
	4” - flathose	3m
	4” - ventilation	15m
Valve	6” – butterfly	1
	50mm ID – Ball	2
	4” – ball	2
Hose clamps	2”	2
	3”	2
	4”	4
Fan	ATEX	1

3.1.2.5 Structural supports

To keep the pipes and equipment in place during displacements, support equipment was made in structural steel. For the design, it was emphasized that the support structure should not influence visibility of the flow in the pipe. Drawings of the support equipment for the parts can be seen in previous sketches, with a parts list in Table 10.

Table 10 - Parts list for the support structures

Part	Description	Quantity
Bottom support	100x50x3.2mm	4.8m
	30x30x2.0mm	1.620m
Main inlet support	30x30x2.0mm	4906.74m
Outlet support	30x30x2.0mm	2.517m
2xLow flow pump support	30x30x2.0mm	0.7095m
	50x5.0mm	0.330m
Low displacement flow system	20x20x2.0 mm	1.46485m
	50x5.0mm	0.2m
Outlet hose support	30x30x2.0 mm	5.5m
	50x5.0mm	0.5m

3.1.3 Liquid selection

The displacement experiment was performed with two different liquids, a displacement liquid and a liquid to be displaced. From the requirements, the liquids shall be representative of a realistic situation and available worldwide, and therefore oil was selected as a liquid to be displaced.

Although crude oil is preferred, it is not feasible for the experiment due to its toxicity and the fact that it cannot be bought through regular channels, hence Exxsol D60 from ExxonMobile Chemicals was selected. This oil is a commonly used for experimental work, with well-known properties and high availability. Notably, it has limitations due to low viscosity. Very few oils and especially the ones from new oil fields is known to have low viscosity. Although the oil is quite flammable, this is not an issue due to the closed-loop design and ATEX classified ventilation.

There are several options of displacement liquids, including Methanol and MEG. Methanol is illegal in the experimental facility and hence, excluded as an displacement liquid. Due to cost and availability, tap water was chosen over MEG. The properties of tap water will vary from location to location and also with seasonal differences, however it should stay consistence for the length of the experiment. The properties of the tap water are available from Trondheim municipality water works. Water also satisfies the requirement of being immiscible with Exxsol D60. The material properties of Exxsol D60 and water can be found in Table 11, see below.

Table 11 - Material properties of Exxsol D60 and water

Property	**Water**	**Exxon Mobile Exxsol D60**
Molar Mass [kg $kmol^{-1}$]	18.02	158
Density @ 15 ºC [kg m^{-3}]	997	792
Dynamic Viscosity @ 25 ºC [cP]	0.8899	1.2989

As both liquids are transparent, red dye Oil Red-O, was added to the oil to distinguish the two liquids. The dye is insoluble in water and "will not affect the surface tension of the oils" (Xuemei Chen, 2016). Inhibitors was added to separator, to prevent formation of algae and bacteria in the separator,. According to SINTEF, the inhibitor IKM CC-33 will not affect the properties of the liquids. The interface tension between exxsol d60 and water has been measure to 36 mN/m in 2016 by SINTEF, with Pendant Drop measurement method with a Teclis Tracker tensiometer from Teclis Instruments (http://www.teclis-instruments.com/index.php/en/offer/products/tensiometer) (Fossen, 2016).

3.2 Displacement procedure

Four cases were developed to test two different displacement strategies for the pipe section. Strategy one displaces the liquid trough the top inlet of the pipe, while strategy two displaces through a dedicated displacement line located at the bottom of the pipe. With strategy two, the first riser section would be closed of 0.4m above the closest ninety degree bend, to create a dead-leg in the pipe. Both strategies would be tested with oil displacing water and water displacing oil, each with four different flowrates. The flowrates was selected based on input from Anna Elisabet Borglund at Onesubsea, simple numerical simulations and available pumping capacity.

The displacement procedure was split into three different sections, establishment of initial conditions, displacement trough the bottom inlet and displacement trough the top inlet. The procedures include visual presentation of the setup via a P&ID made in Microsoft Excel and step by step description of the pump and valve operations. Initial conditions for valves were listed and liquid contained in pipes and hoses displayed prior to onset of each procedure.

In the P&ID, open valves have white collar with black borders, while closed valves are all black. The status of pipes and hoses is indicated by its color, black line indicates empty, red illustrates oil filled, blue illustrates water filled and green implies a mixture of water and oil. The flow path for each step is indicated by glowing lines. The complete procedure developed can be found in appendix A. A picture of the P&ID used for the procedure can be found in Figure 19 below. A short description of the content in the procedures can be found in subchapter 3.2.1 through 3.2.3.

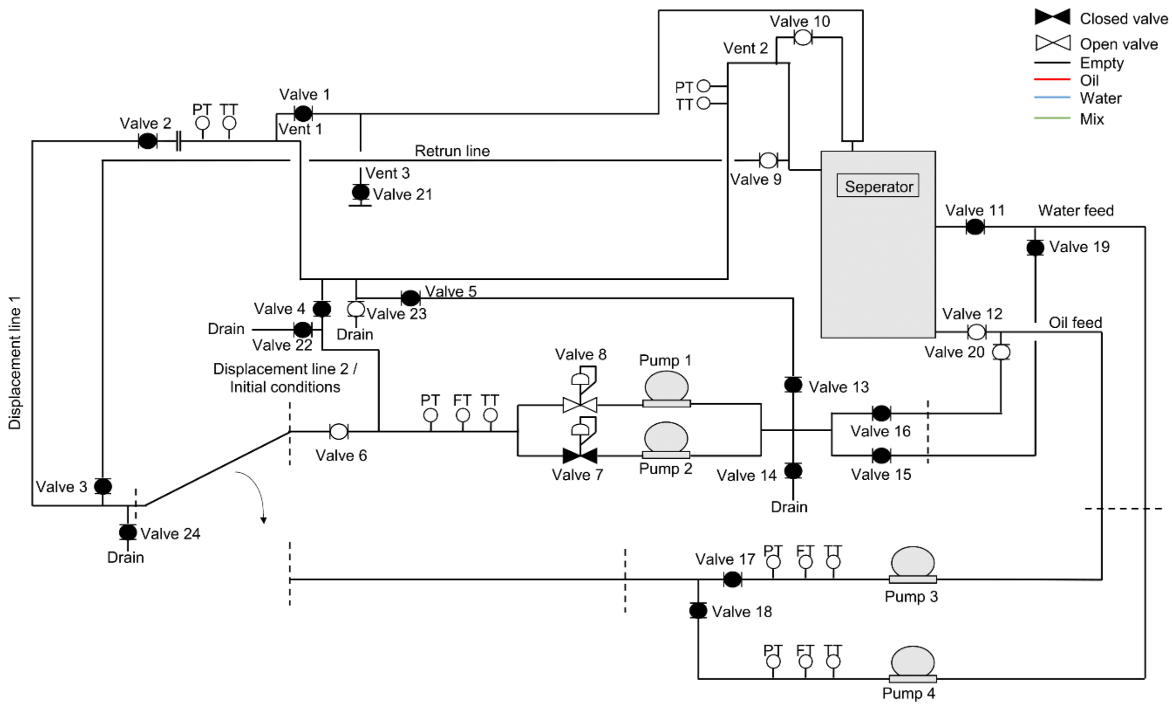

Figure 19 - Complete P&ID

3.2.1 Establishment of initial conditions

The establishment of initial condition were done before onset of the displacement procedure. It is done through a dedicated initial condition line, with the low-flow pump setup and four different sub procedures was developed describe filling the whole jumper or half the jumper with either water or oil.

3.2.2 Displacement trough lower inlet

Displacement trough the lower inlet was performed with the low-flow pumps at four different flowrates, displacement rates and pumps used can be seen in Table 12, see below. Two different scenarios was tested, water displacing oil and oil displacing water.

Table 12 - Displacement rates for the bottom inlet

Test number	Displacement rate [m3/h]	Pump used
1	4	Pump 1
2	6	Pump 1
3	8	Pump 1 & Pump 2
4	10	Pump 1 & Pump 2

3.2.3 Displacement trough top inlet

Displacement trough the top inlet was performed both with the low-flow pumps and with the high-flow pumps with four different flowrates, displacement rates and pups used can be seen in Table 13. Two different scenarios was tested, water displacing oil and oil displacing water with four different flowrates.

Table 13 - Displacement rates for the top inlet

Test number	Displacement rate [m3/h]	Pump used
1	6	Pump 1
2	10	Pump 1 & pump 2
3	20	Pump 3 / Pump 4
4	30	Pump 3 / Pump 4

4 Experimental Results

Results obtained in the experiment are reported numerically in tables for each displacement case at discreet points. An overview of the experiments conducted can be found in Figure 20. Detailed results from the individual cases are presented in subchapter 4.1 through 4.4, results will be further discussed in chapter 7.

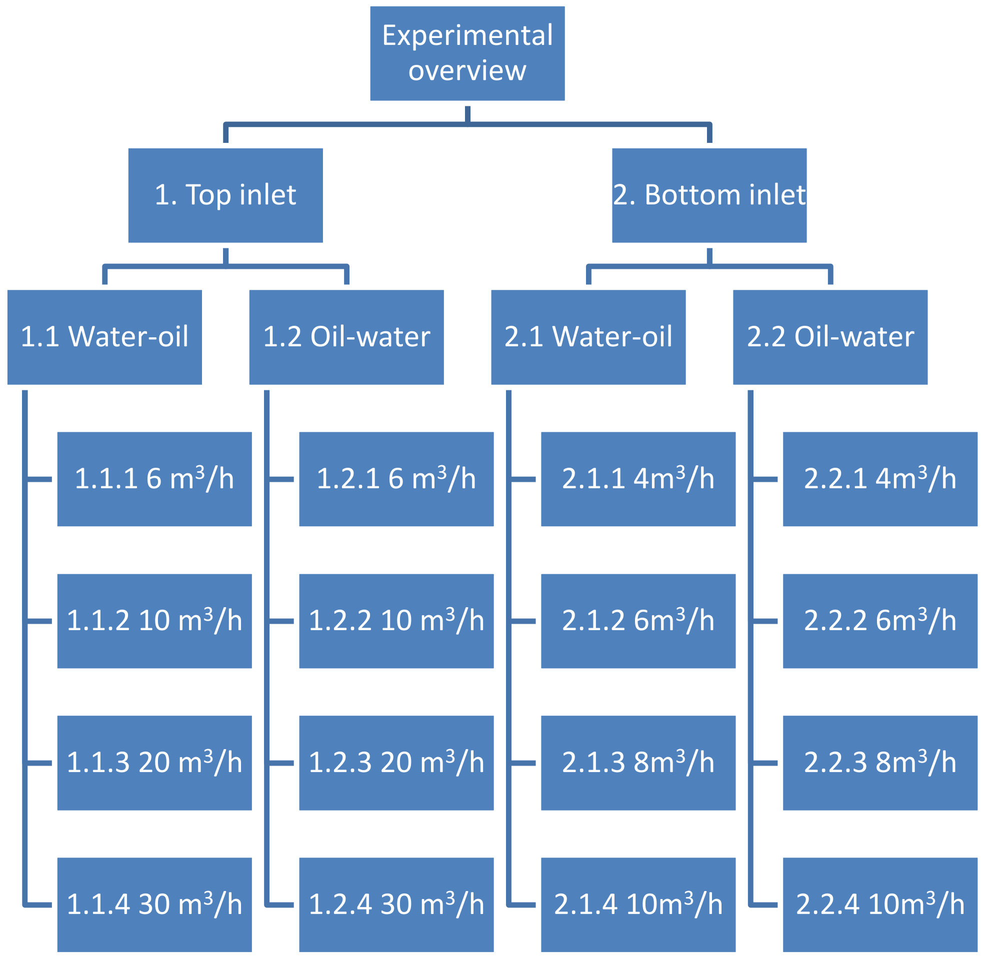

Figure 20 – Overview of experiments

In the detailed results, remaining initial liquid after one, two and three displacement volumes is displayed in tables along with superficial displacement velocity. To further analyze the flow visually, three measurement point were added (left in Figure 21). Movies showing the displacement front height and velocity at the bottom horizontal section and second riser can be found in the digital appendix. Measurement cup used to measure remaining water and oil can be seen to the right in Figure 21.

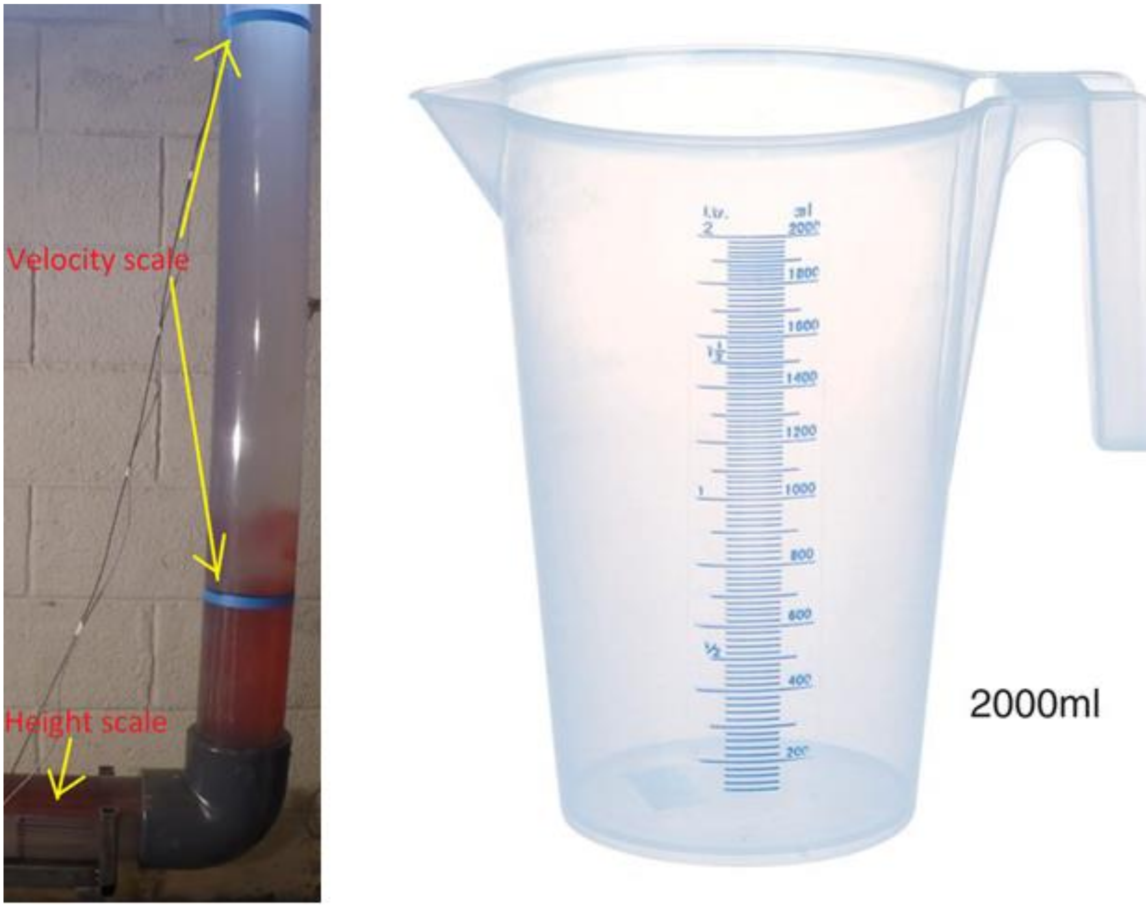

Figure 21 – Measurement scales for experiment (left) and measurement cup (right)

4.1 Displacement 1 - Water displacing oil through the top inlet

Experiment number	Superficial displacement velocity [m/s] +- 0.009 m/s	Displacement rate [m^3/h] +- 0.6 [m^3/h]	Remaining oil - 1 displacement volume [liters] +- 0.01 liter	Remaining oil - 2 displacement volume [liters] +- 0.01 liter	Remaining oil - 3 displacement volume [liters] +- 0.01 liter
1.1.1	0.09	6	29.5	29	29
1.1.2	0.15	10	21	17	16
1.1.3	0.30	20	12.8	4	3.3
1.1.4	0.45	30	1.32	0.35	0.28

4.2 Displacement 2 - Oil displacing water through the top inlet

Experiment number	Superficial displacement velocity [m/s] +- 0.009 m/s	Displacement rate [m^3/h] +- 0.6 [m^3/h]	Remaining water - 1 displacement volume [liters] +- 0.01 liter	Remaining water - 2 displacement volumes [liters] +- 0.01 liter	Remaining water - 3 displacement volumes [liters] +- 0.01 liter
1.2.1	0.09	6	59	56	54
1.2.2	0.15	10	56	44	41.5
1.2.3	0.30	20	49	22.2	16.2
1.2.4	0.45	30	23.42	4.65	1.72

4.3 Displacement 3 - Water displacing oil through the bottom inlet

Experiment number	Superficial displacement velocity [m/s] +- 0.009 m/s	Displacement rate [m^3/h] +- 0.6 [m^3/h]	Remaining oil - 1 displacement volume [liters] +- 0.01 liter	Remaining oil - 2 displacement volumes [liters] +- 0.01 liter	Remaining oil - 3 displacement volumes [liters] +- 0.01 liter
2.1.1	0.06	4	10.6	9.9	9.36
2.1.2	0.09	6	10.3	9.45	9.54
2.1.3	0.12	8	11.52	8.5	8.5
2.1.4	0.15	10	13.7	9.38	8.77

4.4 Displacement 4 - Oil displacing water through the bottom inlet

Experiment number	Superficial displacement velocity [m/s] +- 0.009 m/s	Displacement rate [m^3/h] +- 0.6 [m^3/h]	Remaining water - 1 displacement volume [liters] +- 0.01 liter	Remaining water - 2 displacement volumes [liters] +- 0.01 liter	Remaining water - 3 displacement volumes [liters] +- 0.01 liter
2.2.1	0.06	4	70	59	57
2.2.2	0.09	6	52.6	49	46
2.2.3	0.12	8	50.3	40	39
2.2.4	0.15	10	41	34.7	30.5

5 Numerical simulation

Intending to provide further detailed information regarding the multiphase flow dynamics and to examine the accuracy of the numerical model, numerical simulations were performed. All simulations were conducted using the commercially available CFD software ANSYS CFX 16.2, with ANSYS workbench integration. The simulation domain was meshed using ANSYS ICEM CFD. The process of conducting the numerical simulation was divided into five steps, described in the flowchart in Figure 22.

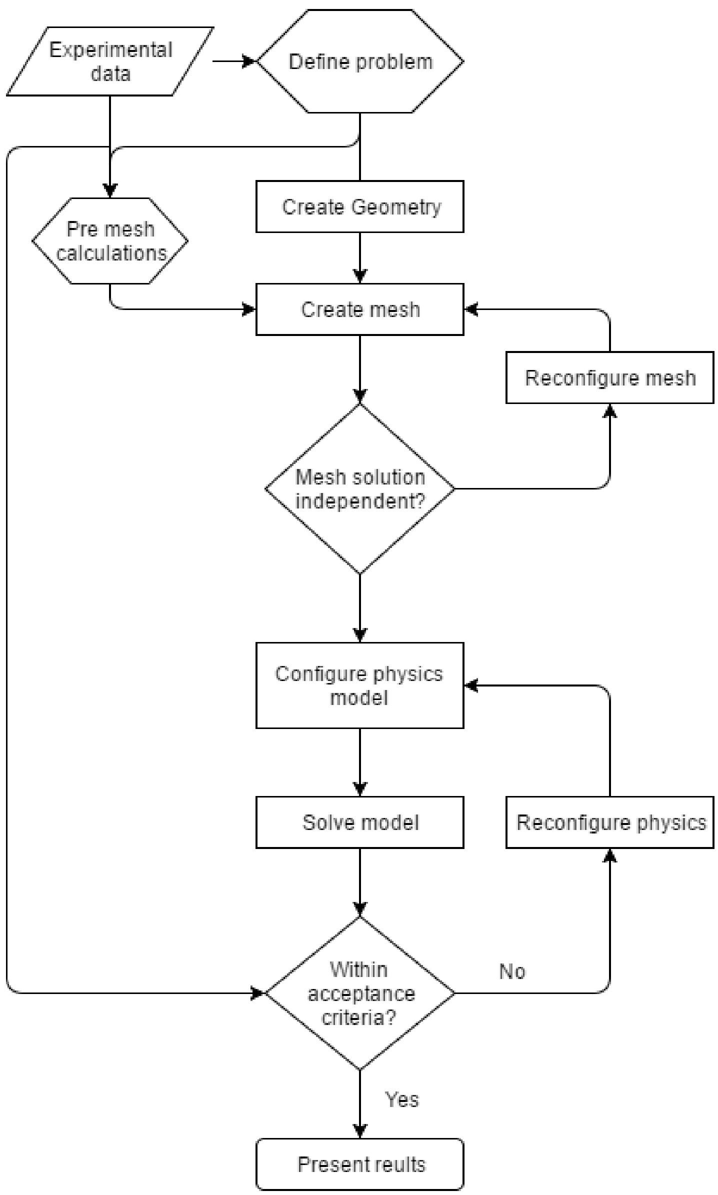

Figure 22 - Numerical simulation process

5.1 Problem definition

Simulations based on the experiment setup described in chapter 3 with the geometry displayed in Figure 22 can be summed up in the following manner:

- Liquid-liquid displacement in a u-shaped pipe geometry.
- Multiphase, with oil and water.
- Four different displacement velocities, ranging between 4 and 30 m3/h.
- Measured values include pressure, temperature and velocity.

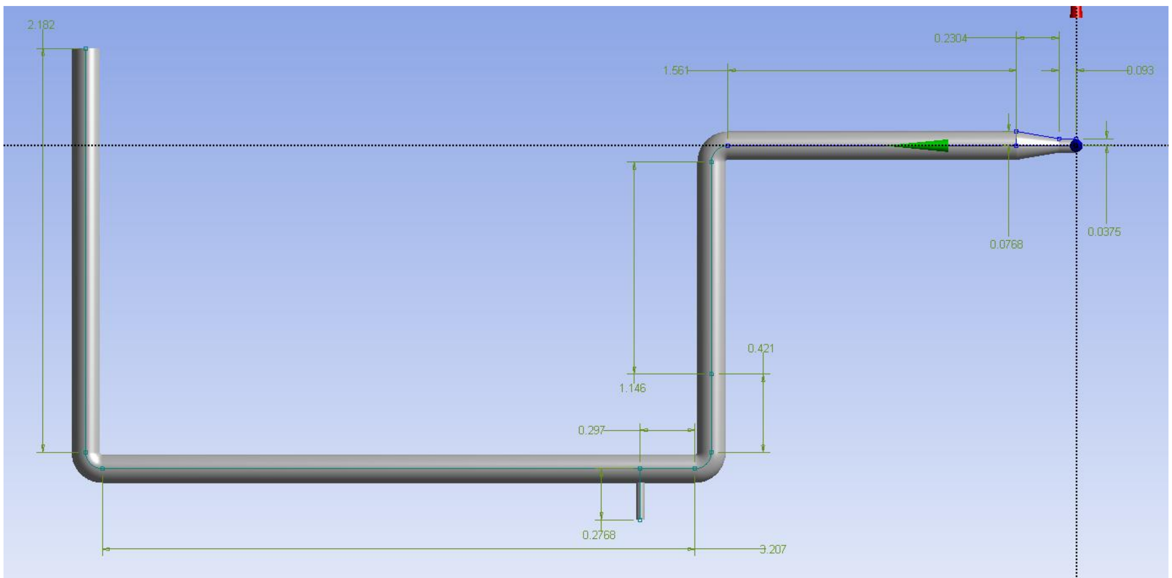

Figure 23 – Pipe geometry with dimensions

As the problem at hand includes two different liquids, a multiphase model has to be applied. Experimental results indicate that the interface between the liquids is inconsistently clear and that they travel with different velocities. This indicates that there is slip between the two liquids, making it an inhomogeneous multiphase flow.

Calculations are required in order to determine if the flow is turbulent or not, before modeling and meshing the domain. With internal flow in pipes, ANSYS recommends using a turbulence model if the Reynolds number is above 1000 (Ansys, 2015). Based on calculated values in Figure 24, the flow will be turbulent for all cases. To model the turbulence, Shear Stress Transport (SST) model was used in combination with an automatic wall function. SST captures the boundary layer and near wall flow with high accuracy, but requires a fine mesh and is therefore computationally expensive.

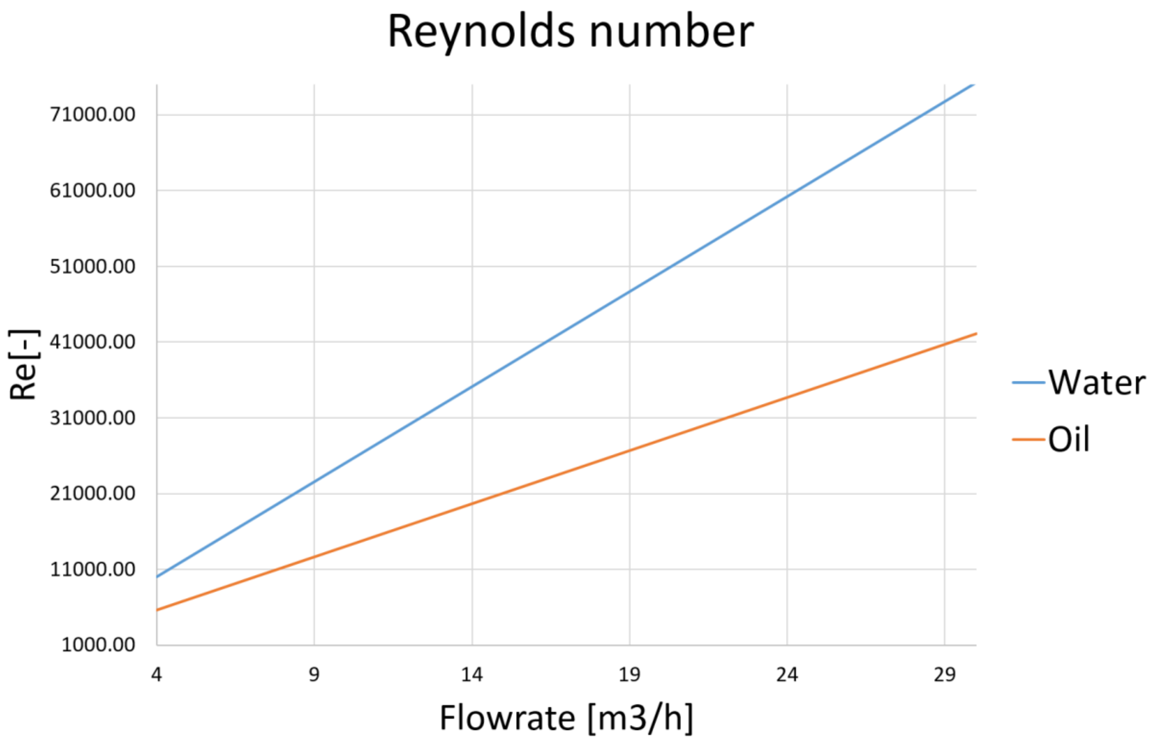

Figure 24 - Reynolds number for flowrates used

5.2 Geometry

The displacement domain for the simulations was developed using the computer aided design (CAD) software ANSYS Geometry. The reason for using this specific software, is that it has great integration with the rest of the ANSYS product family. Two different CADs was developed, described in detail in the next sub chapters.

5.2.1 Case 1

Case 1 of the jumper has a complex inlet; with two transitions reducing the pipe size from 160mm OD to 75mm OD. In order to reduce the mesh complexity and thereby the simulation time, it was decided to simplify the design, while keeping the domain volume constant. Changes to the inlet geometry can be seen in Figure 25 below, with the experimental design to the left and the one used in the simulations to the right. The whole jumper geometry can be seen in Figure 26, along with the dimensions.

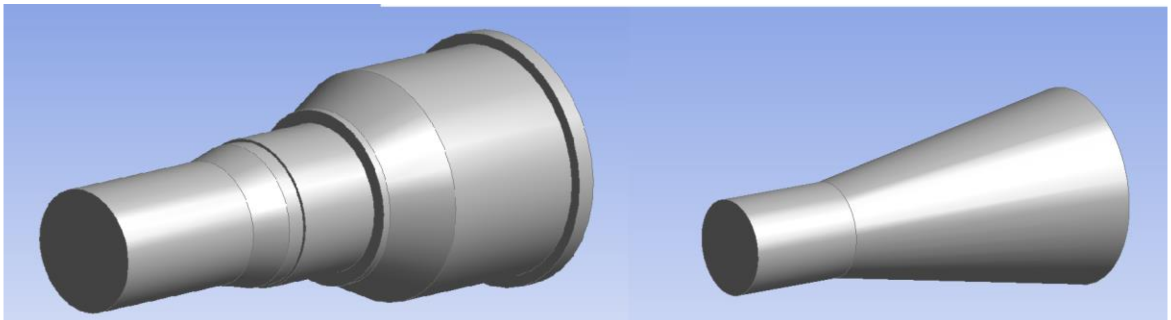

Figure 25 - Simplification of inlet

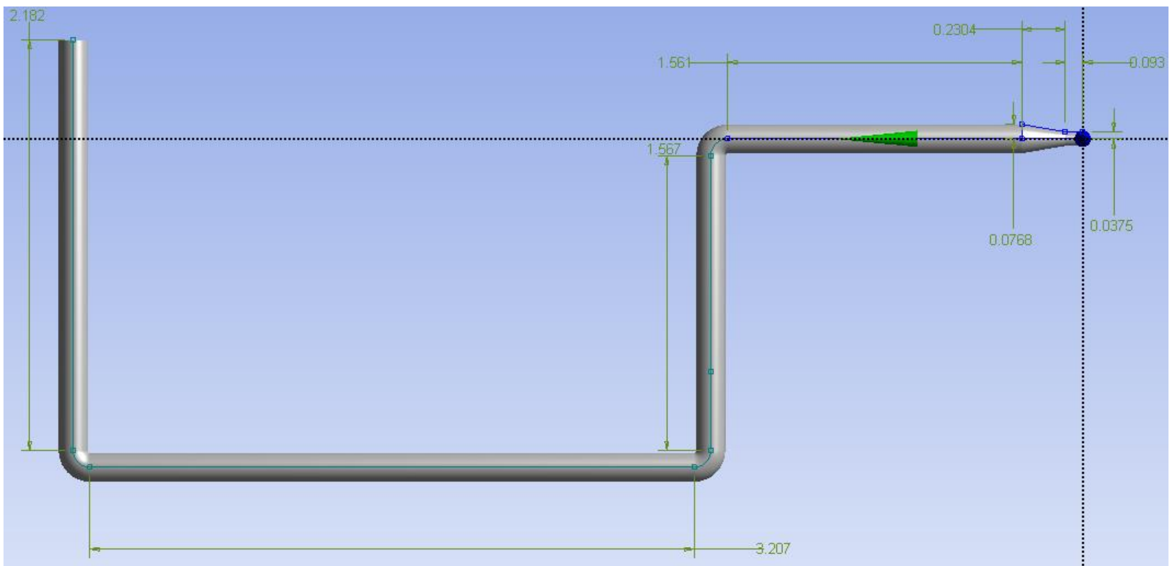

Figure 26 - Full jumper design with units in meters

5.2.2 Case 2

Case 2 of the jumper has an inlet at the bottom, close to the first vertical pipe. The top section of the first vertical pipe was removed, in order to create a dead-leg to the left of the inlet. Jumper design and dimensions can be seen in Figure 27 below.

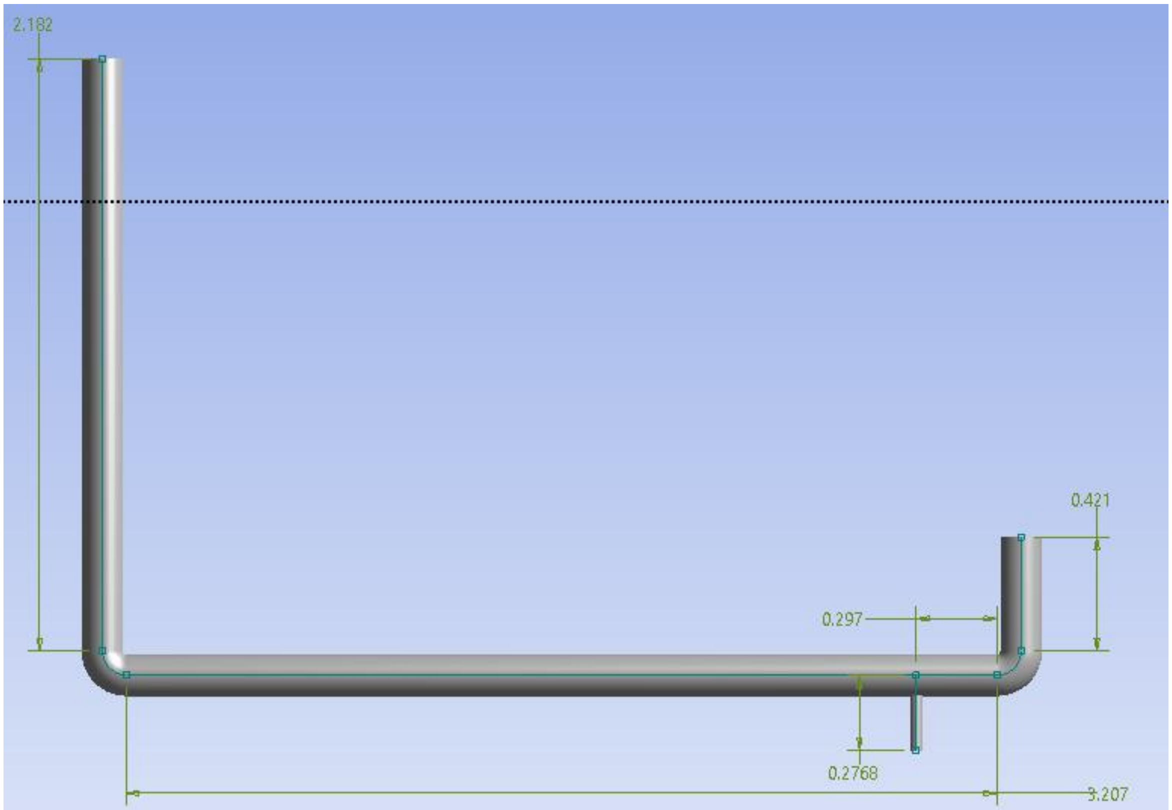

Figure 27 - Reduced jumper geometry with units in meters

5.3 Meshing of domain

Generation of the meshes for the displacement domain was done using ANSYS ICEM CFD. The mesh type selected was unstructured mesh, as this is a required input type by ANSYS CFX and computationally lighter then structured meshes. To limit the number of elements in the mesh, hexahedral elements was selected, as they allow for a high aspect ratio in the flow direction with a high accuracy. An o-grid was placed in the middle of the pipe to increase the mesh quality. To keep the results as consistence as possible, an individual mesh was generated for each displacement case.

5.3.1 Pre mesh calculations

Pre-mesh calculations are done to give some guidelines for creation of the mesh and are dictated by the models applied in the simulations. Although they offer some guidelines, they are not the final settings and the parameters have to be tune with simulations. The selected turbulence model is SST with an automatic wall function, which comes with some requirements for the mesh. The dimensionless wall distance, y^+, should be kept between 20-200 and there should be between 10 and 15 nodes within the boundary layer.

With requirements of the mesh known, the distance between the wall and the first mesh node can be calculated using Equation 9, with a target y^+ of 20. Calculated wall spacing for different pipe dimensions used and flowrates for oil and water can be seen in Table 14 and Table 15.

Equation 4 - Calculation of Reynolds number

$$Re = \frac{\rho * U * D_h}{\mu}$$

Equation 5 – Calculation of skin friction coefficient (empirical estimate)

$$C_f = 0.079 * Re^{-0.25}, for\ internal\ flow$$

Equation 6 - Calculation of wall shear stress

$$\tau_w = \frac{1}{2} * C_f * \rho * U^2$$

Equation 7 - Calculation of friction velocity

$$U_\tau = \sqrt{\frac{\tau_w}{\rho}}$$

Equation 8 – Calculation of y^+

$$y^+ = \frac{\rho * U_\tau * \Delta y_1}{\mu}$$

Equation 9 – Calculation of first cell height

$$\Delta y_1 = \frac{y^+ * \mu}{\rho * U_\tau}$$

Table 14 - dy [m] values for water

Flowrate	6 inch pipe	3 inch pipe	2 inch pipe
4	0.00474348	0.00112797	0.00050273
6	0.003326727	0.000791075	0.000352578
8	0.002586401	0.00061503	0.000274115
10	0.002127647	0.000505941	0.000225495
20	0.001160108	0.000275866	-
30	0.000813614	0.000193472	-

Table 15 - dy [m] values for oil

Flowrate	6 inch pipe	3 inch pipe	2 inch pipe
4	0.008089013	0.001923518	0.000857301
6	0.005673038	0.001349014	0.000601248
8	0.004410566	0.001048805	0.000467447
10	0.003628257	0.000862777	0.000384535
20	0.001978321	0.000470433	
30	0.001387449	0.000329927	

To accommodate for the requirement of minimum 10 nodes in the boundary layer of the flow, calculations regarding the thickness of the boundary layer is required and calculated by Equation 10. Initial placement of the o-grid can be calculated using Equation 11, based on results obtained from boundary layer thickness calculations. It was decided to use 15 nodes between the wall and the o-grid, to achieve maximum accuracy. Calculated o-grid spacing can be seen in Table 16 and Table 17.

Equation 10 – Calculation of boundary layer thickness

$$\delta = 0.035 * D * Re^{-\frac{1}{7}}$$

Equation 11 – Calculation of o-grid spacing

$$n(15) - n(1) \leq \delta$$

Table 16 - Node 15 placement for water in meters from the wall

Flowrate [m3/h]	6 inch pipe	3 inch pipe	2 inch pipe
4	6.18E-03	1.73E-03	8.68E-04
6	4.68E-03	1.36E-03	6.97E-04
8	3.89E-03	1.16E-03	6.05E-04
10	3.39E-03	1.03E-03	5.46E-04
20	2.30E-03	7.51E-04	
30	1.89E-03	6.42E-04	

Table 17 - Node 15 placement for oil in meters from the wall

Flowrate [m3/h]	6 inch pipe	3 inch pipe	2 inch pipe
4	9.65E-03	2.58E-03	1.26E-03
6	7.15E-03	1.96E-03	9.77E-04
8	5.83E-03	1.64E-03	8.29E-04
10	5.00E-03	1.44E-03	7.34E-04
20	3.22E-03	9.89E-04	
30	2.56E-03	8.19E-04	

5.4.2 Tuning of mesh parameters

Prior to the pre-mesh calculations, a simple straight pipe was created in ICEM CFD to vertify the calculated values. ICEM CFD was coupled to ANSYS workbench and ANSYS CFX, so the dimension could be adjusted using input parameters. A simple ICEM script file was created, to generate the mesh based on parameters such as pipe length, pipe diameter, o-grid spacing, dy value and number of nodes in all directions. A snapshot displaying the workbench integration is presented in Figure 28, and the project-file in the digital attachments (StraightPipeCalibration.wbpz).

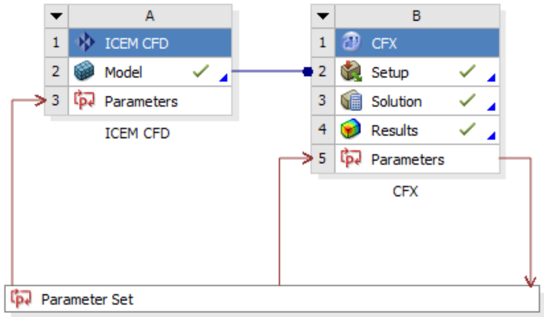

	A	B	C	D
1	ID	Parameter Name	Value	Unit
2	Input Parameters			
3	ICEM CFD (A1)			
4	P3	WallNodes	15	
5	P4	OgridNodes	10	
6	P5	dyvalue	0.00081361	
7	P6	OgridSpacing	0.0018898	
8	P7	znodes	169	
9	P8	Radius	0.0768	
10	P9	Length	1.6896	
11	CFX (B1)			
12	P10	InletVelocity	0.44972	
*	New input parameter	New name	New expression	
14	Output Parameters			
15	CFX (B1)			
16	P11	Ypluss	9.9194	
*	New output parameter		New expression	
18	Charts			

Figure 28 - Workbench integration and parameter adjustment window

Three cases were created, 6”-, 3”- and 2”-pipe with a length of 11xD_h. A length of 11xD_h was selected, as it -takes 10xD_h before a turbulent flow stabilizes and the extra 1xD_h would ensure stabilized flow. All simulations were run with 1 node per cm in Z-direction and an o-grid with 10x10 nodes. CFX was run as steady-state single phase simulation, with SST-turbulence model, max iterations of 1000, residual RMS of 1E-04 and conservation target of 0.01.

First the o-grid was adjusted, to ensure that the whole boundary layer is in a cell parallel to the wall. The number of nodes in the boundary layer was check by plotting the eddy viscosity ratio along the pipe and counting nodes manually. Eddy viscosity ratio was calculated with Equation 12 and give the ratio between the turbulent viscosity and molecular dynamic viscosity. As seen in Figure 29, the automatic wall function resolves the boundary layer successfully, without any turbulence near the wall. As a finale quality check, the boundary layer was inspected at the outlet, by plotting the outlet velocity from 99%-100% of the freestream velocity. Pictures of the eddy viscosity ratio and outlet were extracted by running CFD-POST in batch mode in combination with a CEL script.

Equation 12 – Calculation of eddy viscosity ratio

$$Eddy\ Viscosity\ Ratio = \frac{Eddy\ Viscosity}{Dynamic\ Viscosity}$$

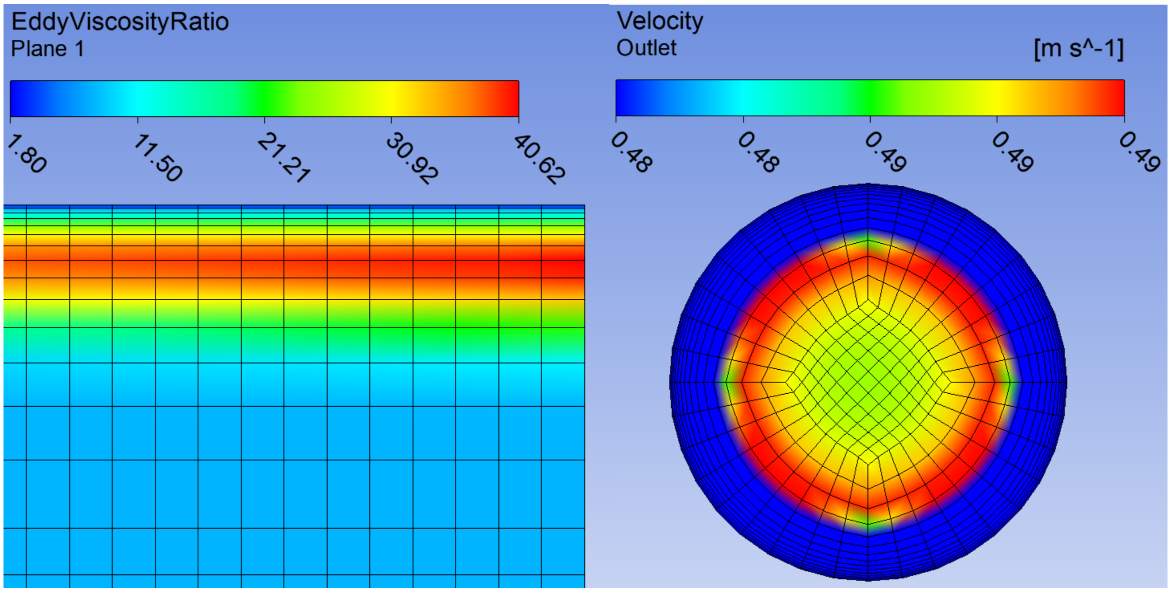

Figure 29 - Eddy viscosity ratio and 99%-100% of max velocity

After the o-grids spacing had been set, the first cell spacing was adjusted in order to achieve a y^+ value that is greater than or equal to 20. The results of the mesh tuning calibrations is listed in Table 18 below.

Table 18 - Derived mesh parameters

Flowrate	**6" pipe**			**3" pipe**			**2" pipe**		
	OgridSpacing [m]	**dy [m]**	**Y^+**	**OgridSpacing [m]**	**dy [m]**	**Y^+**	**OgridSpacing [m]**	**dy [m]**	**Y^+**
30	0.034	0.01522	20.939	0.022	0.0085	20.6381			
20	0.038	0.022	20.1126	0.022	0.012	20.0751			
10	0.042	0.045	20.3335	0.025	0.0248	20.8337	0.02	0.018	20.1183
8	0.042	0.055	20.0863	0.027	0.03	20.5989	0.02	0.0225	20.3876
6	0.042	0.074	20.2877	0.028	0.04	20.6499	0.02	0.03	20.6994
4	0.055	0.3	20.4961	0.03	0.061	20.8245	0.02	0.043	20.3451

As a finale step to making the mesh solution independent, the number of nodes along the pipe and inside the o-gird was calibrated. This was done by adding a bend and a vertical section to the end of the previously described pipe, and adjusting the number of nodes. Differential pressure and velocity in the straight sections and bend was used as mesh independence measurements. A course mesh was set as a baseline, with 0.5 nodes per cm along the pipe and 6x6 nodes inside the o-grid. The number of nodes was increased gradually until the convergence criteria were met. The convergence criteria were set to 1%, meaning that once the change in pressure and velocity decreased below 1%, the mesh was considered solution independent. The geometry used can be seen in Figure 30 below, with calibrated mesh parameters in Table 22. Results from the simulation can be found in Table 19 through Table 21. The workbench file used in the mesh independence study can be found in the digital appendix, named “CalibrationWithBend.wbpz”.

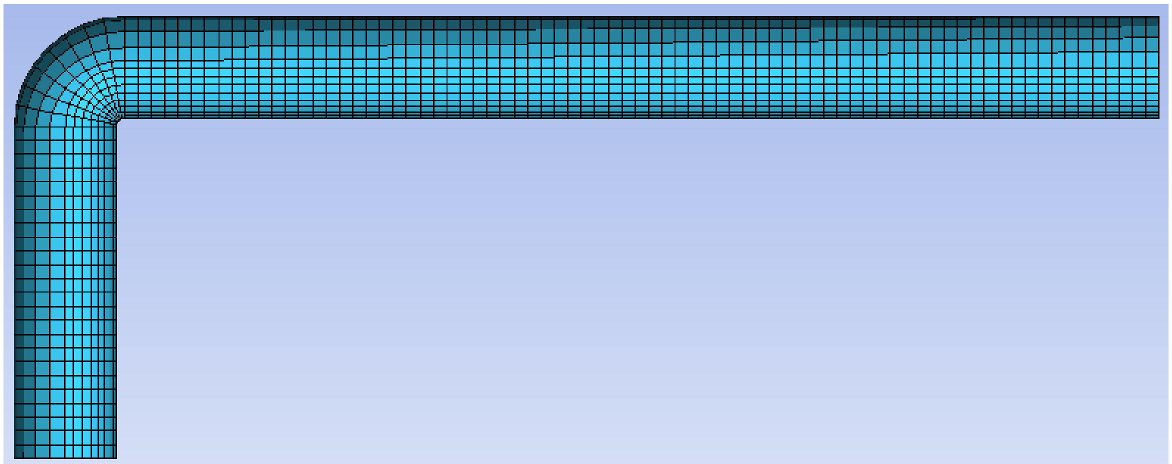

Figure 30 - Mesh independence study geometry

Table 19 - Mesh independence results inside o-grid

Nodes inside o-grid	dp Inlet [Pa]	Error [%]	dv Inlet [m s^-1]	Error [%]
6x6	36.6032	0.00	-0.0145171	0.00
10x10	36.3277	0.75	-0.0143499	1.15
15x15	36.2426	0.23	-0.0142707	0.55
20x20	36.2138	0.08	-0.0142505	0.14

Table 20 - Mesh independence results along pipe

Nodes straight [Nodes per cm]	dp Inlet [Pa]	Error [%]	dv Inlet [m s^-1]	Error [%]
0.50	36.8814	0.00	-0.0142973	0.00
1.00	37.9465	-2.89	-0.0155118	-8.49
1.50	38.1648	-0.58	-0.0157129	-1.30
2.00	38.2321	-0.18	-0.0157499	-0.24

Table 21 - Mesh independence results for bends

Nodes Bends [Nodes per cm]	dp Bend [Pa]	Error [%]	dv Bend [m s^-1]	Error [%]
1	36.3277	0	-0.0143499	0
2	37.3654	-2.9	-0.0149864	-4.4
3	37.9254	-1.5	-0.0155075	-3.5
4	38.1648	-0.6	-0.0157129	-1.3
5	38.3081	-0.4	-0.0158096	-0.6

Table 22 - Tuned mesh parameters

Location	Number of nodes
Inside o-grid	10x10
Straight pipe	1.5 per cm
Bend	4 per cm

5.4.3 Meshing of geometry

Once the mesh parameters had been calculated and tuned, meshes for the two geometries was created with the same approach as described in the mesh tuning chapter. The derived mesh parameters was applied to the meshes, followed by a finale quality check verifying that the mesh met the mesh quality recommendation found in appendix B (Ansys, 2015)

Due to the complex inlet geometry for case two, were a 2” pipe meets a 6” pipe to form a T, the number of nodes inside the o-gird had to be increased to 15x15 in order to meet the mesh quality requirements. Mesh smoothing was applied to increase the overall quality of the mesh. Finally, a transient simulation was done with oil and water to verify that the resolution of the mesh was good enough to be able to visually inspect the flow pattern. A picture of multiphase flow for both geometries can be seem in Figure 31 and Figure 32.

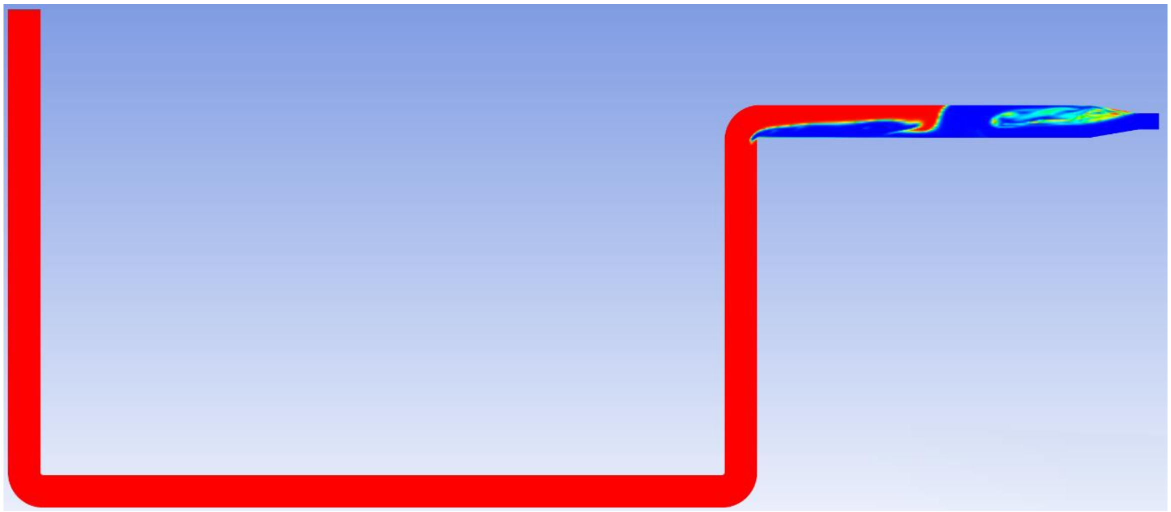

Figure 31 – Water-oil displacement of geometry one

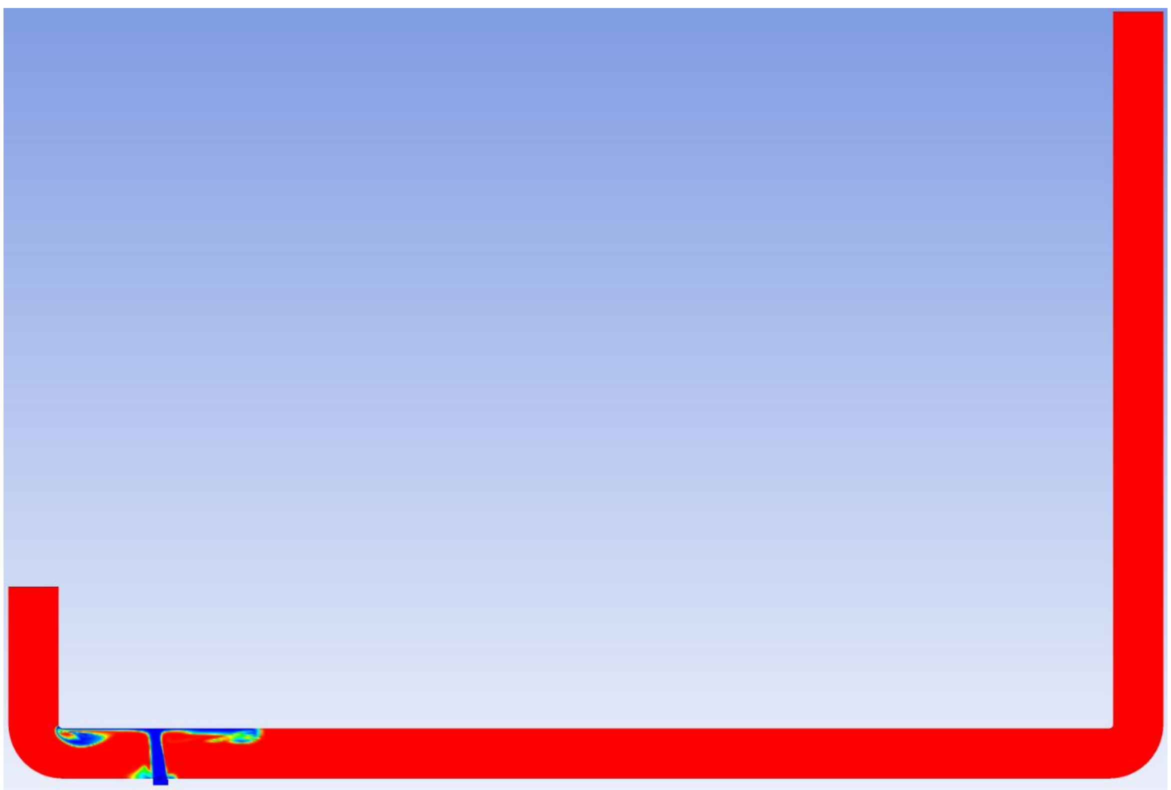

Figure 32 – Water-oil displacement of geometry two

5.4 CFX-pre setup

The physics model in CFX-pre was configured to be representative of the displacement experiment, using Navier-Stokes equation with additional equations for turbulence and multiphase. The models are applied to the domain inside the mesh and solved by Finite Volume Method (FVM).

Additionally, as the simulations are transient, the total time and time steps had to be configured. The total time of the simulations were set according to the required time to displace the jumper volume three times with the given inlet velocity. Adaptive time steps were selected, with relation to the number of coefficient loops. The solver then adjusts the time step to reach the target number of coefficient loops, between 3 and 5 respectively.

After the analysis type had been configured, the boundaries of the mesh could be configured. To make the solution as robust as possible, the inlet was set to velocity inlet, outlet to pressure outlet with an average static pressure of 1 atm and smooth wall for the pipe (Baukal, 2013). At the inlet, the displacement liquid volume fraction was set to 1 and trapped liquid to 0. In the default domain a buoyancy model was added to model gravity, with reference buoyancy density determined by the least dense liquid. Shear Stress Transport model with automatic wall function was used to model turbulence. Both of the liquids were set to continues, as they would be in the start of the displacement procedure. Two different multiphase models were test, inhomogeneous mixture model and homogenous free surface model.

For the solver control, the advection scheme was set to high resolution, with a second order backward Euler transient scheme and high resolution turbulence numerics. Minimum coefficient loops was set to two, in order to reduce the residuals in the domain and 50 as maximum to ensure convergence for the first time steps. As convergence criteria, residuals should be less than 1e-05, calculated by root mean square, and the conservation target less than 0.01 to ensure domain balance.

A transient file was written every 0.1 seconds of the simulations, with information about density, turbulence kinetic energy, velocity and volume fraction of oil and water. Monitor points were added to the domain, so that the volume fraction could be monitored throughout the solver run. A complete CEL script for the different simulation setups is presented in appendix C for homogenous multiphase model and appendix D for inhomogeneous multiphase model.

5.5 Solver setup

As the domain contains a large number of elements and therefore requires large amounts of computational power, the solver was ran on a high performance computer cluster. The cluster selected, Maur, runs Linux with a SLURM batch server. However, SLURM is not officially supported by ANSYS and hence, several steps needed to be taken in order to run the simulations on the cluster. A complete guide for running CFX5SOLVE with SLURM can be found in appendix E, with job scripts for local parallel in appendix F and distributed parallel in appendix G.

As the number of computer nodes on the cluster is reasonably low, only 21, and shared with fellow students at IPT, only two computer nodes was used for case one and four for case two. The number of mesh partitions was set to a maximum of 20 per node, as the nodes consist of two CPUs with ten cores each. NetDisk2 was used to mount the Linux cluster remotely, so that the simulations could be monitored in real time from a third party Windows based computer.

6 Simulation results

Obtained results from the numerical simulations are reported at discrete times with measurements of remaining initial liquid in the domain. The Results from each case was extracted using a PERL enchanted CEL script for CFD-Post. The script was ran with CFD-Post in batch mode locally on the cluster, in order to avoid exporting transient result files onto a local computer for further post processing. The CFD-post script can be found in appendix I, with a job script for running CFD-Post in batch mode in appendix H. An overview of the simulation cases is listed in Figure 33, some cases did not finish in time due to time and computational power limitations.

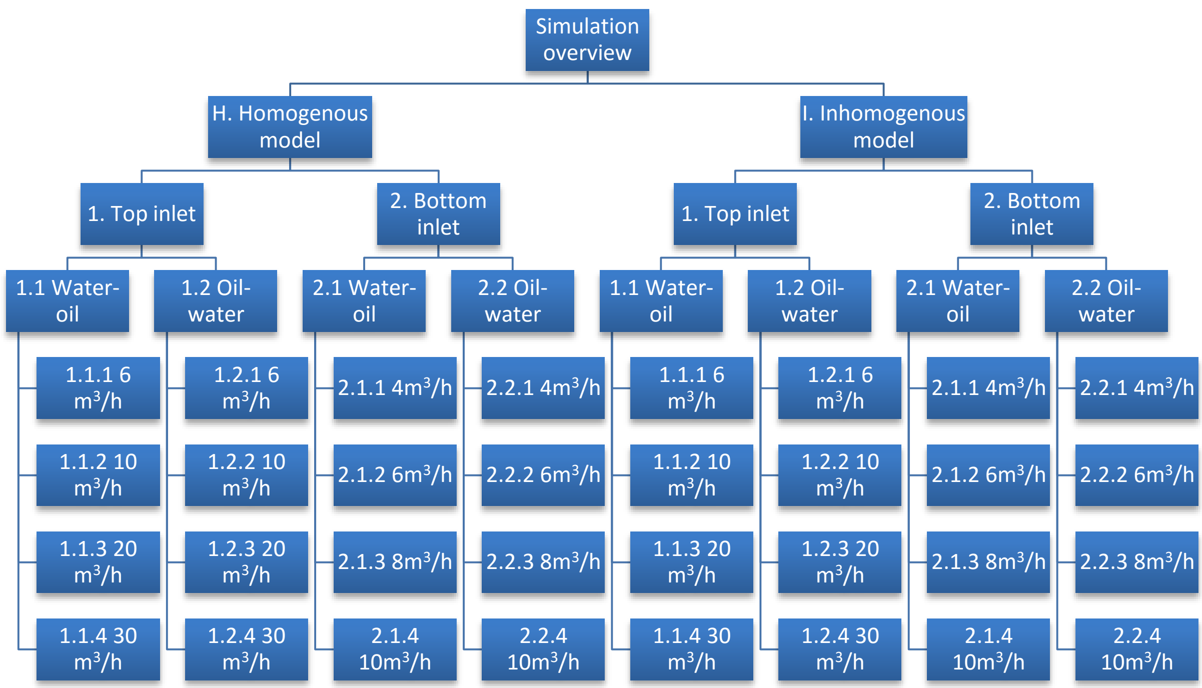

Figure 33 – Overview of simulated cases

Detailed results are presented in subchapter 5.1 through 5.4, and will be further discussed in chapter 7, along with a comparison to the experimental results to see which multiphase model that fits best. .Out, .res, .def, liquid hold-up vs time and transient files for one, two and three displacement volumes can be found in the digital appendix.

The sub-chapters includes measured liquid hold-up for one, two and three displacement volumes, and are displayed in tables along with the superficial displacement velocity, front velocity and height. Front velocity was calculated by measuring the time the front uses between two planes on the second riser in the U, seen to the left in Figure 34. Once the area average displacement liquid volume fraction exceeded 0.5 on the plane the clock was started and later stopped once the same conditions were reached on the second plane. The height of the displacement front was measured 0.03m from the second vertical section, when the area average volume fraction reached 50% at the first cut plane measurements were taken. The height, h, was calculated using Equation 13 and Equation 14.

Equation 13 – Calculation of circle segment angle

$$A = \frac{R^2}{2}(\theta - \sin(\theta))$$

Equation 14 – Calculation of displacement front height based on covered area

$$h = R\left(1 - \cos\left(\frac{\theta}{2}\right)\right)$$

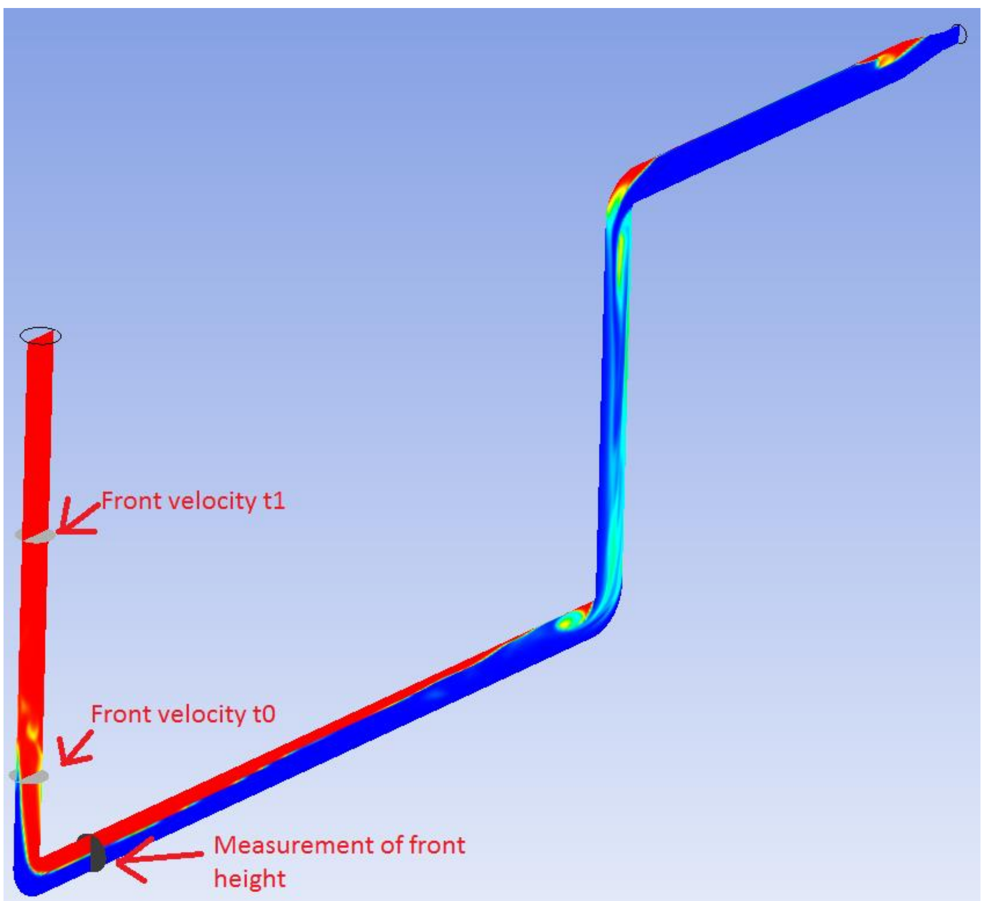

Figure 34 – Measurement points on the geometry

6.1 Homogenous free surface model

6.1.1 Displacement 1 - Water displacing oil through the top inlet

Experiment Number	Displacement rate [m^3/h]	Remaining Oil - Displacement Volumes			Front velocity [m/s]	Front height [m]
		1 volume [liter]	2 volumes [liter]	3 volumes [liter]		
H.1.1.1	6	30.2753	19.2909	15.8602	0.062892686	0.124127191
H.1.1.2	10	25.011	10.155	5.812	0.109851481	0.087268589
H.1.1.3	20	13.7094	5.28135	3.36094	0.232660943	0.069152943
H.1.1.4	30	7.57074	1.22245	7.28E-02	0.314594016	0.069625998

6.1.2 Displacement 2 - Oil displacing water through the top inlet

Experiment Number	Displacement rate [m^3/h]	Remaining Water - Displacement Volumes			Front velocity [m/s]	Front height [m]
		1 volume [liter]	2 volumes [liter]	3 volumes [liter]		
H.1.2.1	6	44.2115	27.3795	22.894	0.019304199	0.042155253
H.1.2.2	10	25.9595	14.2827			
H.1.2.3	20	22.1145	6.02906	3.69876	0.133344001	0.149940333
H.1.2.4	30	14.9967	1.5148	0.327285	0.328904092	0.146053762

6.1.3 Displacement 3 - Water displacing oil through the bottom inlet

Experiment Number	Displacement rate [m^3/h]	Remaining Oil - Displacement Volumes			Front velocity [m/s]	Front height [m]
		1 volume [liter]	2 volumes [liter]	3 volumes [liter]		
H.2.1.1	4	11.496	8.76634	8.3499	0.048313847	0.129692997
H.2.1.2	6	12.9058	8.50332	-	-	-
H.2.1.3	8	15.0362	7.86454	-	-	-
H.2.1.4	10	15.791	7.88181	6.22574	0.120452903	0.103764724

6.1.4 Displacement 4 - Oil displacing water through the bottom inlet

Experiment Number	Displacement rate [m^3/h]	Remaining Water - Displacement Volumes			Front velocity [m/s]	Front height [m]
		1 volume [liter]	2 volumes [liter]	3 volumes [liter]		
H.2.2.1	4	57.791	46.1922	-	-	-
H.2.2.2	6	47.798	31.3763	25.1245	0.0257078	0.06603469
H.2.2.3	8	41.9077	24.0319	18.5711	0.045254398	0.075825467
H.2.2.4	10	36.366	17.2527	12.6905	0.04524764	0.081012954

6.2 Inhomogeneous mixture model

6.2.1 Displacement 1 - Water displacing oil through the top inlet

Experiment Number	Displacement rate [m^3/h]	Remaining Oil - Displacement Volumes			Front velocity [m/s]	Front height [m]
		1 volume [liter]	2 volumes [liter]	3 volumes [liter]		
I.1.1.1	6	-	-	-	-	-
I.1.1.2	10	33.072	-	-	-	-
I.1.1.3	20	18.1216	9.72943	4.71277	0.217438574	0.066402888
I.1.1.4	30	9.35697	4.70204	3.71694	0.312910695	0.072817688

6.2.2 Displacement 2 - Oil displacing water through the top inlet

Experiment Number	Displacement rate [m^3/h]	Remaining Water - Displacement Volumes			Front velocity [m/s]	Front height [m]
		1 volume [liter]	2 volumes [liter]	3 volumes [liter]		
I.1.2.1	6	47.456	41.8382	35.3106	-	-
I.1.2.2	10	33.365	20.4595	-	-	-
I.1.2.3	20	23.0588	12.5193	4.23345	0.152868683	0.149940333
I.1.2.4	30	15.955	3.65947	2.18474	0.166694449	0.152868683

6.2.3 Displacement 3 - Water displacing oil through the bottom inlet

Experiment Number	Displacement rate [m^3/h]	Remaining Oil - Displacement Volumes			Front velocity [m/s]	Front height [m]
		1 volume [liter]	2 volumes [liter]	3 volumes [liter]		
I.2.1.1	4	11.6826	9.23599	-	-	-
I.2.1.2	6	10.532	-	-	-	-
I.2.1.3	8	15.1041	9.08405	7.65567	0.090933891	0.107033291
I.2.1.4	10	15.8124	7.29383	6.18627	0.12047467	0.103580572

6.2.4 Displacement 4 - Oil displacing water through the bottom inlet

Experiment Number	Displacement rate [m^3/h]	Remaining Water - Displacement Volumes			Front velocity [m/s]	Front height [m]
		1 volume [liter]	2 volumes [liter]	3 volumes [liter]		
I.2.2.1	4	60.429	59.4937	59.4667	-	-
I.2.2.2	6	46.9701	38.4873	35.286	0.021833966	0.06267195
I.2.2.3	8	40.5142	32.4405	28.7214	0.07939596	0.07088546
I.2.2.4	10	48.3784	41.6566	39.496	-	-

7 Discussion

In this chapter, results obtained through the experiments and numerical simulations will be discussed and compared. Firstly, the potential error sources from the experiment will be highlighted, in order to set baseline for comparison with numerical simulations. Thereafter, liquid hold-up, displacement front height and velocity will be discussed. Finally, the accuracy of the multiphase models and how they fit with the experimental results for different velocities will be discussed.

7.1 Error sources during experiment

There are several parameters that can influence the accuracy of experiment and thereby influence the results. Some of the main concerns include:

- Reliability of sensor calibration
- Pump flow variation
- Separation of the liquids
- Wall wetting
- Human errors during measurement of liquid hold-up
- Pressure buildup at outlet

The sensors were calibrated before conducting the experiment. However, with a lot of parallel work in the experimental hall, signal noise is a concern to considerate. Although signal noise should be low due to shielded wiring, it could possibly introduce errors. Furthermore, human errors during calibration are potentially an even greater source of error. This might especially regard the flowmeter, which is possibly the most critical instrument used in the experiment. Although the flowmeter was calibrated by filling 50 liters into a tank and the accumulated flow tested three times for validation, some variation in accumulated flow was observed. However, only minor variations were observed. The largest error observed was a variation of 0.2 liters for the 50 liter test, introduction an error margin of 0.04 for the accumulated flow.

Additionally, some variation in the flowrate was observed during the experiments, typically +- 10 liters/min for steady-state conditions for the low-flow setup. Experience suggest that the source of the steady-state flow variation might be variation in pump speed. An inspection of the pumps was performed, which revealed worn rotor bearings due to use with mud and insufficient cleaning. The pump housing was therefore cleaned and the bearings re-greased, which caused somewhat improved performance.

Another concern relates to the separation of the oil and water, although the liquids are immiscible, there might be some oil bubbles in the water phase if an insufficient separation time is given. However, due to the quick separation time and the use of transparent pipe for visual inspection, this is considered as a minor issue. A bigger concern is that oil/water sticks to the pipe wall, this was observed in some of the transparent sections of the pipe during displacement, seen in Figure 35. For the bends it is not possible to visually inspect, however since they are made from the material as the transparent pipes (PVC), similar behavior should be expected. While draining the water/oil, the bubbles sticking to the wall were mostly captured on the surface of the drained liquid, limiting this margin. Nevertheless, as a safety measure, the volume was flushed with a high rate of the initial condition liquid before conducting new experiments to remove liquids at the wall.

Figure 35 - Bubbles on wall of vertical section (left) and horizontal section (right)

Measurements of the liquid hold-up were performed with a transparent measuring cup, at a tapping point controlled by a 3/8" ball valve. As the pipes located close to the tapping point is transparent, the flow could be reduced with the valve as the liquid of interest was getting close to the valve. If over-tapping occurred, this should be detected and measured by observing the scale on the measurement cup. As an error of margin, this issue is therefore negligible and should not influence the overall results.

A concern that should be tackled by the next user of the rig, is the pressure build up at the outlet of the jumper caused by the reduction from 160mm pipes to a 4" hose, unable to flow all the liquid exiting the domain. However, this was only observed for the two highest flowrates, 20- and 30-m^3/h. Review of the data log showed a pressure build-up of 0.5 barg, which is within the pressure rating of the pipes and is therefore safe. Although this problem lead to accumulation of liquid in the horizontal section at the outlet, no flow-back of liquid into the domain was observed once the pump was stopped. This issue can be seen in Figure 36, with oil accumulating at the outlet during water-oil displacement with a flowrate of 30 m^3/h.

Figure 36 – Accumulation of oil at the outlet

7.2 Experimental results

In the following subchapters the experimental results will be discussed, focusing on the liquid hold-up, displacement front and flow pattern for the four different displacement cases.

7.2.1 Water-oil displacement bottom inlet

During the water-oil displacement, the buoyance effect was clear and made major impacts on the results for displacement of the reduced jumper. With the tested displacement rates, water was unable to displace the oil in the dead-leg, yet most of the oil located on the right side of the inlet was displaced. From the results displayed in Figure 37, it is clear that the displacement velocity did not play a key role on the total displaced volume after three displacement volumes. All of the experiments lead towards the same results, with a variation of just 1.04 liters.

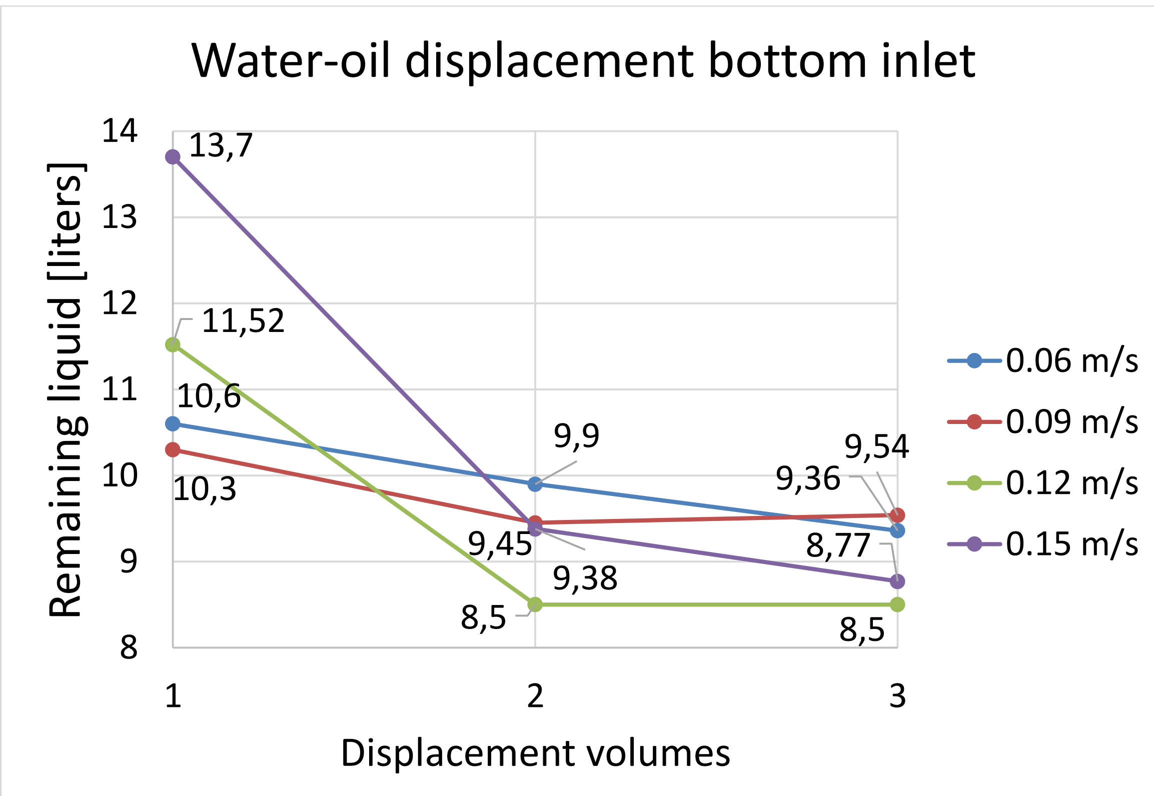

Figure 37 – Plotted water-oil displacement through bottom inlet results

7.2.1.1 Liquid hold up

Our results indicate limited variation of the hold-up with displacement rates. Most surprisingly, the two lowest displacement rate gave a better displacement efficiency than the two high rates for one jumper volume of displacement. With the highest rate, 10 m^3/h, water had problems displacing liquid to the left of the inlet in the start of the experiment. This was due to a powerful jet going from the inlet to the top of the pipe, trapping the liquid to the left as seen in Figure 38. Later, the turbulence caused the oil to spin and the water was able to displace it as bubbles.

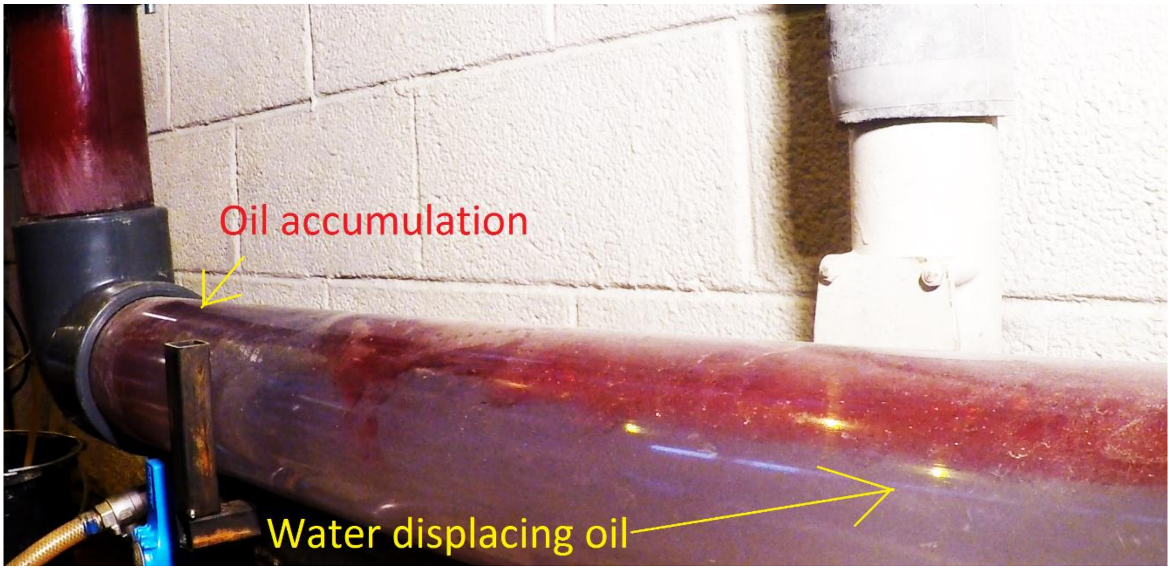

Figure 38 - 10 m^3/h water-oil displacement at bottom inlet

As the volume of the vertical section of the dead-leg is 7.8 liters (not including the pars of the bend exceeding the horizontal section) and the whole volume is 113.18 liters, water was able to displace most of the jumper by one jumper volume of accumulated flow.

7.2.1.2 Displacement front

By water-oil displacement, the water established itself by filling the lower horizontal section first, with oil occupying the top 0.04m of the pipe as seen in Figure 39. Water with low velocity had problems displacing the oil at the top of the pipe, due to drag introduced by wall and displacement of the small oil drops at the wall shown to be more difficult than large droplets.

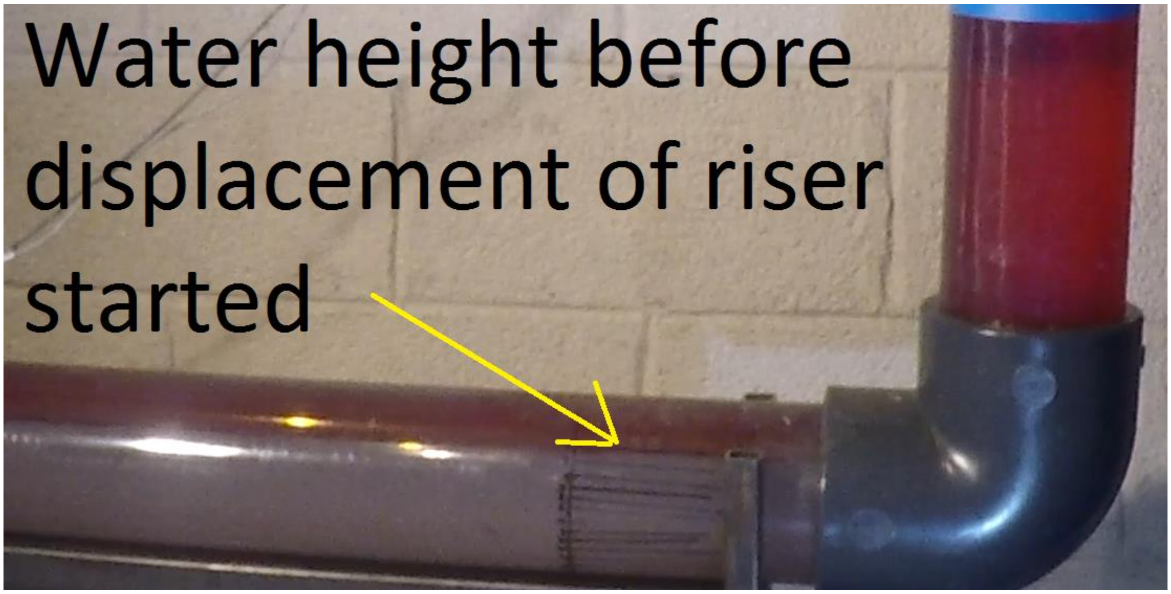

Figure 39 - Water-oil displacement front height for flowrate of 10 m^3/h

Oil was exclusively exiting the domain as the water established itself at the bottom section. Once the water was dominant in the horizontal section; displacement of the second vertical started. The vertical was displaced in one push, by a water column with oil bubbles from the oil layer in the bottom horizontal section, as seen in Figure 40. Once the oil in the vertical section was displaced, only droplets from the oil strip located at the bottom horizontal was observed exiting the domain.

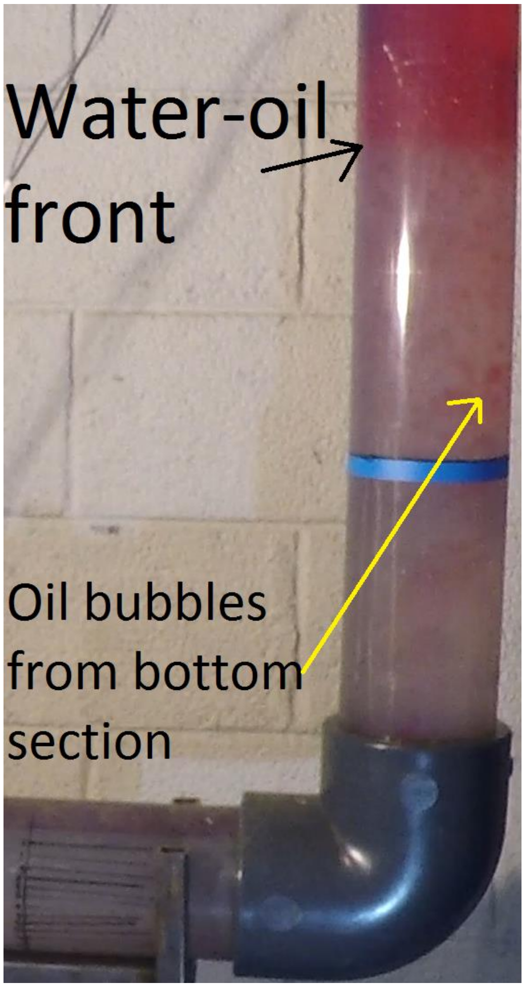

Figure 40 - Water-oil front in second riser with flowrate of 10m^3/h

7.2.2 Oil-water displacement bottom inlet

Oil-water displacement show a large dependency on the displacement rate, compared to the water-oil displacement. Oil was able to displace water to the left of the inlet and displacement of the dead-leg was achieved, probably due to buoyancy. A full displacement of the jumper was not observed with three jumper volumes. However, the results displayed in Figure 41 points towards a full displacement of water if a sufficient displacement time is given.

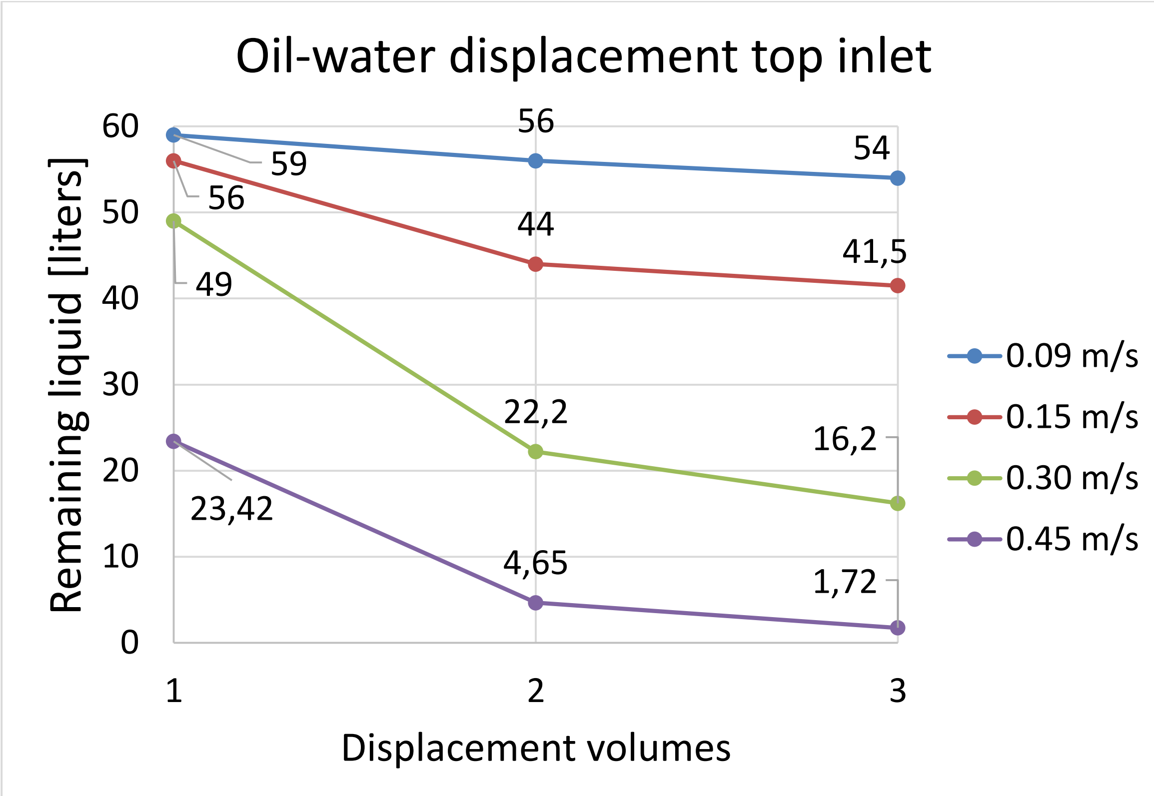

Figure 41 – Plotted oil-water displacement through bottom inlet results

7.2.2.1 Liquid hold up

The results presented here, indicate a large velocity dependence for the oil-water displacement. With the lowest rates 4 m^3/h, oil had problems displacing water throughout the domain, this could be seen by liquid exiting the domain was mainly consisting of oil. The oil used some time to establish itself in the domain and a clear interfaces between the liquid was observed in the dead-leg and the bottom horizontal section, seen in Figure 42.

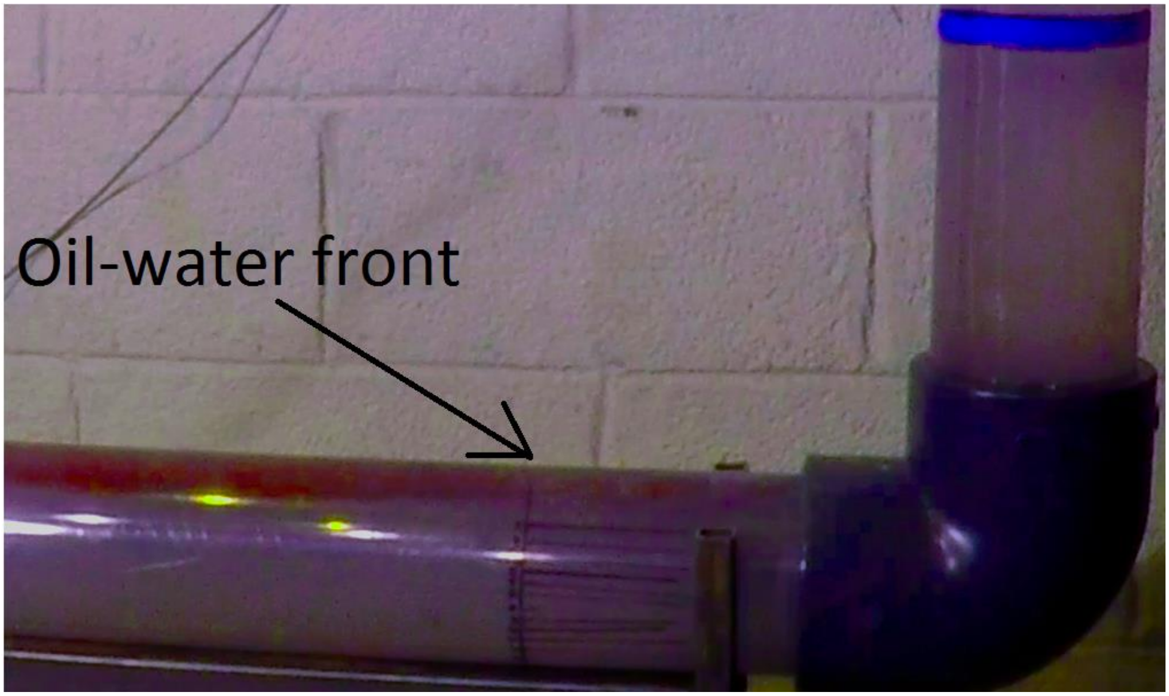

Figure 42- Oil-water displacement front reaching the second riser with 8m3/h flowrate

7.2.2.2 Displacement front

The oil established itself as a thin strip at the top of the bottom section as it entered the volume, with increasing displacement volumes the oil occupied more and more of the bottom section. The oil going to the left displaced water by natural buoyancy in the dead-leg, the water then moved towards the right underneath the established oil strip, creating a wavy interface, seen in Figure 43. High flowrates established itself much quicker than the low rates, but met resistance after one displacement volumes. After one displacement volumes, the displacement efficiency for high rates was reduced.

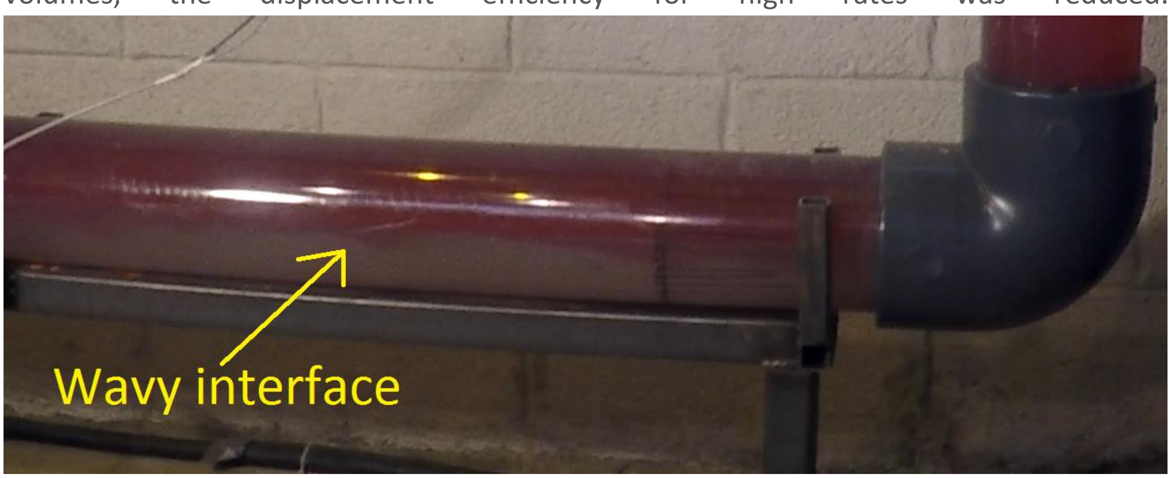

Figure 43 - Wavy interface between oil-water during displacement of dead-leg (8m^3/h)

In the second vertical section, no clear interface between the oil and water was observed. Once the oil reached the second riser, it accelerated and broke up into bubbles (left Figure 44) as it rose in the vertical section. This lead to a mixture of the two liquid, with formation of oil and water bubbles. After some time, with high rates, the mixture evolved from water dominant to oil dominant (right Figure 44), with small water bubbles exiting the domain. With the lowest rate, 4 m^3/h, the oil had problems establishing itself in the second riser as some of the oil bubbles were sinking down in the low pressure zones of the riser.

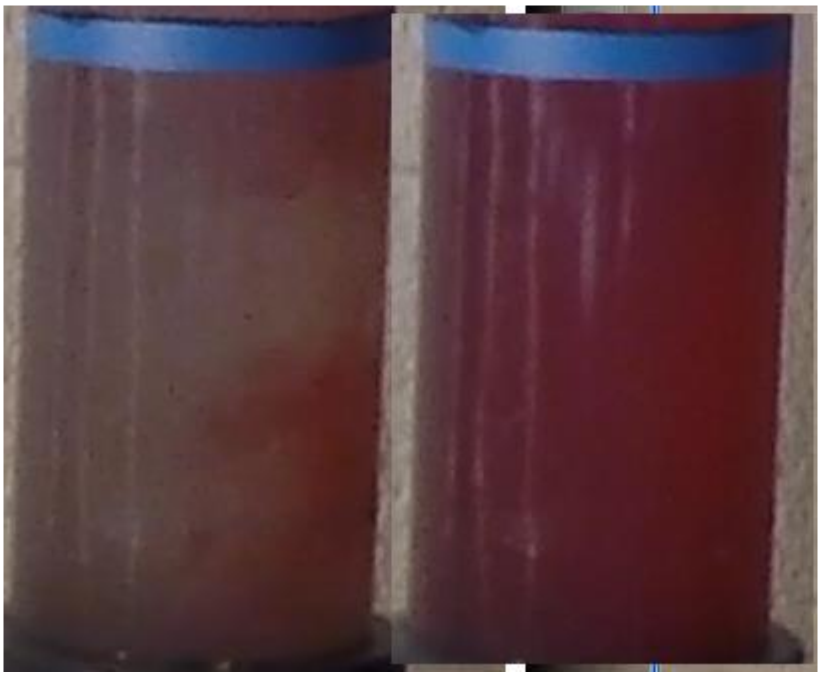

Figure 44 - Oil bubbles (left) and oil dominant (right) in bottom of second riser (8m^3/h)

7.2.3 Oil-water displacement top inlet

Oil-water displacement was helped by the buoyancy effect for the first horizontal and vertical section, as it took the easiest way down the riser and out of the domain. Water was displaced efficiently for all velocities in both the first horizontal and vertical section. For the rest of the domain, similar displacement as for the reduced jumper was observed. For the lowest rates, 6 m^3/h, the oil had problems displacing water in the rest of the domain as it was unable to establish a clear displacement front. A full displacement of the domain was not observed, but results displayed in Figure 45 look promising for the two highest velocities.

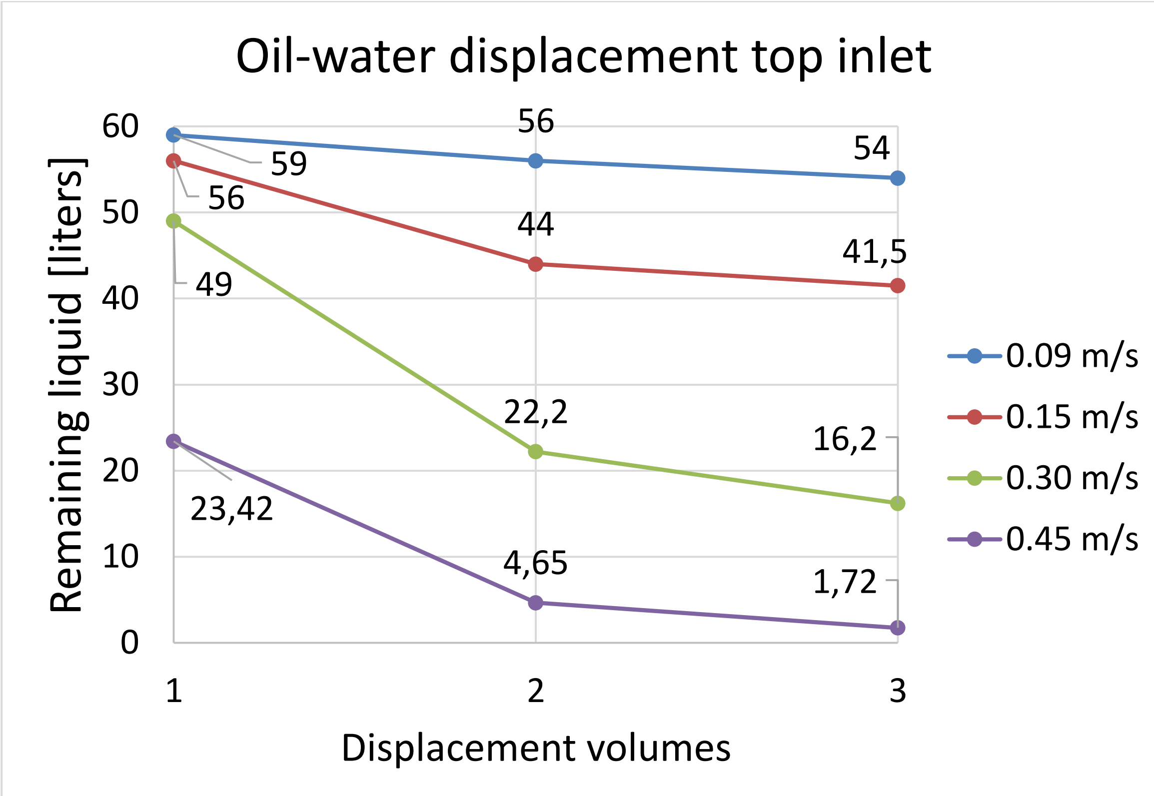

Figure 45 – Plotted oil-water displacement through top inlet results

7.2.3.1 Liquid hold up

The water hold-up was similar at the inlet for all velocities, with some water accumulation at the bottom of the first horizontal section, presented in Figure 46. This water was displaced for velocities after one jumper volume. In the bottom horizontal section, the oil had problems displacing water with the two lowest velocities and a large water hold-up was observed. It is unlikely that the oil would be able to displace this water within a reasonable time.

Figure 46 – Accumulation of water at bottom of first horizontal section (6m^3/h).

7.2.3.2 Displacement front

For the lowest velocities, the oil established itself at the top of the bottom horizontal section before starting displacement of the second riser, with an approximately height of 0.05 meters, left in Figure 47. With the two highest velocities, displacement of the second riser started once the front reached the bend, with a height of 0.04 m, right in Figure 47. With high displacement velocities, wavy interface between the oil and water was observed as the oil dragged the water out.

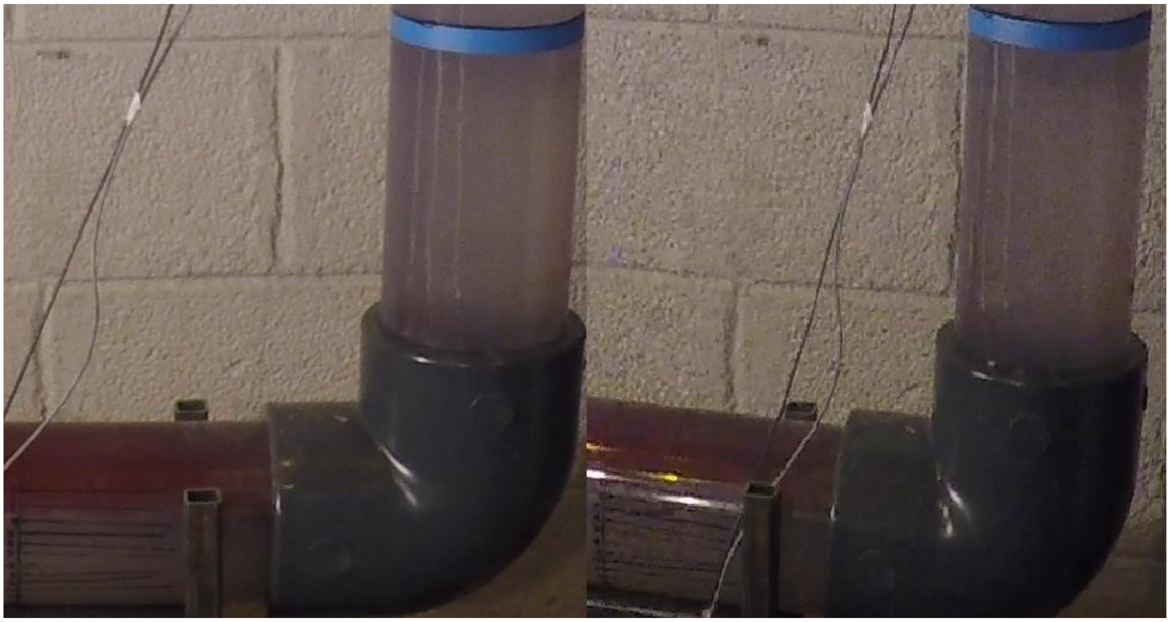

Figure 47 – Front height at displacement of second riser start (6m^3/h left and 30m^3/h right)

Due to the density difference, the oil front quickly broke up as it rose in the second riser for the lowest velocities. With time, the flow went from water dominant dispersed to oil dominant dispersed. With the highest velocities, 20- and 30 m^3/h, the oil established a displacement front in the second riser, efficiently displacing the water. Some breakup of the front was observed, with oil accelerating in the water and leaving the front, as seen in Figure 48.

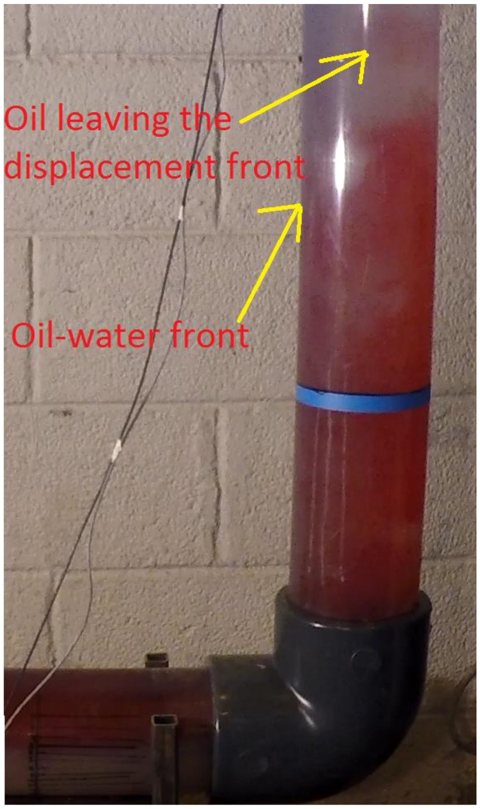

Figure 48 – Accelerating oil in the oil-water displacement front

7.2.4 Water-oil displacement top inlet

Water-oil displacement at the top inlet was largely influenced by the oil located at the first horizontal section. Due to buoyancy, water was unable to displace all of the oil located in the first horizontal and vertical section. A full displacement of the jumper was not observed with three jumper volumes with the tested rates, although results indicate that it is possible with the highest rate, given a sufficient displacement time.

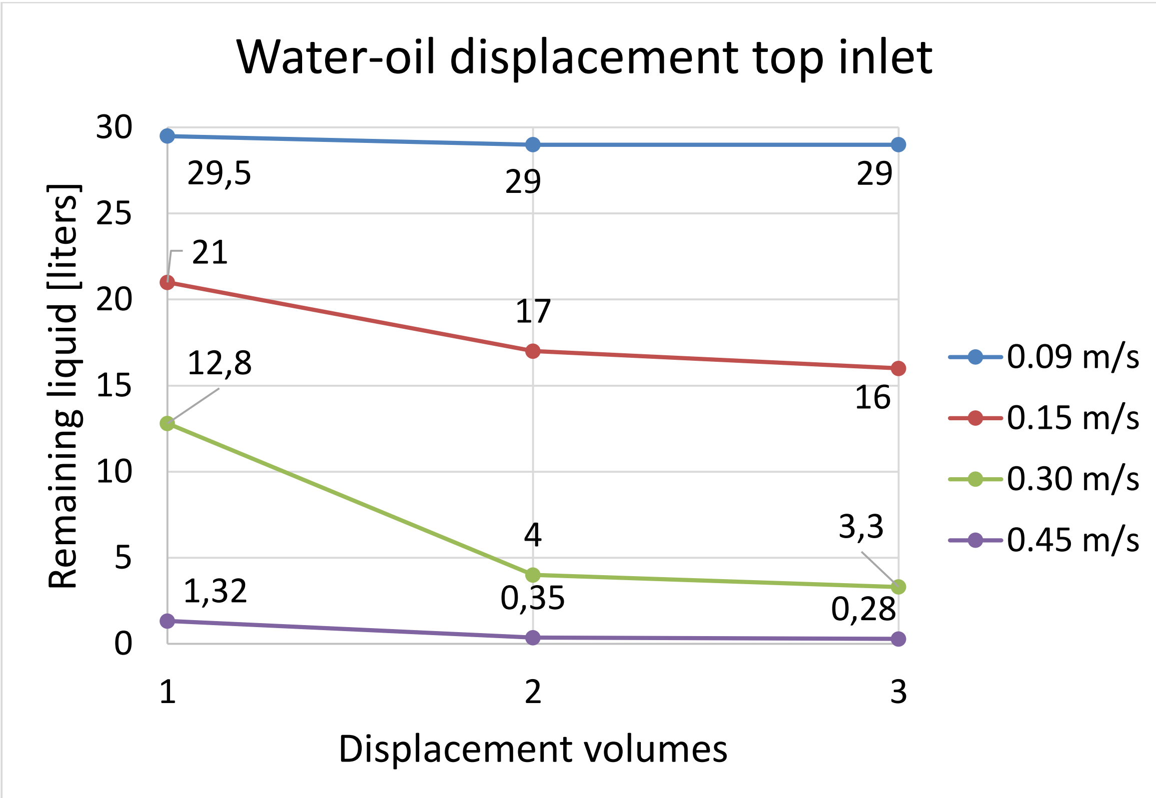

Figure 49 – Plotted water-oil displacement through top inlet results

7.2.4.1 Liquid hold up

Displacement velocity played a key role on the oil hold-up for water-oil displacement at the top inlet. As previously described, the oil forced the water down at the horizontal section, leading to accumulation of oil at the top. With high velocities, most of the oil was displaced due to the interface tension. Large turbulent eddies was observed after the first bend, leading to oil accumulation in the low pressure side of the first vertical section, as seen in Figure 50. For the rest of the jumper, bottom horizontal section and second riser, oil hold-up was observed in the same locations as the reduced geometry.

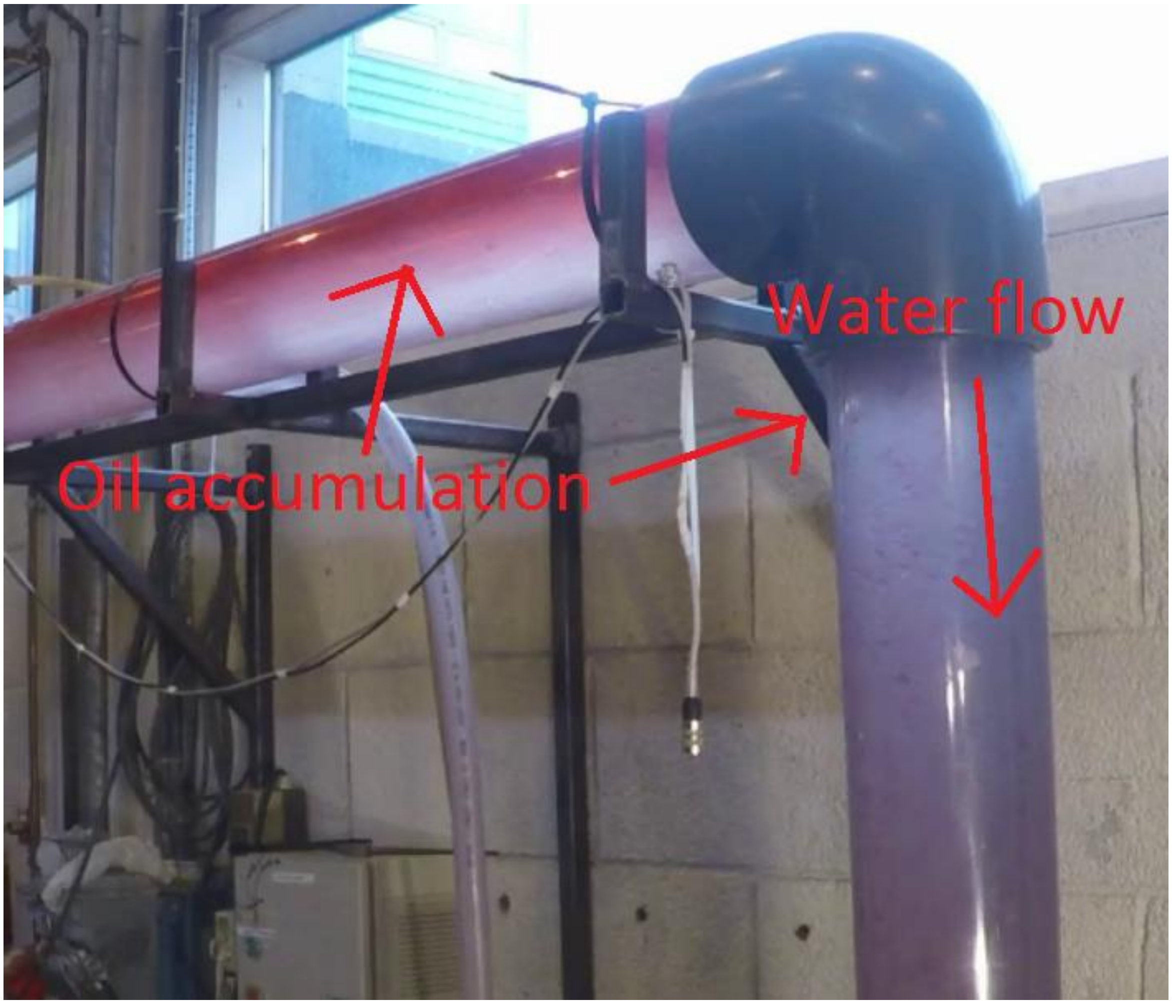

Figure 50 - Oil bubbles (left) and oil dominant (right) in bottom of second riser (8m^3/h)

7.2.4.2 Displacement front

For the lowest velocities, water established itself in the bottom horizontal section in the same manner as for the reduced geometry. Displacement of the second riser started once the oil strip was reduced to 0.05meters for the lowest velocity, seen in Figure 51. With the two highest velocities, water introduced displacement of the second vertical section once the front reached the riser, without filling up the horizontal section, leaving a 0.1m high strip of water at the top.

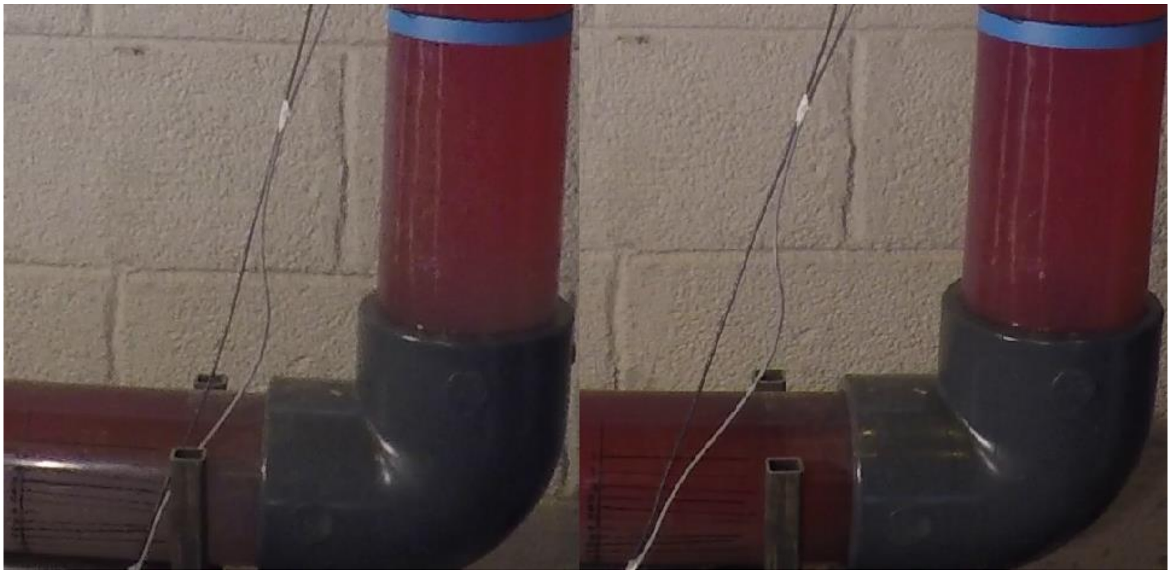

Figure 51 – Water-oil displacement front for displacement via top inlet (6 m^3/h left, 30 m^3/h right)

Displacement of the second riser was done as one column after the water had established itself in the bottom section for the lowest velocities. The displacement front was then traveling with approximately the superficial velocity of the water. With the highest velocities, the water front penetrated the trapped oil volume and displaced most of the oil with the first displacement volume. The flow went from oil continues to water continues after one volume of displacement.

7.3 Accuracy of numerical simulations

Based on the results obtained through the numerical simulations, some observations have been made regarding the accuracy of the different models, the cost of performing the simulations and the predicted flow-pattern.

- Low displacement velocities are more computationally heavy than high velocity cases
- The homogenous free-surface model predicts water-oil displacement better than the inhomogeneous model and is considerable less computational heavy for those cases.
- The inhomogeneous mixture model predicts best for oil-water displacement, where there is a lot of mixing between the liquids.
- Errors seem to decrease with increasing velocity.

Each of the numerical simulation cases will be individually analyzed in the next four sub-chapters, with graphs comparing experimental and numerical simulation results. In the graphs, experimental results are indicated with a blue square, inhomogeneous mixture model with a red triangle and homogenous mixture model with green circle. Each of the dots are connect with a line to indicate trend of the displacement and colored based on the displacement velocity.

7.3.1 Water-oil displacement bottom inlet

For the water-oil displacement of the reduced jumper, simulated results are consistent with the experimental results. Results indicate better displacement after one jumper volume with low velocities, as suggested by experimental results. For all cases, both models underestimated the oil displacement after one displacement volume and over predicts for two and three displacement volumes. The difference between the simulations and experiments seems to increase with high velocity and is closest for the lowest displacement velocity tested. Overall the inhomogeneous mixture model seems to be closest to the experimental results minimum reporter error is an under prediction of 2.20% for the inhomogeneous mixture model for one displacement volumes at 6 m^3/h. Maximum reported error is an over prediction of 41.77% for the inhomogeneous mixture model after three displacement volumes at 10 m^3/h.

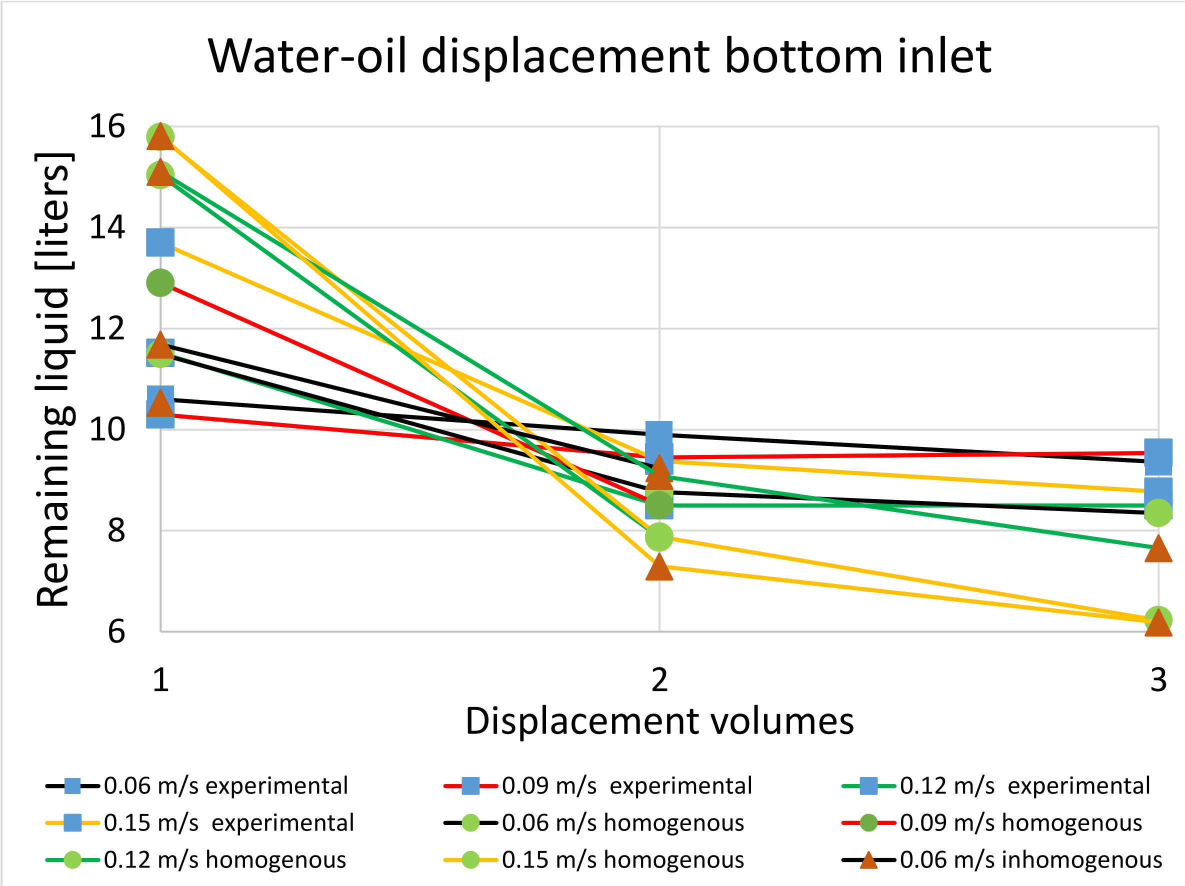

Figure 52 – Water-oil displacement simulated vs experimental results for reduced jumper

Based on the .out file, the inhomogeneous model seem to have bigger convergence problems than the homogenous and was computational heavy for the lowest velocities. Overall all, the homogeneous model showed lower imbalance, the highest reported mass imbalance was 0.5545% for oil during the 4 m^3/h case.

7.3.2 Oil-water displacement bottom inlet

With oil displacing water through the bottom inlet, both models over predicted the displacement, except for the under prediction for the inhomogeneous model after two and three displacement volumes. The difference between the simulations and experiments seems to increase with high velocity and is closest for the lowest displacement velocity tested. Overall the inhomogeneous mixture model seems to be closest to the experimental results minimum reporter error is an under prediction of 0.83% for the inhomogeneous mixture model for two displacement volumes at 4 m^3/h. Maximum reported error is an over prediction of 140.34% for the homogenous free-surface model after three displacement volumes at 10 m^3/h.

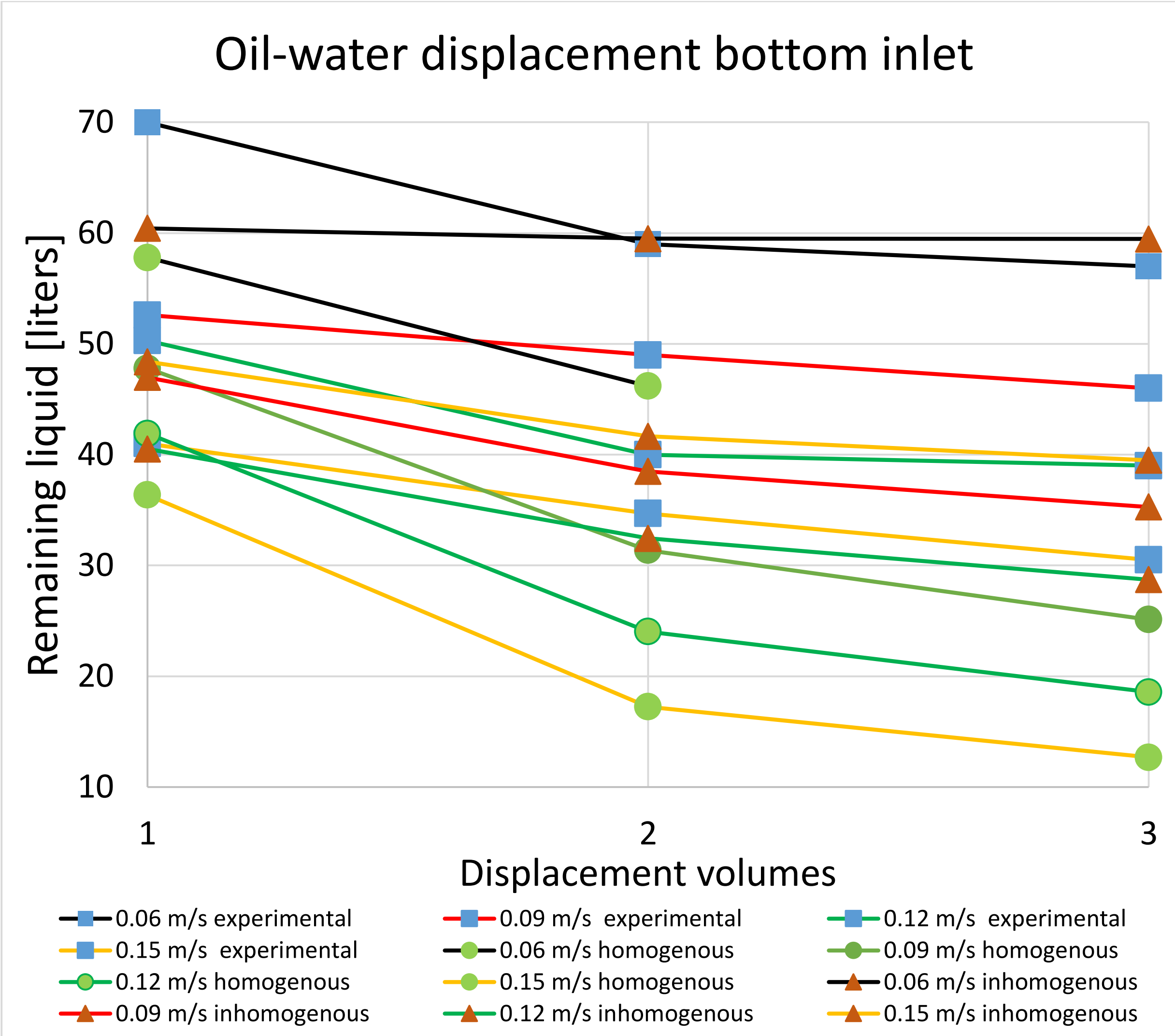

Figure 53 – Oil-water displacement simulated vs experimental results for reduced jumper

Based on the .out file, the inhomogeneous model seem to have bigger convergence problems than the inhomogeneous and was computational heavy for the lowest velocities. Some issues was seen, with formation of a wall at the outlet to block inflow into the domain.

7.3.3 Water-oil displacement top inlet

For the water-oil displacement of the full jumper the homogenous and inhomogeneous model under predicts the displacement for most cases at high velocities. The difference between the experimental and simulated results seems to decrease with number of displacement volumes. From the results shown in Figure 54, the homogeneous free-surface model seems to best fit with the experimental results. Maximum reported error is an under prediction of 284.62% for the homogenous free surface model for three displacement volumes at 30 m^3/h. Minimum reported error is an over prediction of 2.56 for the homogeneous mixture model after one displacement volumes at 6 m^3/h.

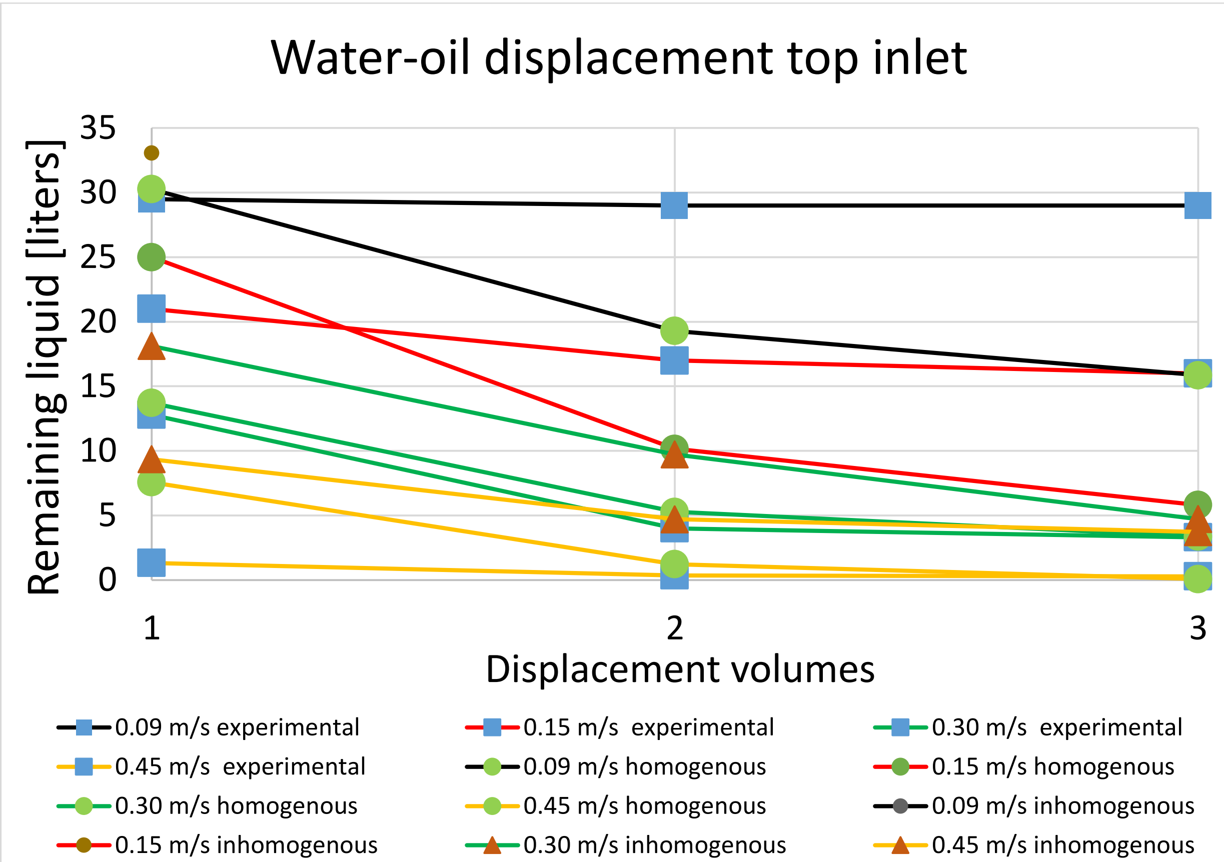

Figure 54 – Water-oil displacement simulated vs experimental results for full jumper

Due to lacking number of results for the inhomogeneous mixture model, clear conclusion cannot be drawn. Computational time from each case indicates that the inhomogeneous model is computationally heavier than the homogenous model, which is the reason that the simulations did not finish in time.

7.3.4 Oil-water displacement top inlet

For the oil-water displacement of the full jumper the homogenous and inhomogeneous model were inconsistent in comparison with the experimental results, as seen in Figure 55. For all cases, both models over-predicted the water displacement. The error seems to decrease with increasing velocity and is closest for the highest velocity. Overall the inhomogeneous mixture model seems to fit best with the experimental results Maximum reporter error is an under prediction of 425.54% for the homogenous free surface model for three displacement volumes at 30 m^3/h. Minimum reported error is an over prediction of 21.27% for the inhomogeneous mixture model after three displacement volumes at 30 m^3/h.

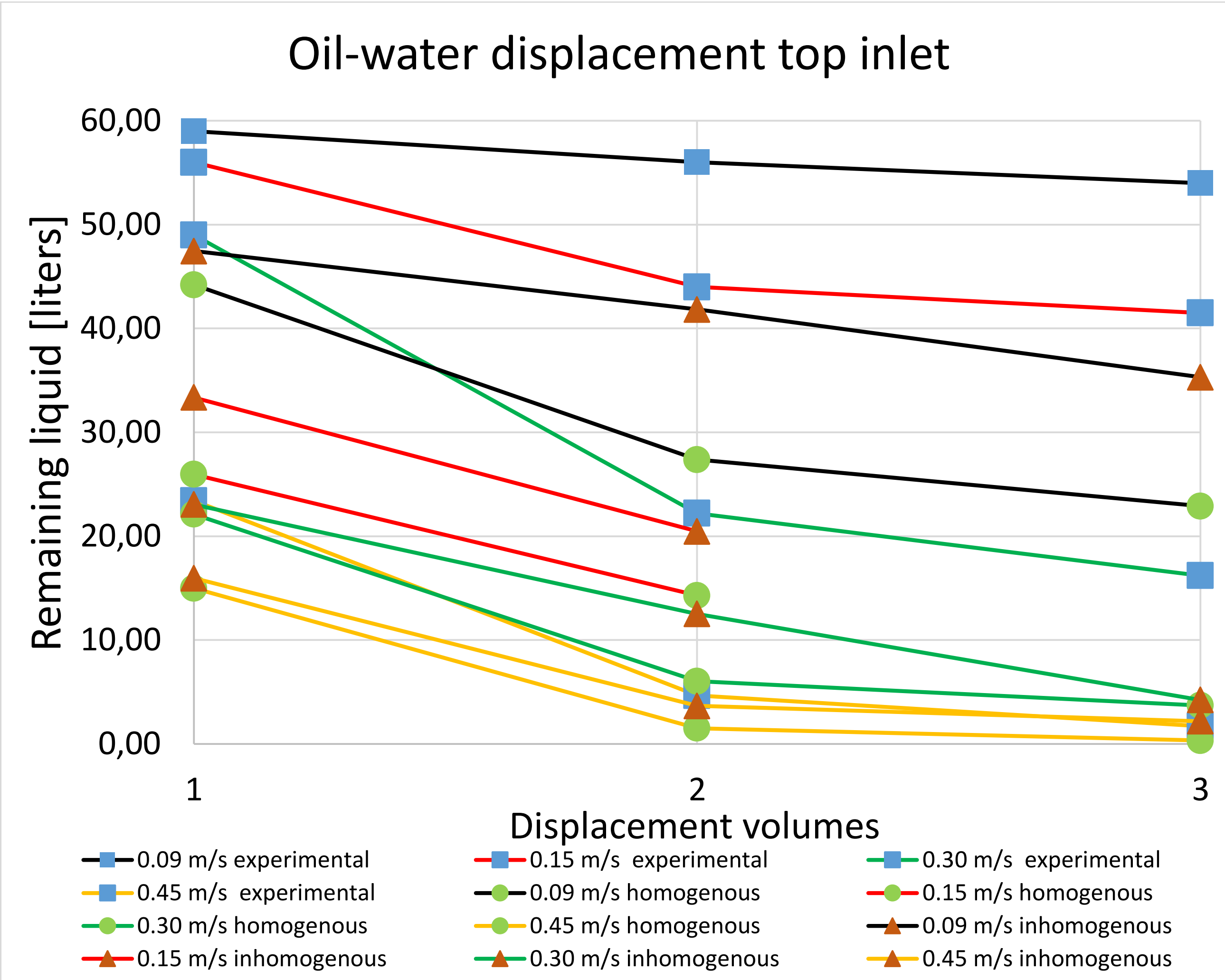

Figure 55 – Oil-water displacement simulated vs experimental results for full jumper

Based on the .out file, the results reported by the solver are true to the models set in CFX-pre. The highest reported mass imbalance was 0.1833% for water with the homogenous model. Overall all, the inhomogeneous model showed lower imbalance and was the least computational heavy.

8 Conclusions

Based on results obtained in the experiment and numerical simulations, the following conclusions can be drawn:

- Displacement of dead-leg only observed for oil-water displacement, this indicates that a less dense liquid is required as expected.
- Water has the best displacement efficiency [1] with one jumper volume of displacement, mainly due to its higher density
- Displacement efficiency is reduced quicker with water-oil than oil-water at a fixed displacement velocity, with regards to displacement volumes.
- For the full jumper, high displacement velocity proven to be best for both oil-water and water-oil displacement.
- For the reduced jumper, the total amount of displaced oil was consistence with all water velocities. Oil-water displacement efficiency increased with oil displacement velocity.
- The flow pattern was stratified in horizontal sections and dispersed bubble flow in vertical sections for low and medium velocities.
- High velocities created a piston shaped displacement front, when displacing from the top inlet, leading to high displacement efficiency.
- Homogenous free surface model fits best with experimental results with water-oil displacement and inhomogeneous mixture model for oil-water displacement, min max average error
- CFX is better at predicting high displacement velocities than low.

[1] Displacement efficiency: amount of original liquid in the domain after x displacement volumes

9 Future work

Based on our results and the conclusions drawn, suggested points for future investigation include:

- Add a multiphase meter to the outlet, to reduce the time use of future experiments.
- Rebuild the outlet of the jumper so it has the same dimension the whole way to the separator. Parts have been acquired and it just needs to be built.
- Do maintenance on the low-flow pumps/replace
- Try to add an angle to the jumper, to check if the displacement efficiency is increased.
- Experiment with a heavier displacement liquid, such as MEG.
- Numerical simulations with LEDA and OLGA, to see how they compare with CFD.
- Try to tune the CFD model to see if better results are obtained, adjust interface length and tension.
- Re-run some of the experiments to verify the results.

Nomenclature

Latin letters

D	Diameter [m]
A	Cross-section area [m^2]
V	Volume [m^3]
F	Force [N]
f	Friction factor[-]
g	Gravity force [9.81 m/s^2]
P	Pressure [Pa]
Q	Mas flow rate [m^3/s]
s	Phase slip ratio [-]
U	Velocity [m/s]
H	Phase holdup [-]

Greek letters

λ	Volume fraction [-]
μ	Viscosity [Pa s]
ρ	Density [Kg/m^3]
β	Inclination [Degrees]

Abbreviations

CFD	Computational Fluid Dynamics
FVM	Finite Volume Method
MSL	Mean Seal Level
OVF	Oil Volume Fraction
HC	Hydrocarbon
MEG	Mono ethylene glycol
PLONOR	Pose Little Or No Risk

Subscripts

m	Mixture
o	Oil
s	Superficial
w	Water
avr	Average

10 References

Ansys, 2015. *ANSYS Help.* s.l.:s.n.

Bardon, F., Hudson, W. L., Vigne, C. & Cretenet, A., 2007. *Hydrate Prevention With Electrically Heated Jumpers.* s.l., 2007 Offshore Technology Conference.

Baukal, C. E., 2013. *The John Zink Hamworthy Combustion Handbook.* Second red. Hoboken : Taylor and Francis .

Brauner, N., 2003. Liquid-Liquid Two-Phase Flow Systems. I: V. Bertola, red. *Modelling and Experimentation in Two-Phase Flow.* s.l.:Springer Vienna, pp. 221-279.

Cagney, T., Hare, S. & Svedeman, S., 2006. *Hydrate inhibition of subsea jumpers during Shut-in.* s.l., Society of Petroleum Engineers.

Cagney, T. L. & Hare, S. C., 2006. *Hydrate Inhibition of Subsea Jumpers During Shut-in.* Texas, Society of Petroleum Engineers.

Coletta, A., Volk, M. & Delle-Case, E., 2011. *Investigations of Flow Behavior in Well-Head Jumpers during Restart with Gas and Liquid.* s.l., IPTC.

Dellecase, E., Solano, S. M., Lu, H. & Volk, M., 2013. *Hydrate inhibitor displacement experiments in jumper-like pipe configurations.* s.l., BHR Group.

Fossen, M., 2016. Trondheim: Sintef.

Herrmann, B., Bargas, C., Svedeman, S. J. & Buckingham, J. C., 2004. *Hydrate Inhibition in Headers With No Production Flow.* s.l., Society of Petroleum Engineers.

Kazemihatami, M., 2013. *Experimental study of displacement of viscous oil in pipes by water,* Trondheim: NTNU.

Lubeena, r., Mohammed, E. & Mohan, S., 2011. *CFD Simulation of Methanol Flushing in Subsea Jumpers,* s.l.: Ansys, Inc..

M-107 Retningslinjer for rapportering fra petroliumsvirksomhet til havs (2014).

Miljødirektoratet, 2015. *Tillatelse til forbruk og utslipp av kjemikalier i forbindelse med installasjon av havbunnskompressorstasjon på Gullfaksfeltet.* s.l.:s.n.

Mo, S., Ashrafian, A. & Johansen, S. T., 2013. *Two phase flow prediction of fluid displacement operations.* s.l., CRIStin 1113427.

Opstvedt, J. A. K., 2015. *Numeric Simulation on Displacement and Flushing of Hydrocarbon Fluid in Subsea Systems,* Trondheim: NTNU.

Petoro, 2012. *petoro - Miljørapport for SDØE 2012.* [Internett] Available at: https://www.petoro.no/petoro-aarsrapport/2012/hms/miljo/utslipp-til-kjemikalier

Schumann, H. et al., 2014. *Liquid-Liquid Displacement in a Horizontal and Inclined Pipe Section.* s.l., BHR Group.

Schümann, H., Kazemihatami, M. & Nydal, O. J., 2013. *Oil-Water Flushing Experiments with Complex Pipe Geometry.* s.l., s.n.

Solheim, K. T. & Nysveen, A., 2014. *Hydrate Management of Jumpers by Electrical Heating.* s.l., International Society of Offshore and Polar Engineers.

Thomas, M., 2010. Subsea Developments Key To Future Production. *Journal of Petroleum Technology*, oktober.

Xuemei Chen, J. A. W. a. S. V. G., 2016. Continuous Oil - Water Separation Using Polydimethylsiloxane - Functionalized Melamine Sponge. *American Chemical Society,* Volum 55, p. 3596.

Young, R. R., 2006. *Project Requirments - A Guide to Best Practices.* s.l.:Managment Concepts, Inc.

Appendixes

Appendix A – Displacement procedure

Displacement Procedure

This document describes operation of the experimental rig and includes procedures for establishment of initial conditions, displacement trough the lower inlet and displacement trough the top inlet. The procedures include visual presentation of the setup via a P&ID made in Microsoft Excel and step by step description of the pump and valve operations. At the start of each procedure, initial status of valves are listed. Only open valves are listed, all other valves are assumed to be closed.

Open valves has white collar with black borders, while closed valves will be all black. The status of a pipe or hose is indicated by its color, black line indicates empty, red oil filled, blue water filled and green filled with a mixture of water and oil. Glowing lines will indicate the flow path of the liquid for each step.

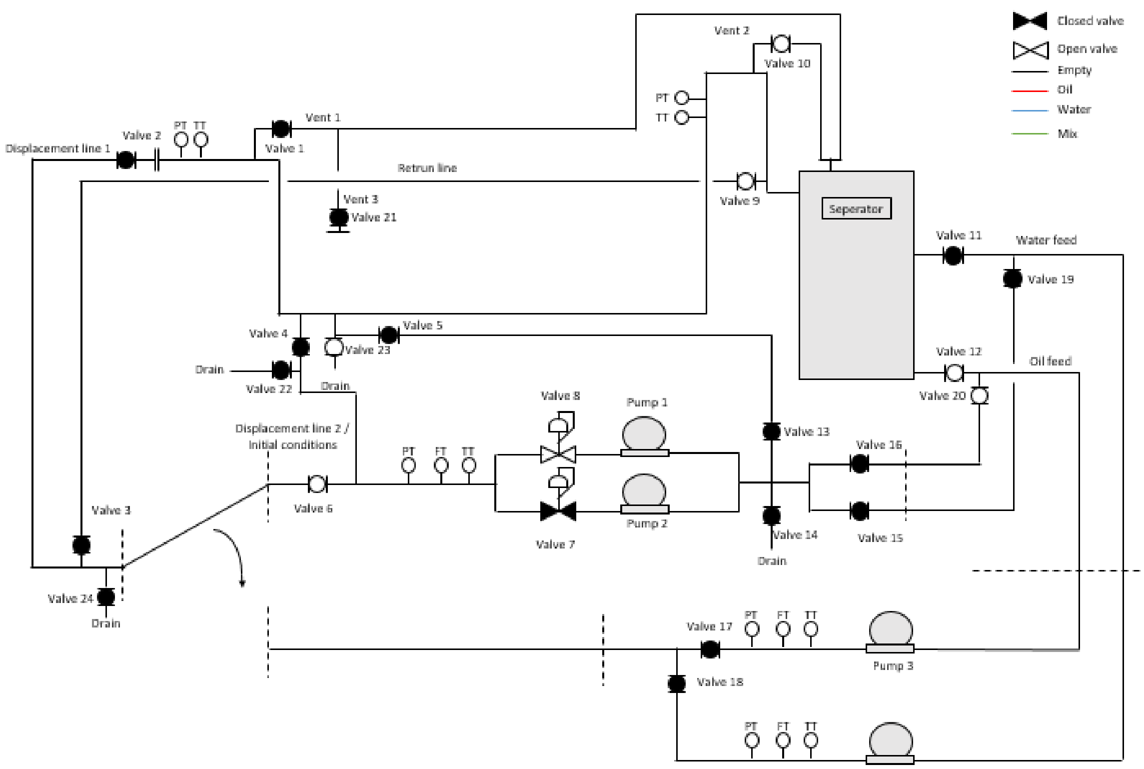

1 Establishment of initial conditions

The establishment of initial condition is done before starting the displacement procedure. Liquid is filled through the dedicated initial condition line, using the low-flow pump setup. Set the flowrate to two m3/h and ensure that the bleeding valves are open. Procedure 1.1 through 1.4 describes in detail how to fill the whole jumper and half the jumper with either water or oil. If only half the jumper is used, ensure that the blind flange is connected and bolts are tighten to prevent leaks. Before starting the procedures, all pipes shall be drained to ensure clean initial condition liquid is supplied.

1.1 Filling the whole jumper with water

Table 23 - Shows the initial valve status

Valve	Status
Valve 1	Open
Valve 4	Open
Valve 8	Open
Valve 9	Open
Valve 10	Open
Valve 11	Open
Valve 15	Open
Valve 19	Open

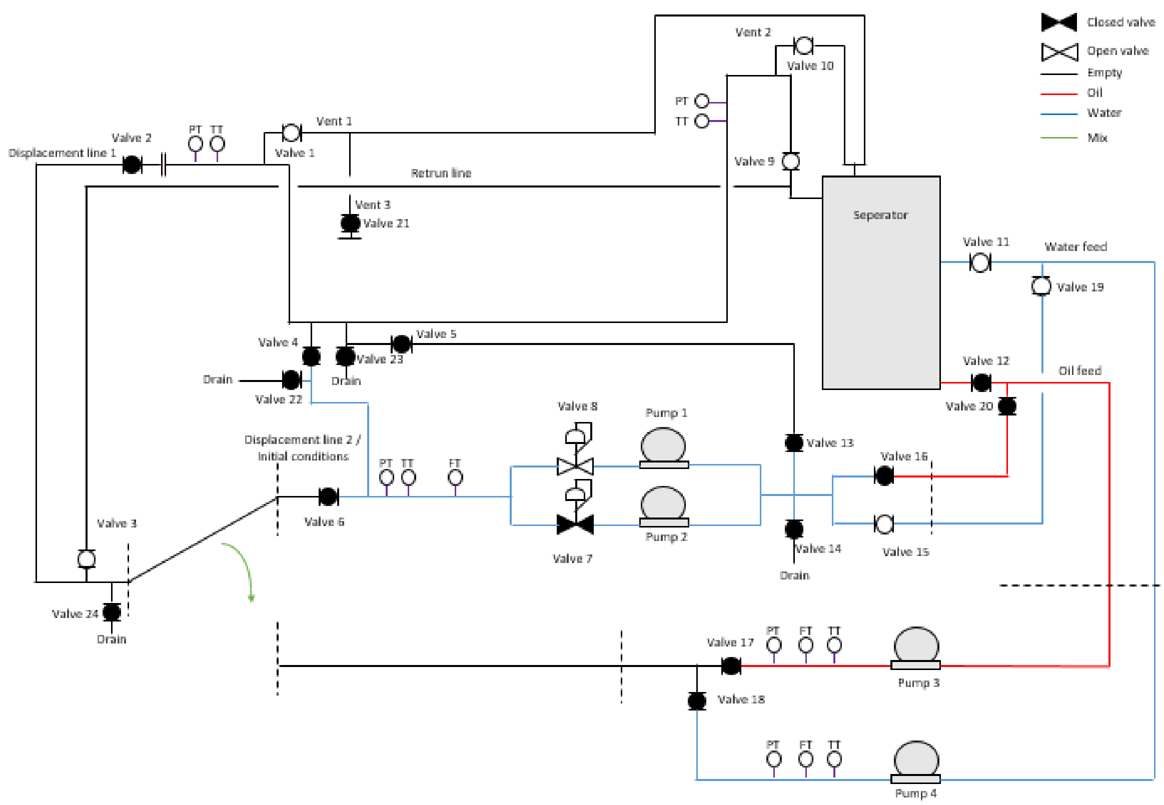

Step	Operation
1	Put valves in initial status
2	Set frequency converter to 3 m^3/h
3	Start pump 1
4	Observe vent 1, wait until trapped air has been displaced from the top inlet

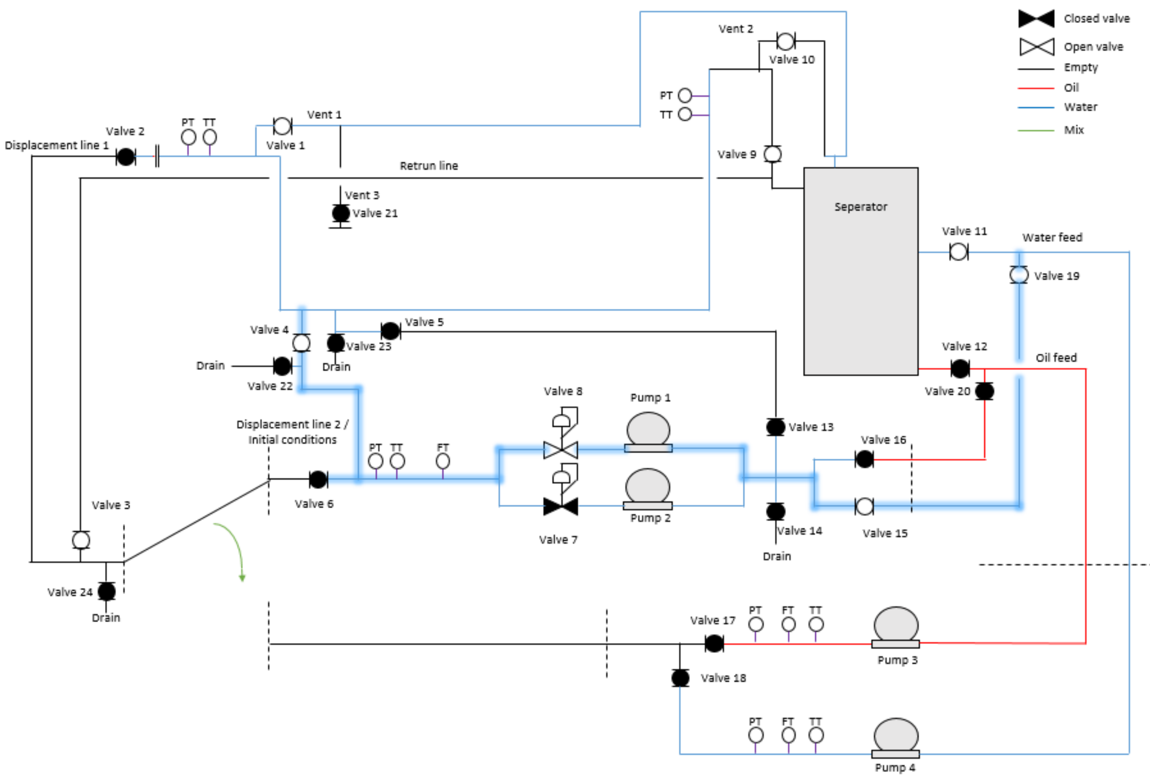

Step	Operation
5	Close valve 1
6	Stop pump 1
7	Close valve 4
8	Drain initial condition line from any remaining liquid

1.2 Filling the whole jumper with oil

Table 24 - Shows the initial valve status

Valve	Status
Valve 1	Open
Valve 4	Open
Valve 8	Open
Valve 9	Open
Valve 10	Open
Valve 12	Open
Valve 16	Open
Valve 20	Open

Step	Operation
1	Put valves in initial status
2	Set frequency converter to 3 m^3/h
3	Start pump 1
4	Observe vent 1, wait until trapped air has been displaced from the top inlet

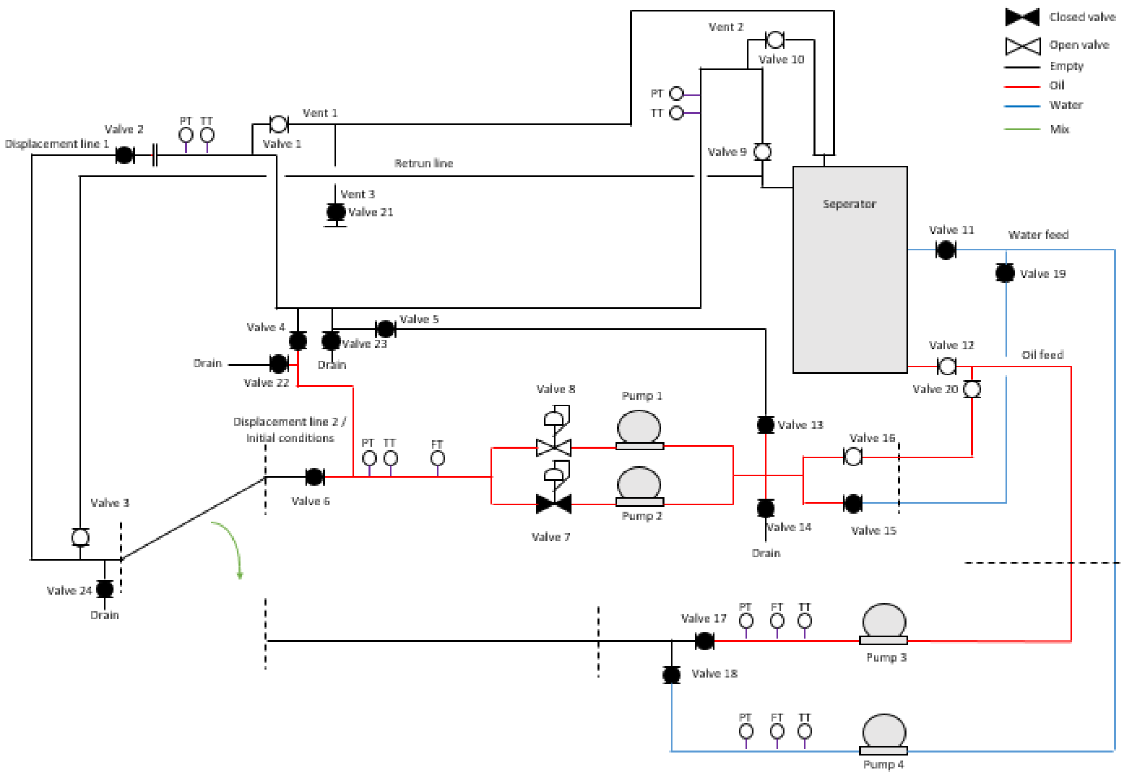

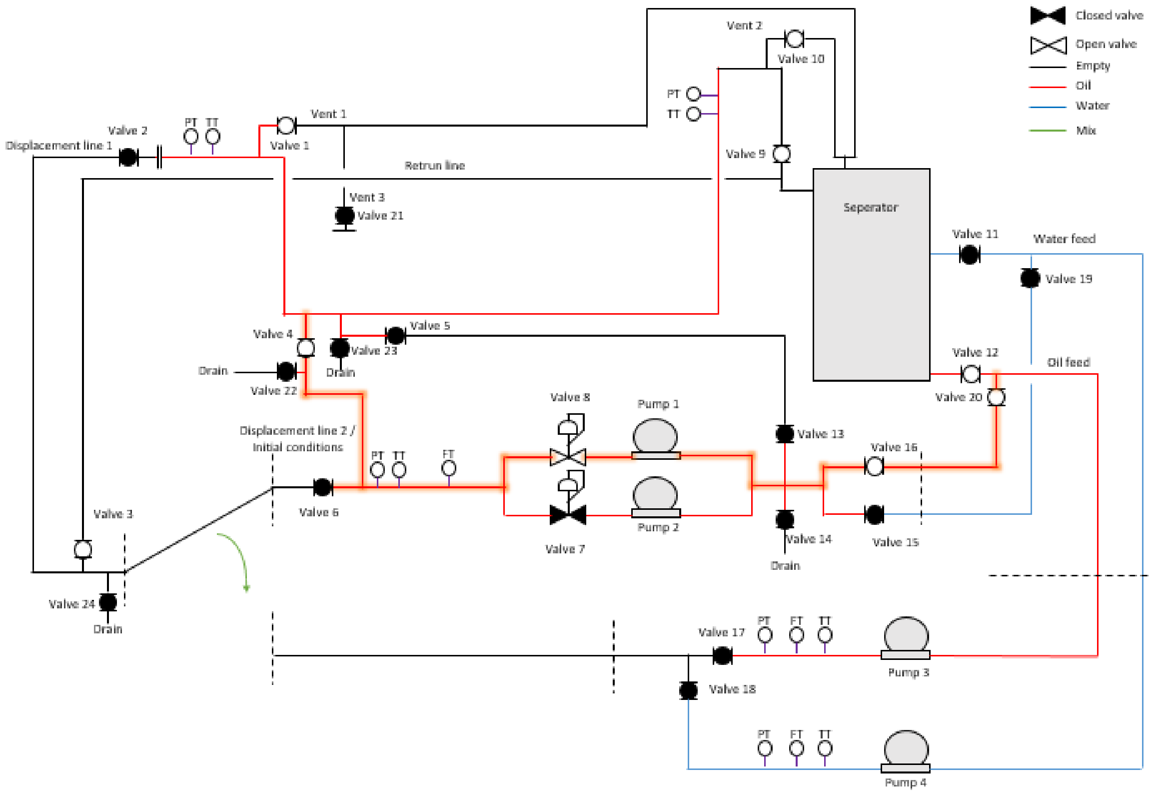

Step	Operation
5	Close valve 1
6	Stop pump 1
7	Close valve 4
8	Drain initial condition line from any remaining liquid

1.3 Filling half the jumper with water

Table 25 - Shows the initial valve status

Valve	Status
Valve 4	Open
Valve 8	Open
Valve 9	Open
Valve 10	Open
Valve 11	Open
Valve 15	Open
Valve 19	Open
Valve 21	Open

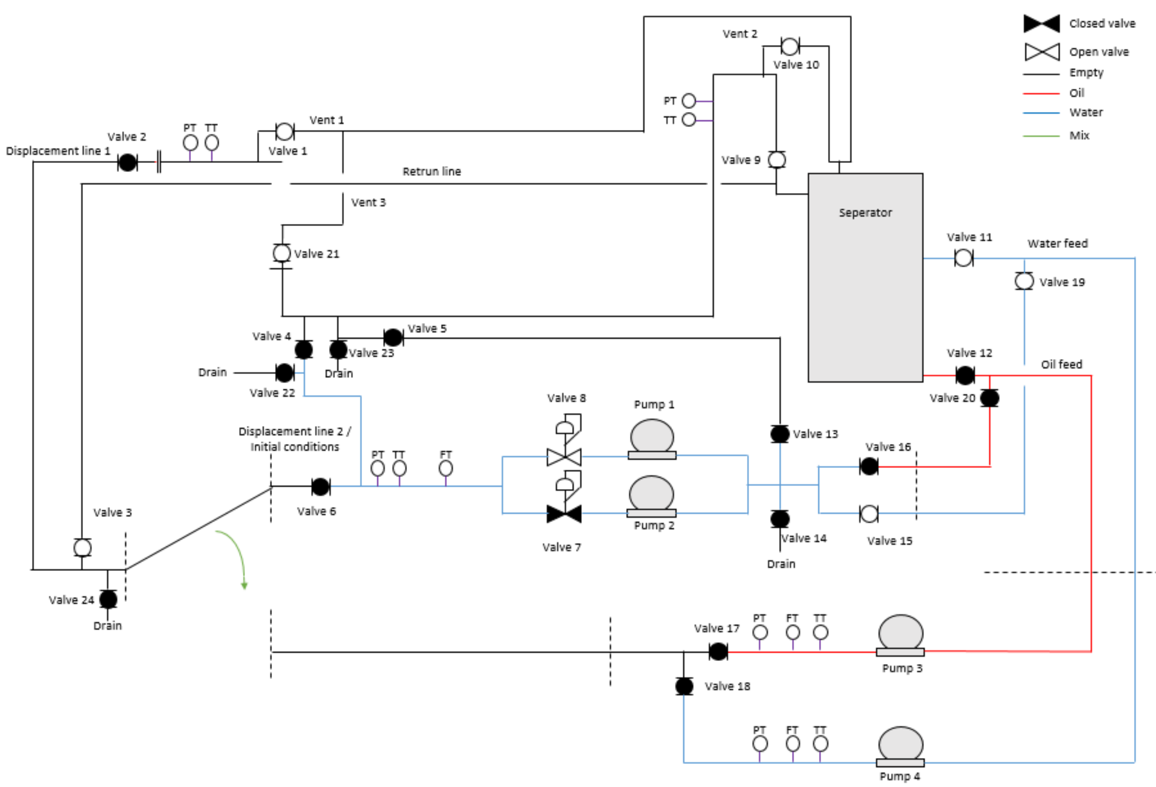

Step	Operation
1	Put valves in initial status
2	Set frequency converter to 3 m^3/h
3	Start pump 1
4	Observe vent 1, wait until trapped air has been displaced from the top inlet

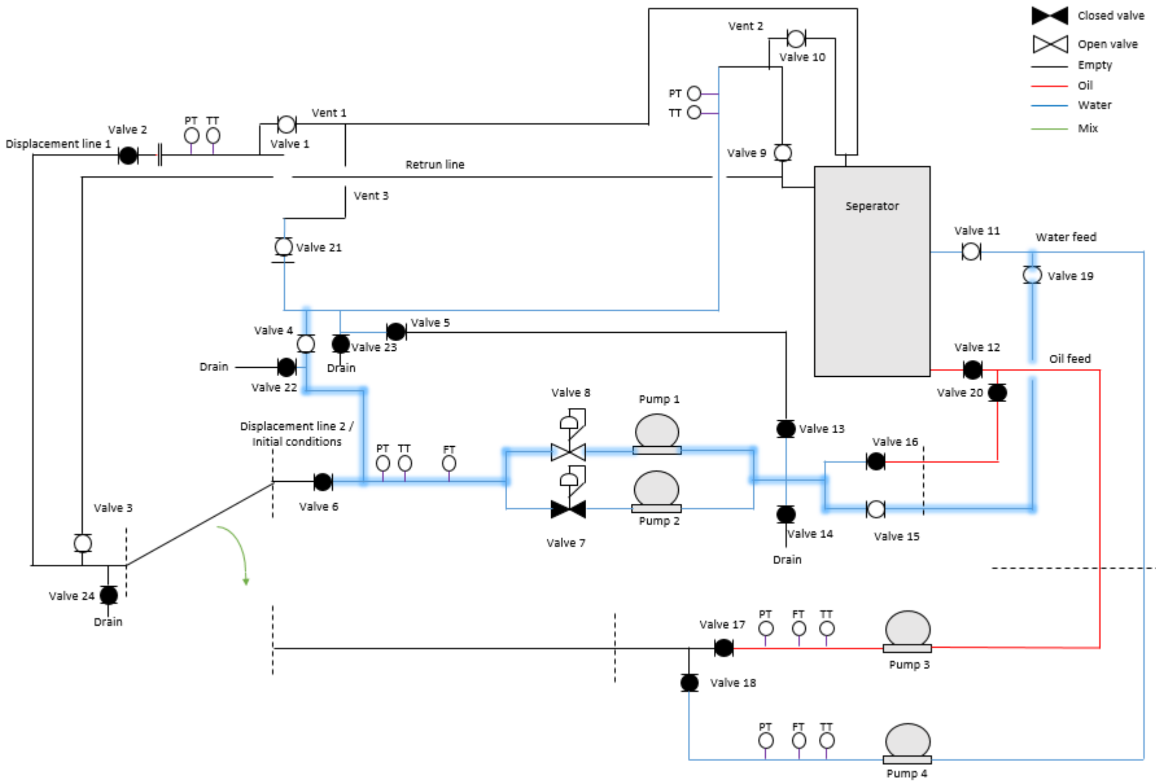

Step	Operation
5	Close valve 21
6	Stop pump 1
7	Close valve 4
8	Drain initial condition line from any remaining liquid

1.4 Filling half the jumper with oil

Table 26 - Shows the initial valve status

Valve	Status
Valve 4	Open
Valve 8	Open
Valve 9	Open
Valve 10	Open
Valve 12	Open
Valve 15	Open
Valve 20	Open
Valve 21	Open

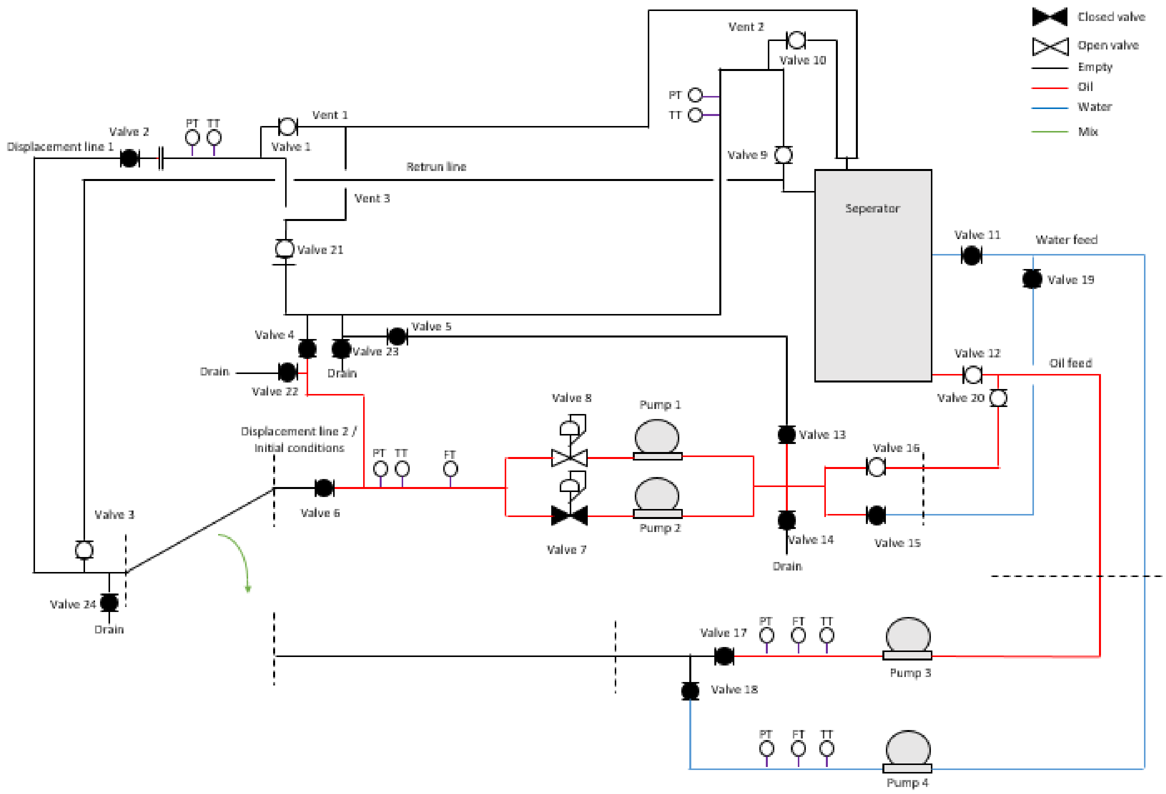

Step	Operation
1	Put valves in initial status
2	Set frequency converter to 3 m^3/h
3	Start pump 1
4	Observe vent 3, wait until trapped air has been displaced from the vertical section

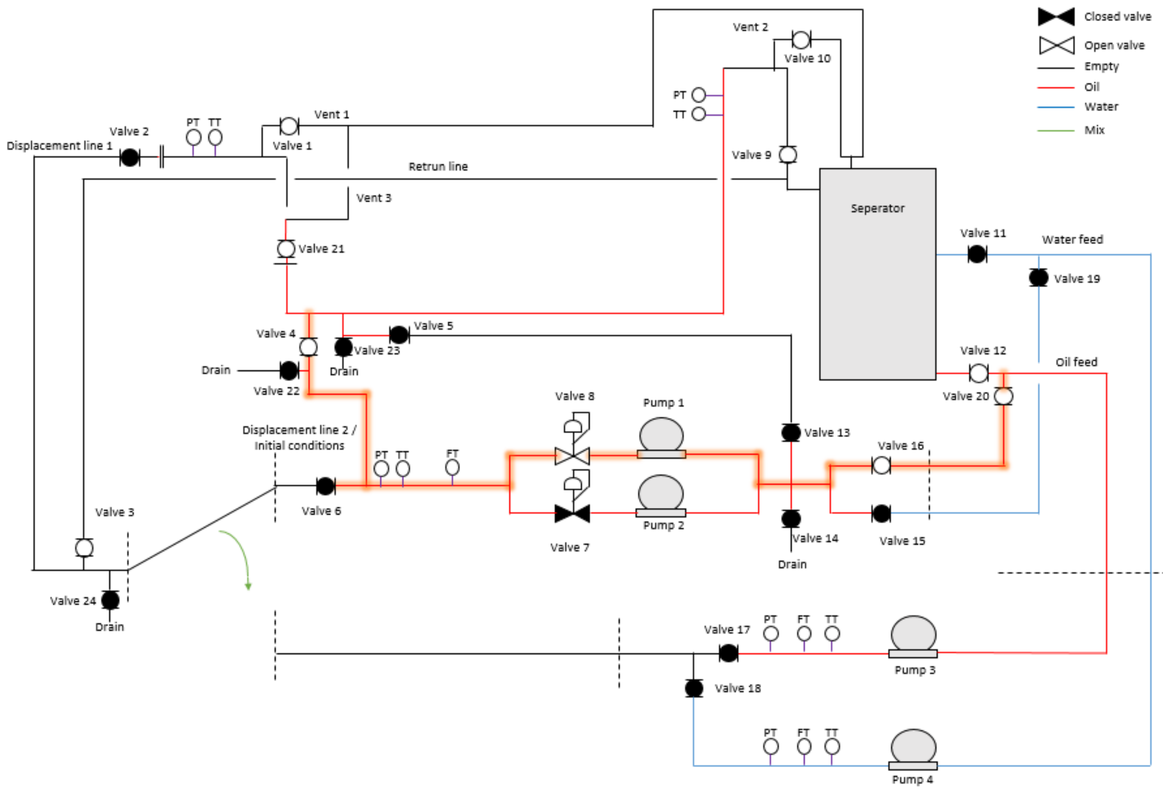

Step	Operation
5	Close valve 21
6	Stop pump 1
7	Close valve 4
8	Drain initial condition line from any remaining liquid

2 Displacement trough lower inlet

Displacement trough the lower inlet is done using the low-flow pumps at four different flowrates, the displacement rates and pumps used can be seen in *Table 27* bellow. The pumps accept both oil and water as input liquid, but the turbine meter needs to be calibrated to the specific liquid. Before starting the displacement procedures, the piping surrounding the low-flow pumps shall be emptied, to ensure that pure displacement liquid is used.

Table 27 - Shows the displacement rates for the lower inlet

Test number	Displacement rate [m3/h]	Pump used
1	4	Pump 1
2	6	Pump 1
3	8	Pump 1 & Pump 2
4	11	Pump 1 & Pump 2

2.1 Water displacing oil

Table 28 - Shows the initial valve status

Valve	Status
Valve 3	Open
Valve 6	Open
Valve 7	(Open)
Valve 8	Open
Valve 9	Open
Valve 10	Open
Valve 11	Open
Valve 15	Open
Valve 19	Open

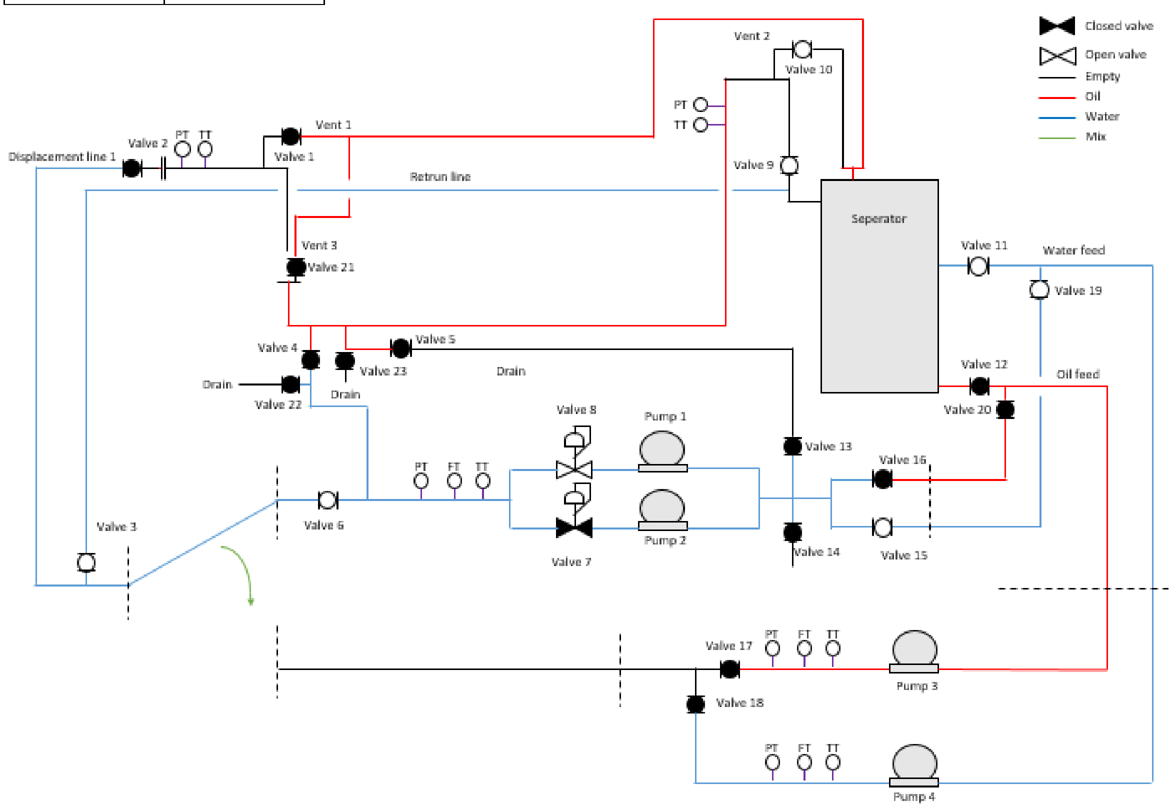

Step	Operation
1	Put valves in initial status
2	Start pump(s), and adjust flow to desired rate
3	Wait to flow stabilizes

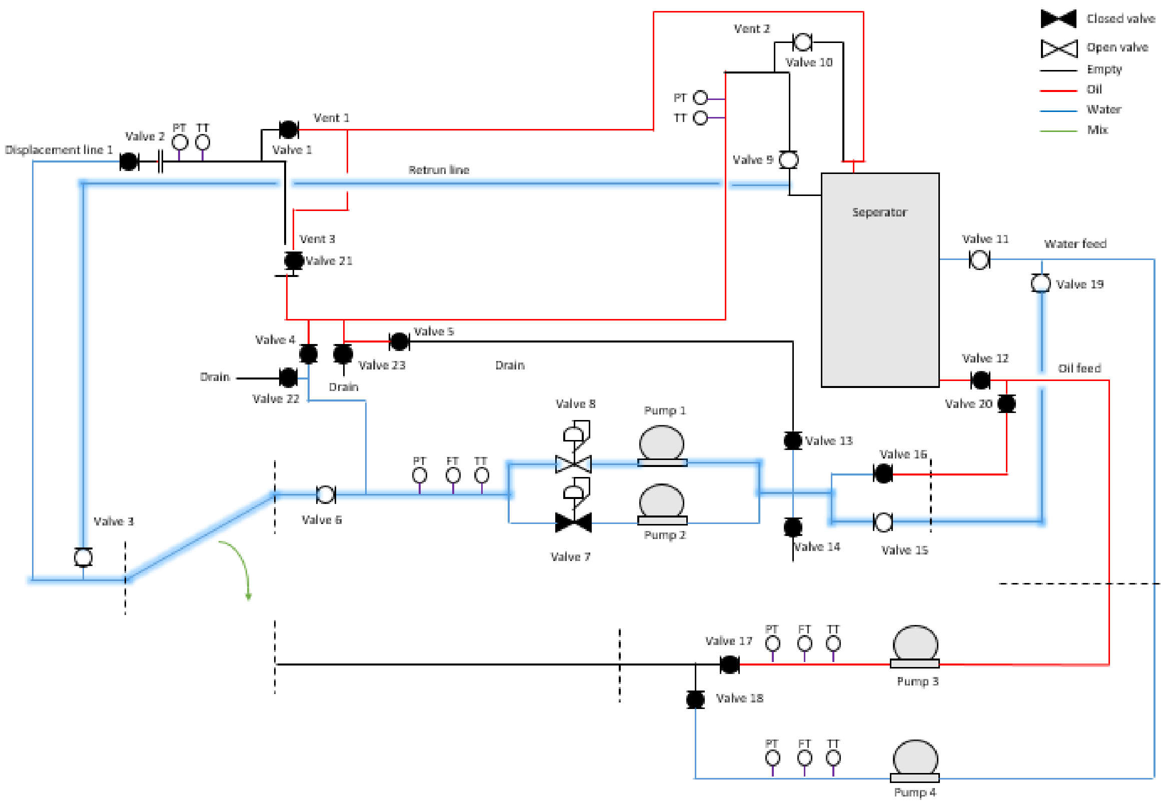

Step	Operation
4	Close valve 6
5	Open Valve 4
6	Monitor accumulated flow

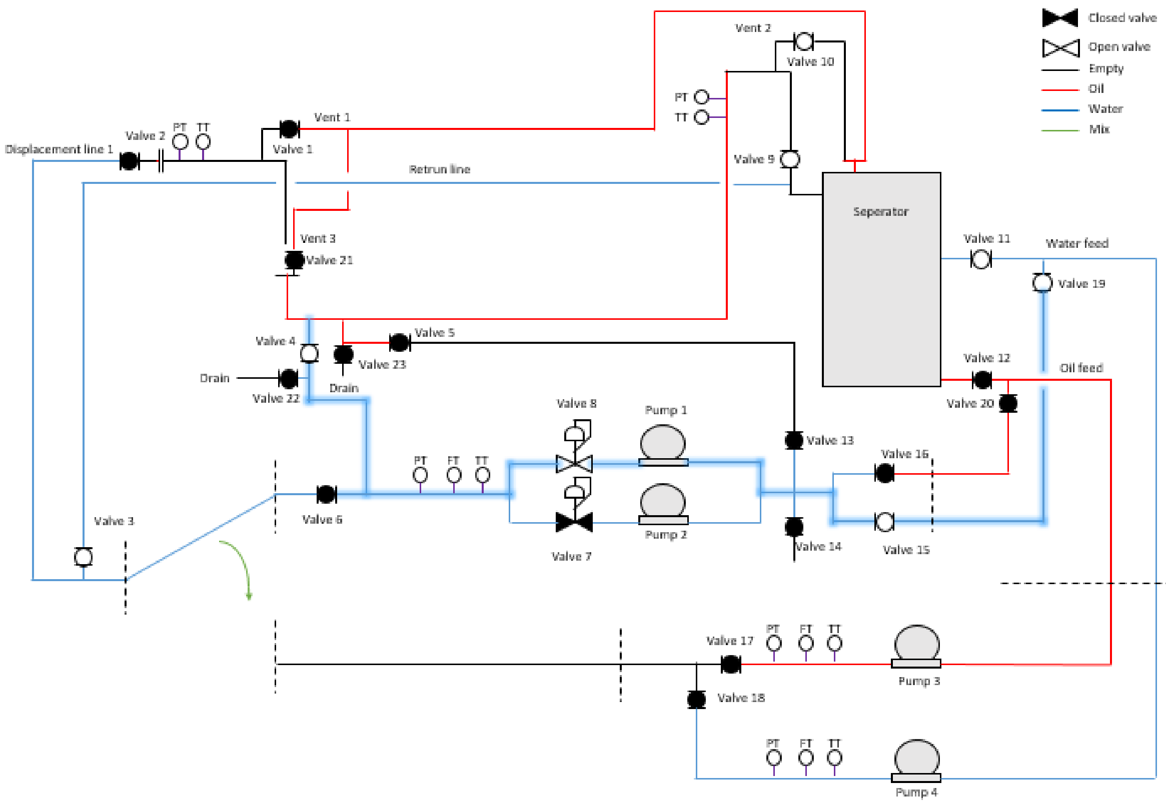

Step	Operation
7	Wait to one jumper volume has been displaced
8	Close valve 4 and stop pump
9	Close valve 15

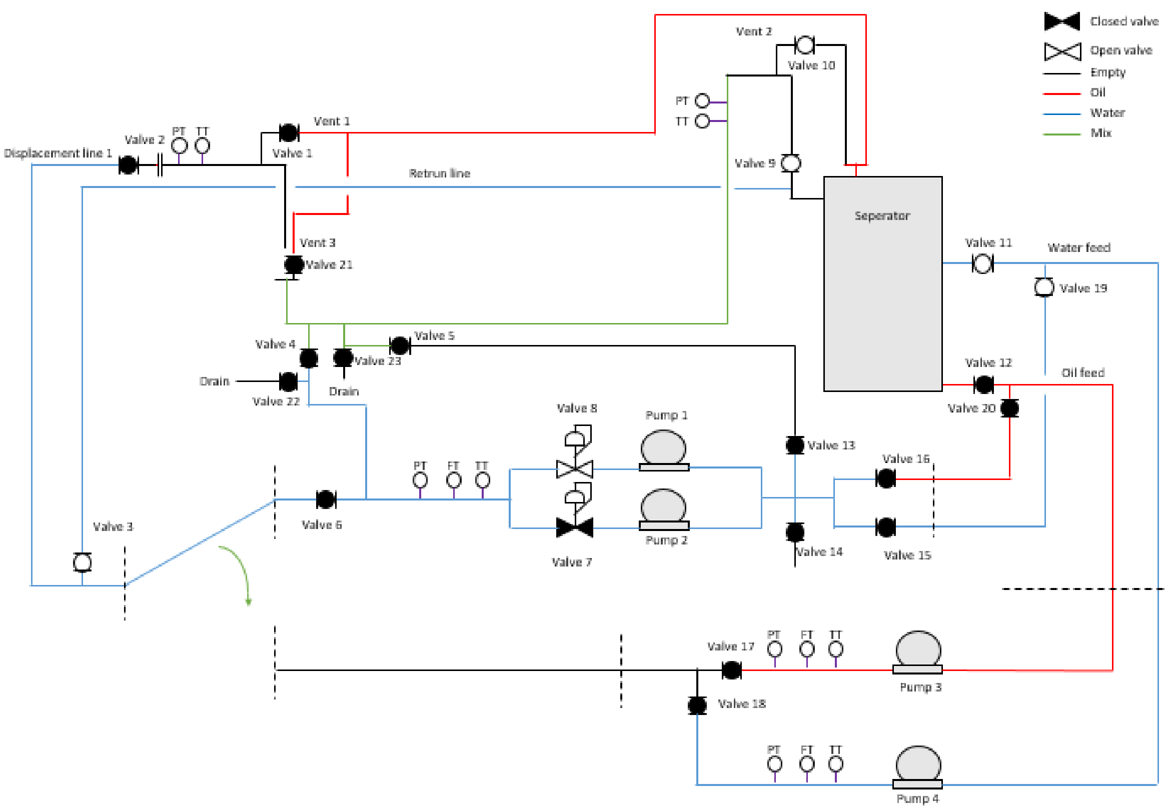

Step	Operation
10	Wait until the water and oil is completely separated
11	Open valve 5
12	Open valve 13
13	Open valve 6
14	Open Valve 21
15	Start pump 1, set rate to 2 m3/h
16	Monitor remaining water in jumper

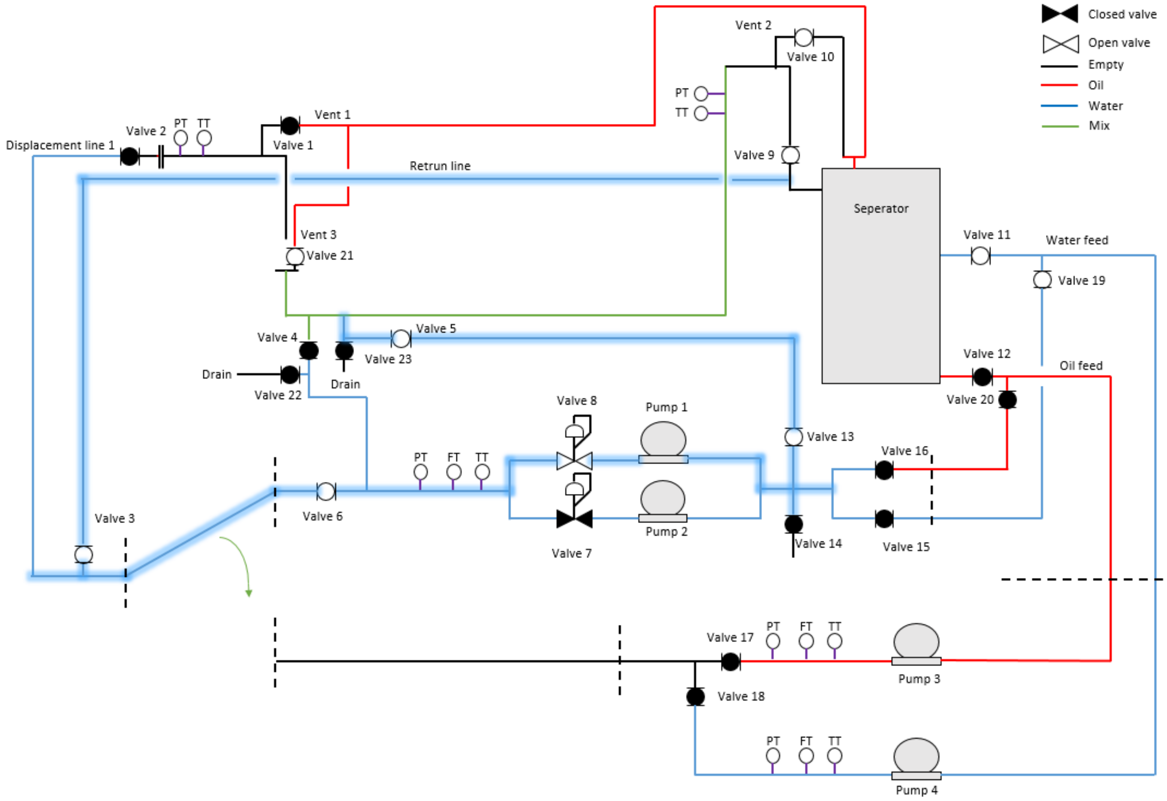

Step	Operation
17	Close valve 13 and stop pump once remaining water is low
18	Close valve 5
19	Open valve 23
20	Measure remaining oil

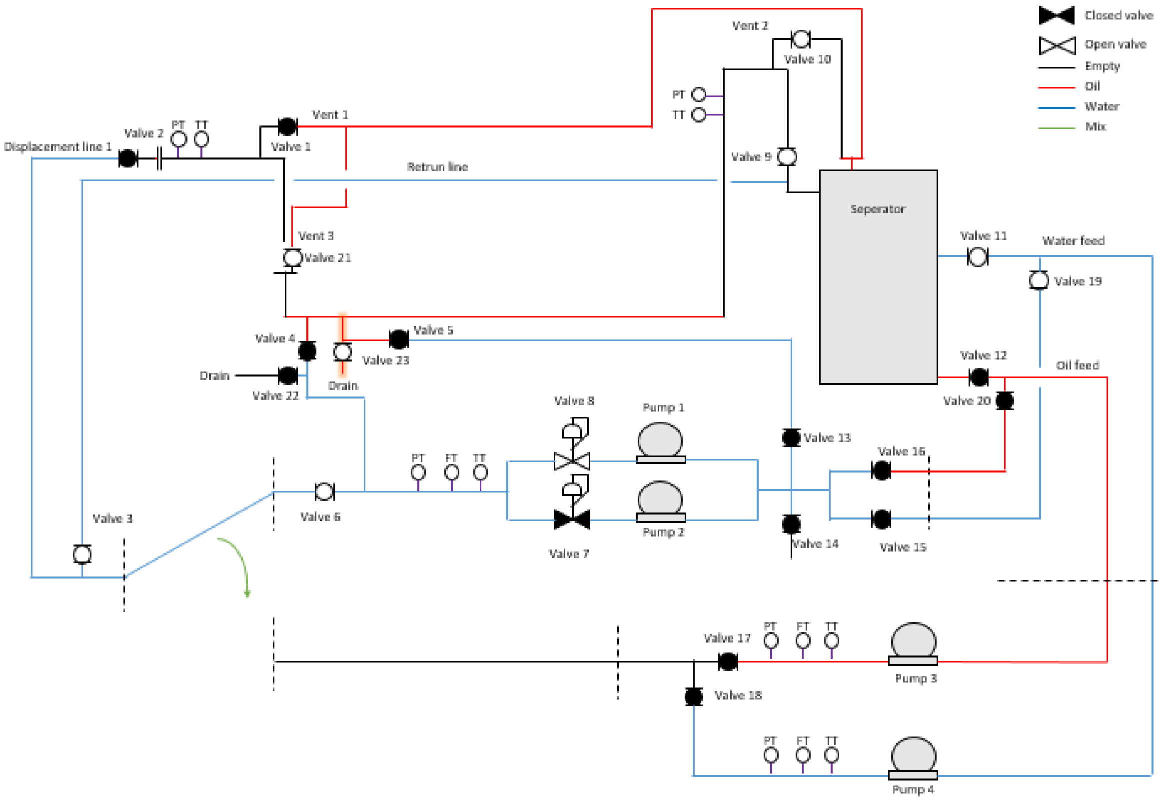

Step	Operation
21	Once jumper is completely empty, reestablish initial conditions
22	Repeat step 1 to 6
23	Wait until two jumper volumes has been displaced
24	Repeat step 8 to 17
25	Repeat step 1 to 6
26	Wait until three jumper volumes has been displaced
27	Repeat step 8 to 16
28	Experiment finished

2.2 Oil displacing water

Table 29 - Shows the initial valve status

Valve	Status

Valve 3	Open
Valve 6	Open
Valve 7	(Open)
Valve 8	Open
Valve 9	Open
Valve 10	Open
Valve 12	Open
Valve 16	Open
Valve 20	Open

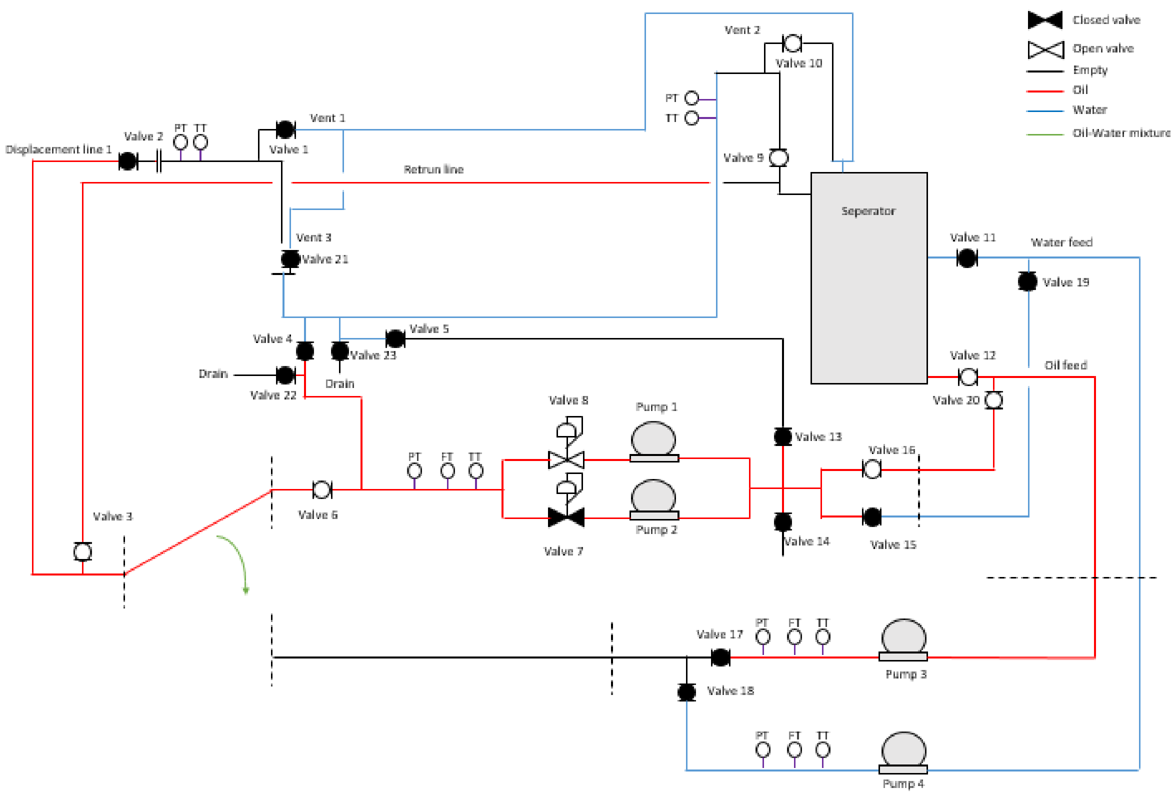

Step	Operation

1	Put valves in initial status
2	Start pump(s), and adjust flow to desired rate
3	Wait to flow stabilizes

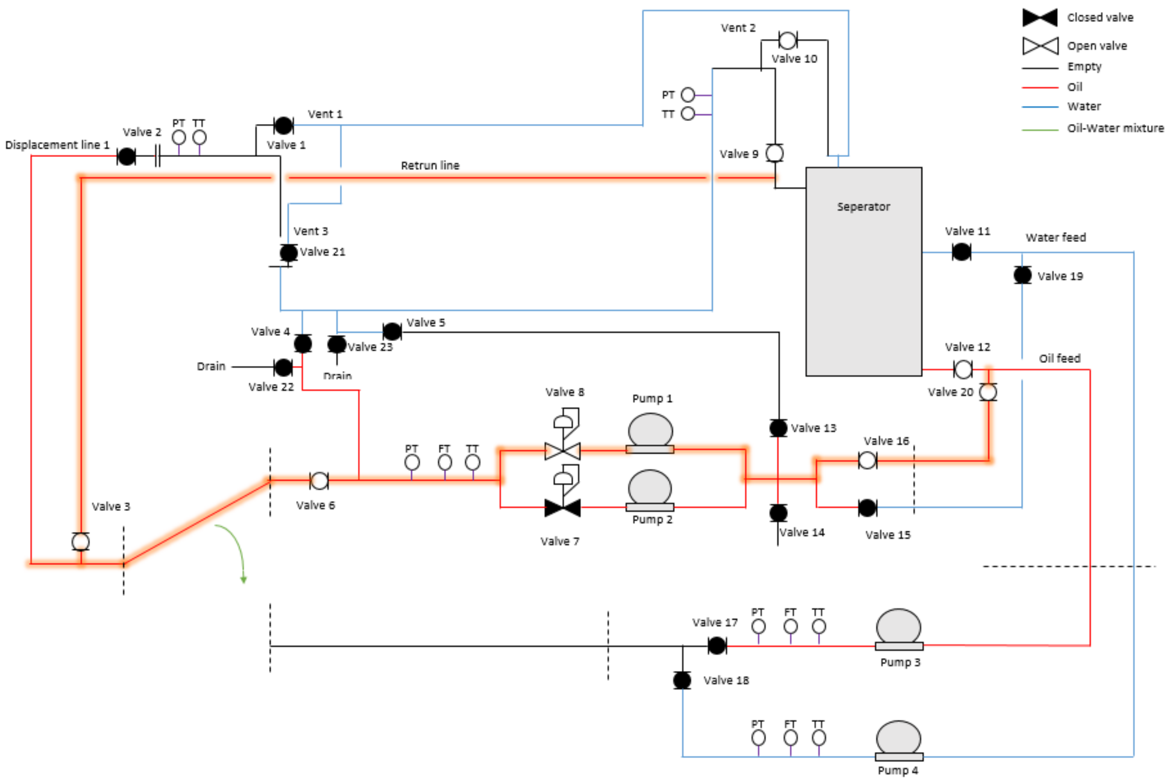

Step	Operation
4	Close valve 6
5	Open Valve 4
6	Monitor accumulated flow

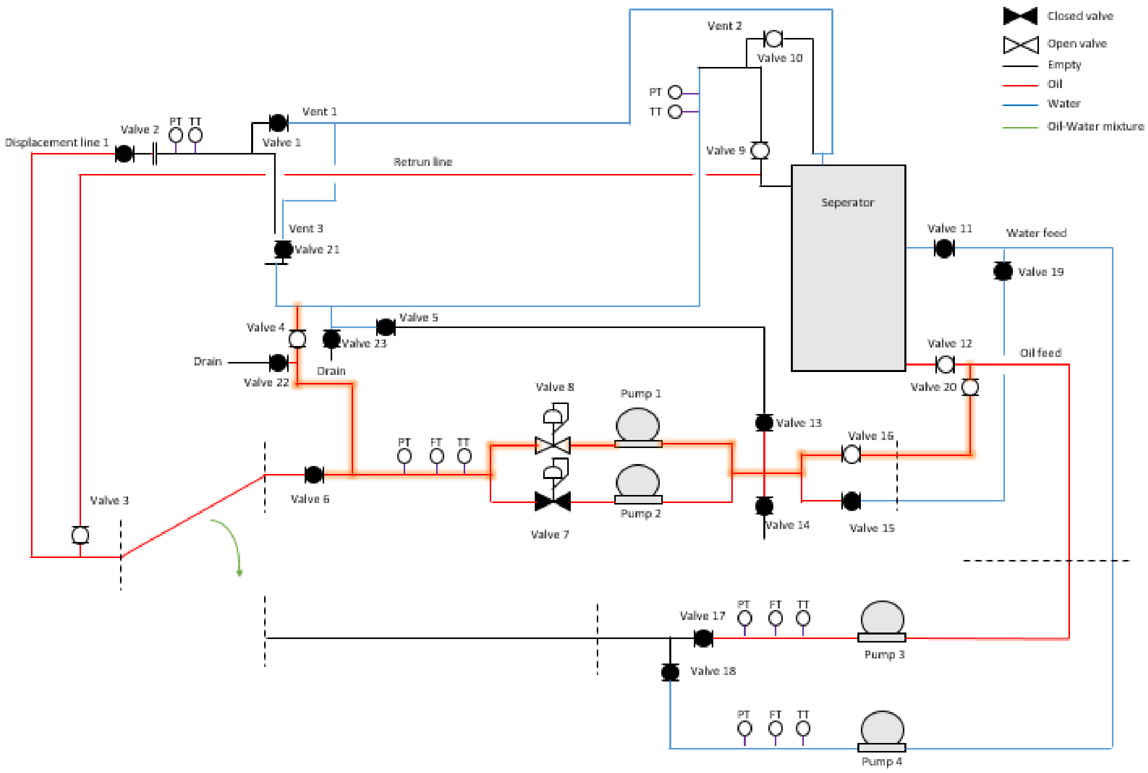

Step	Operation
7	Wait to one jumper volume has been displaced
8	Close valve 4 and stop pump
9	Close valve 16

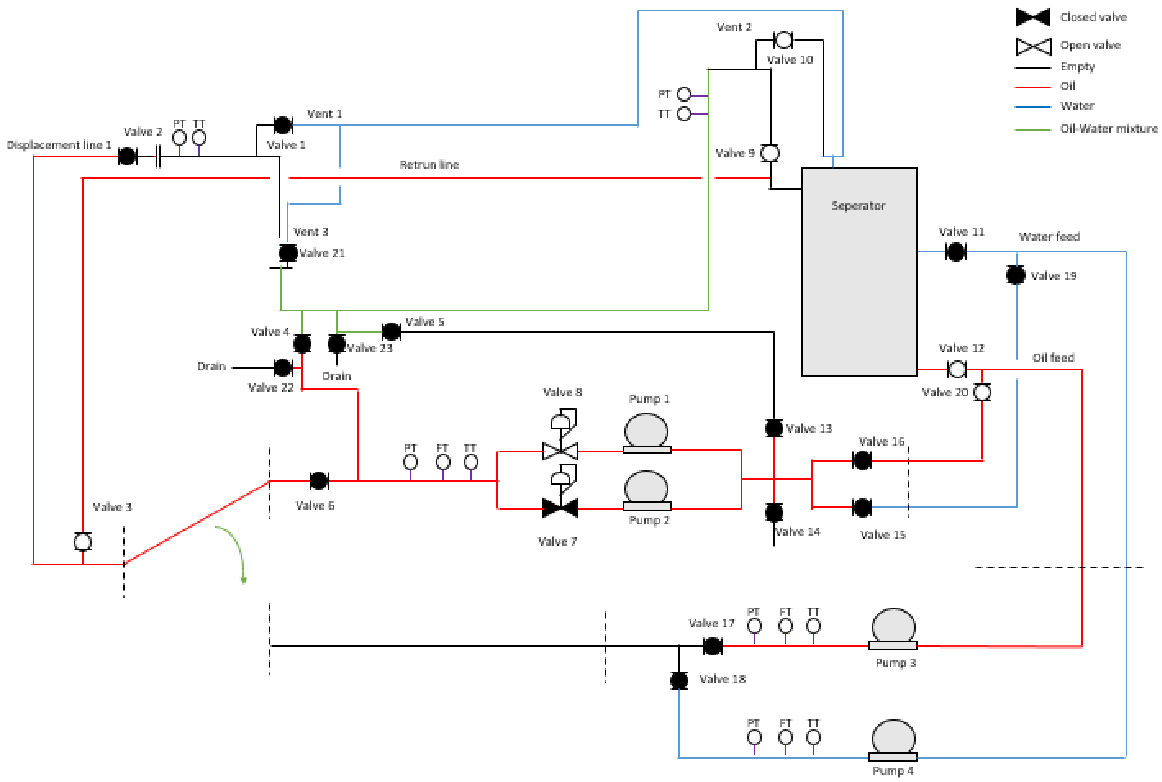

Step	Operation
10	Wait until the water and oil is completely separated
11	Open valve 21
12	Open Valve 23
13	Measure remaining water

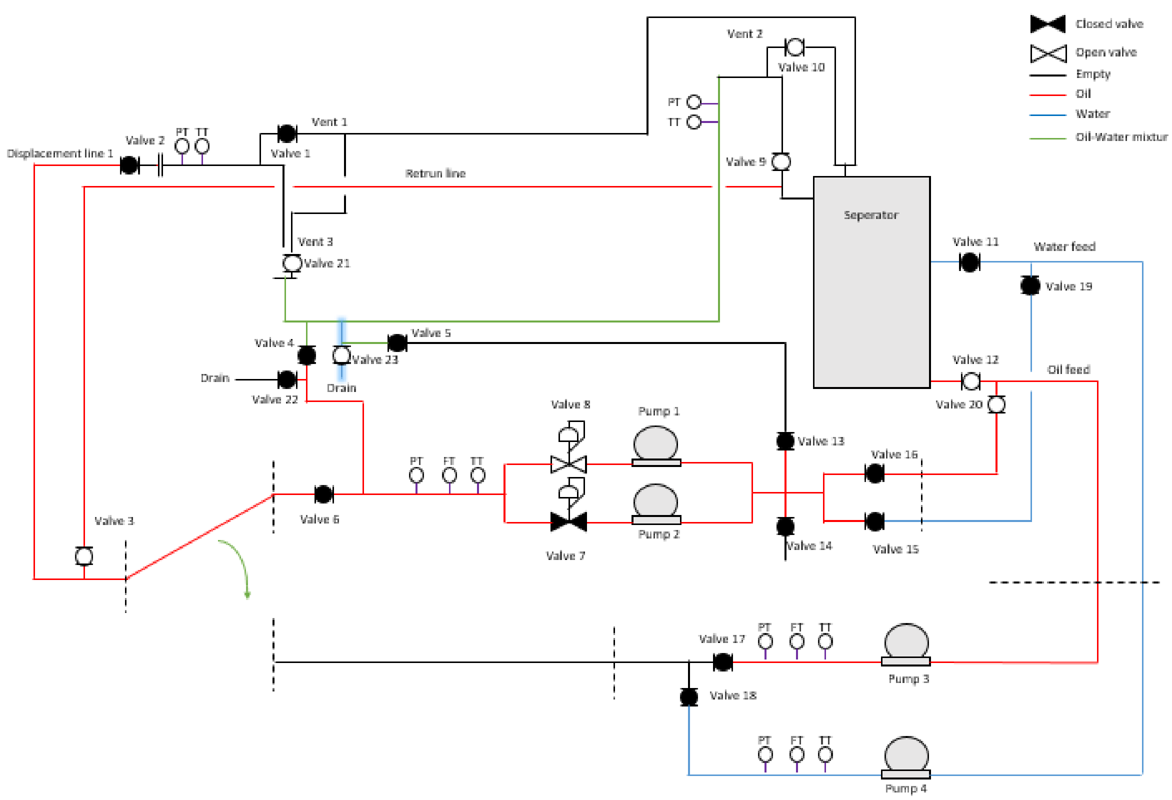

Step	Operation
14	Close valve 23
15	Open valve 5
16	Open valve 13
17	Open valve 6
18	Start pump 1, set rate to 2 m3/h
19	Run pump until jumper is empty

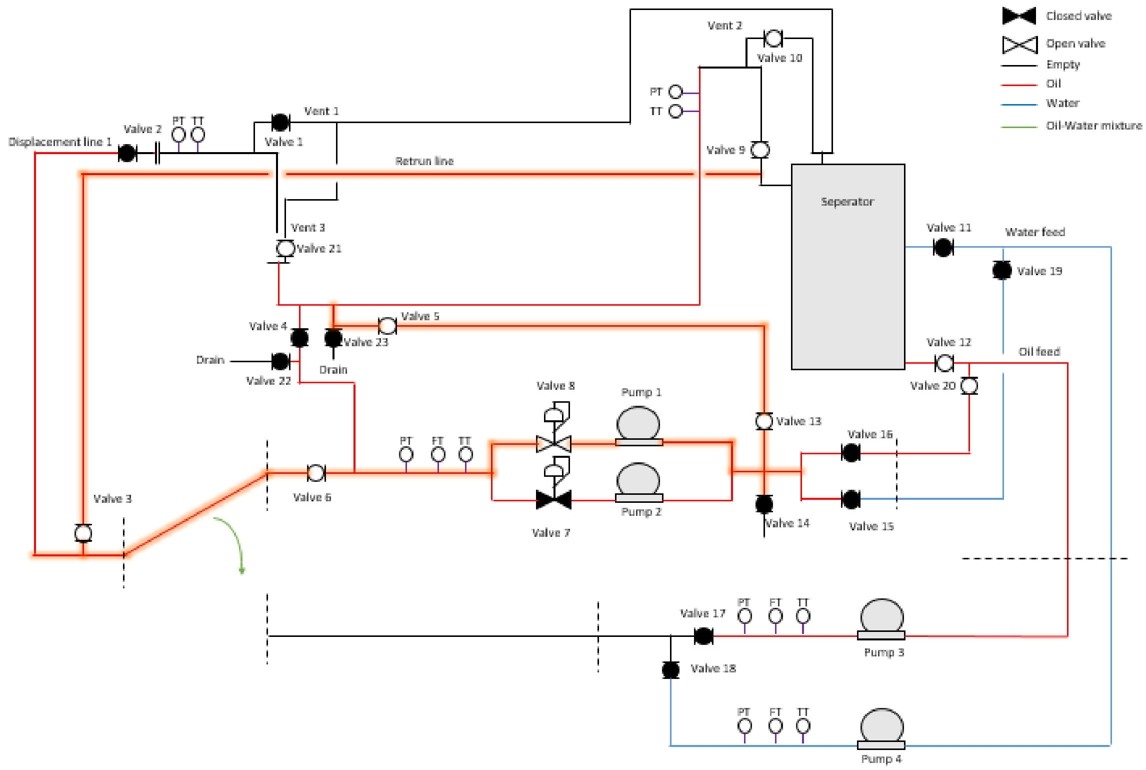

Step	Operation
20	Reestablish initial conditions
21	Repeat step 1 to 6
22	Wait until two jumper volumes has been displaced
23	Repeat step 8 to 17
24	Repeat step 1 to 6
25	Wait until three jumper volumes has been displaced
26	Repeat step 8 to 16
27	Experiment finished

3 Displacement trough top inlet

Displacement trough the top inlet is done using the low-flow pumps or high-flow pumps with four different flowrates, rates and pumps used can be seen in *Table 30* bellow. The pumps accept both oil and water as input liquid, but the turbine meter needs to be calibrated to the specific liquid. Before starting the displacement procedures, the piping surrounding the pumps shall be emptied, to ensure that pure displacement liquid is used.

Table 30 - Shows the displacement rates for the top inlet

Test number	**Displacement rate [m3/h]**	**Pump used**
1	6	Pump 1
2	11	Pump 1 & pump 2
3	20	Pump 3 / Pump 4
4	30	Pump 3 / Pump 4

3.1 Water displacing oil with low-flow pump(s)

Table 31 - Show initial valve status

Valve	Status
Valve 3	Open
Valve 6	Open
Valve 7	(Open)
Valve 8	Open
Valve 9	Open
Valve 10	Open
Valve 11	Open
Valve 15	Open
Valve 19	Open

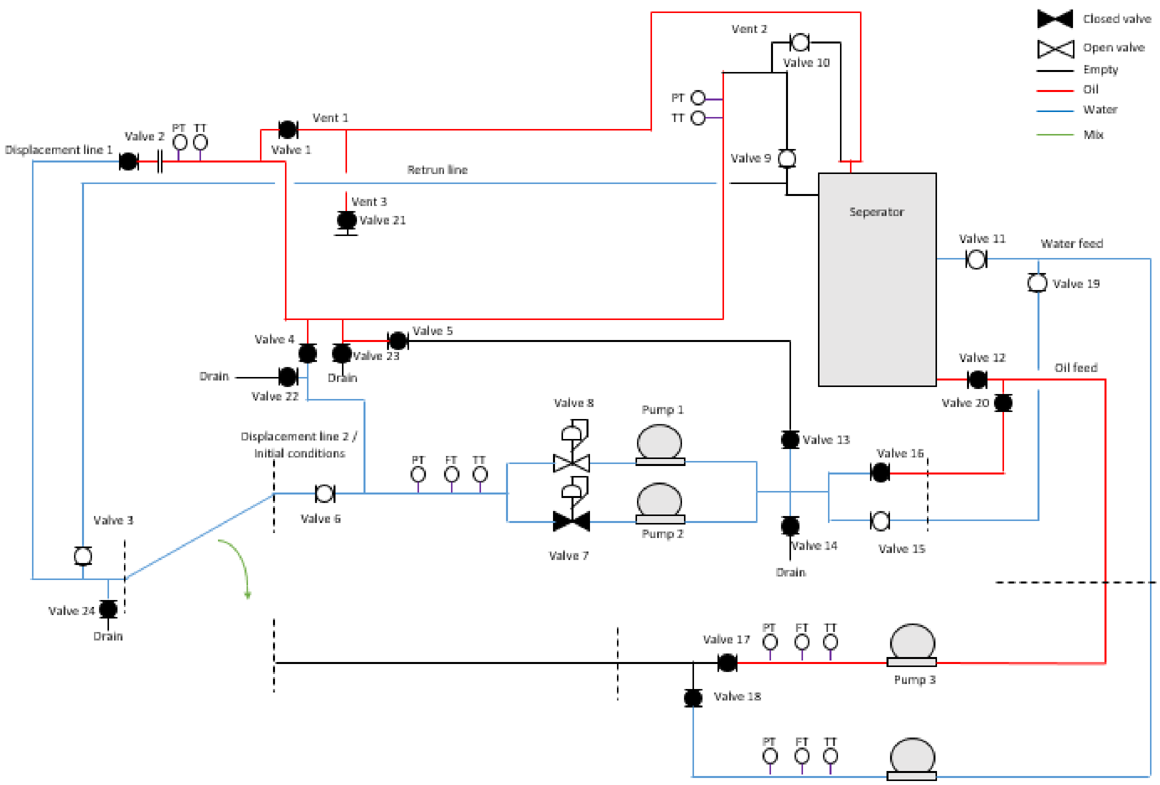

Step	Operation
1	Put valves in initial status
2	Start pump 1(2), and adjust flow to desired rate

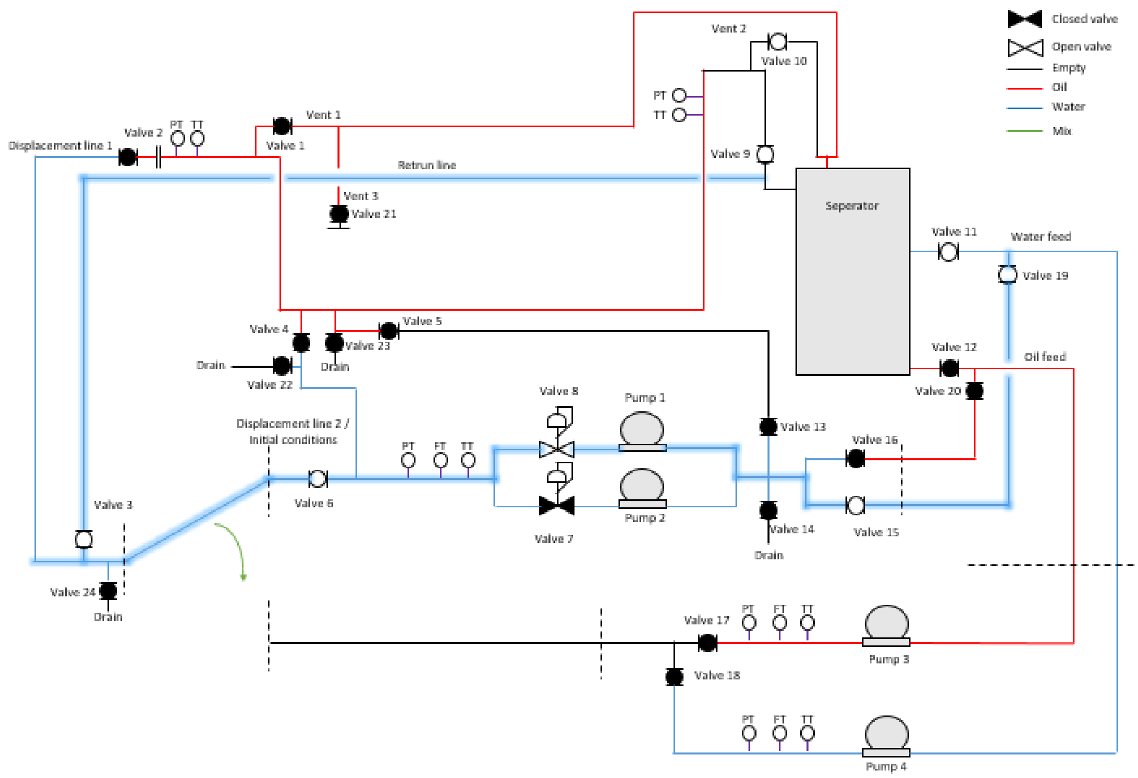

Step	Operation
3	Wait to flow stabilizes
4	Close valve 3
5	Open Valve 2
6	Monitor accumulated flow

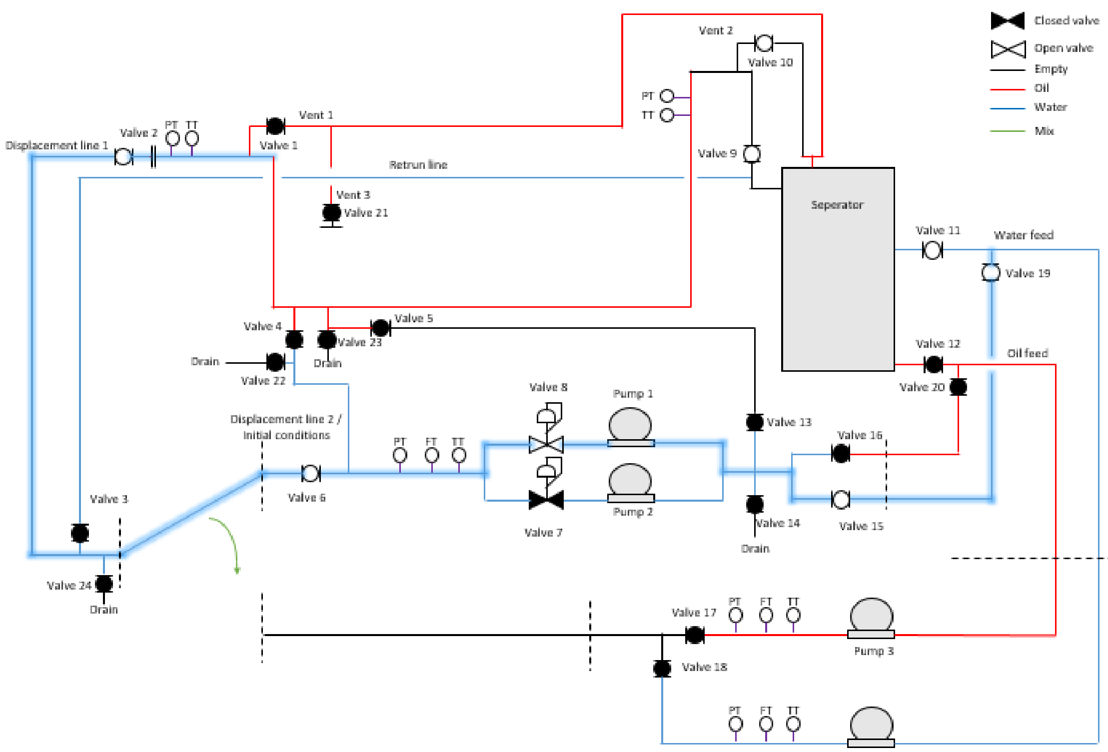

Step	Operation
7	Wait until one jumper volume has been displaced
8	Close valve 2 and stop pump

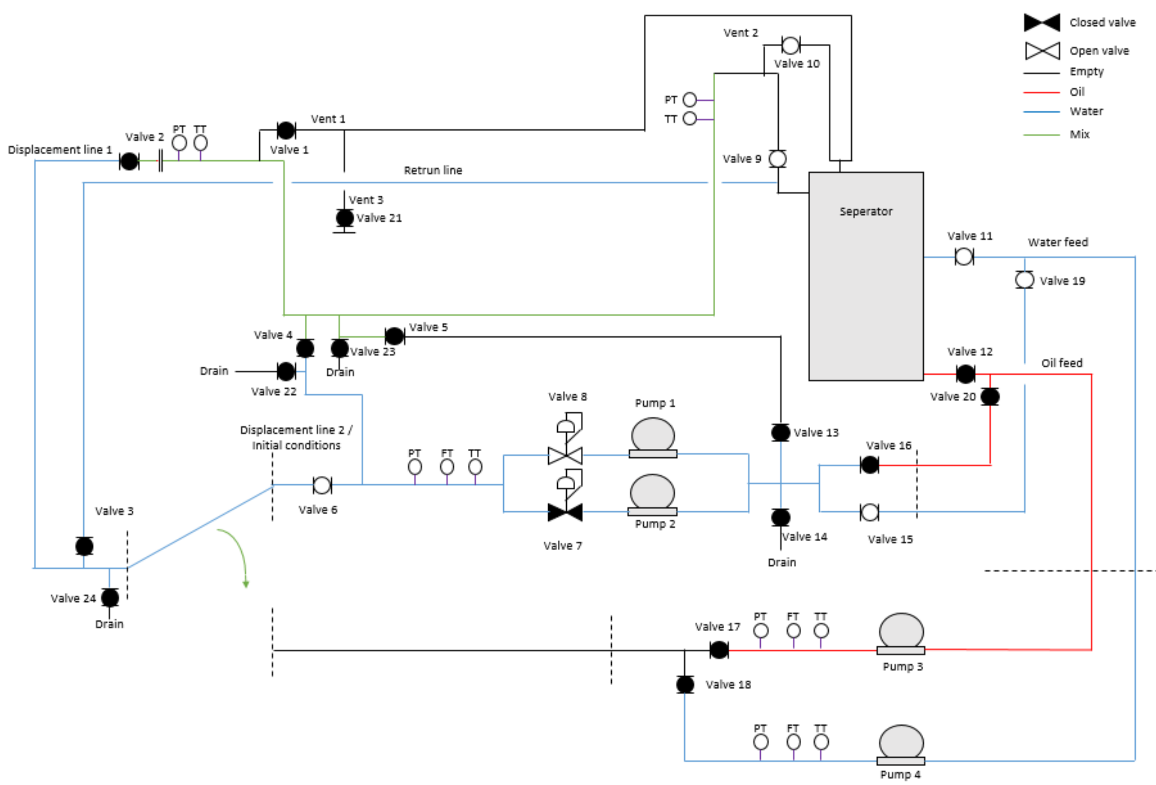

Step	Operation
9	Wait until the water and oil is completely separated
10	Close valve 15
11	Open valve 5
12	Open valve 13
13	Open Valve 3
14	Open Valve 1
15	Start pump 1, set rate to 2 m3/h
16	Monitor remaining water in jumper

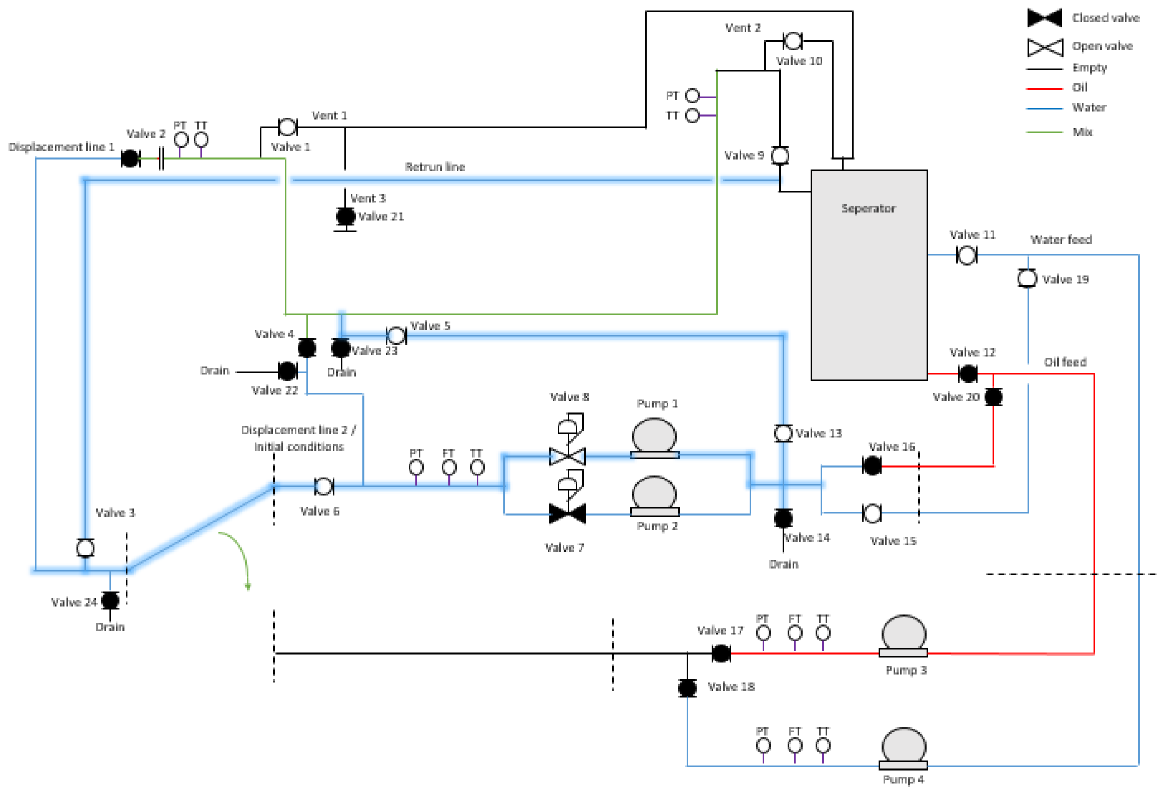

Step	Operation
17	Close valve 5 and stop pump once remaining water is low
18	Open valve 23 and measure remaining oil

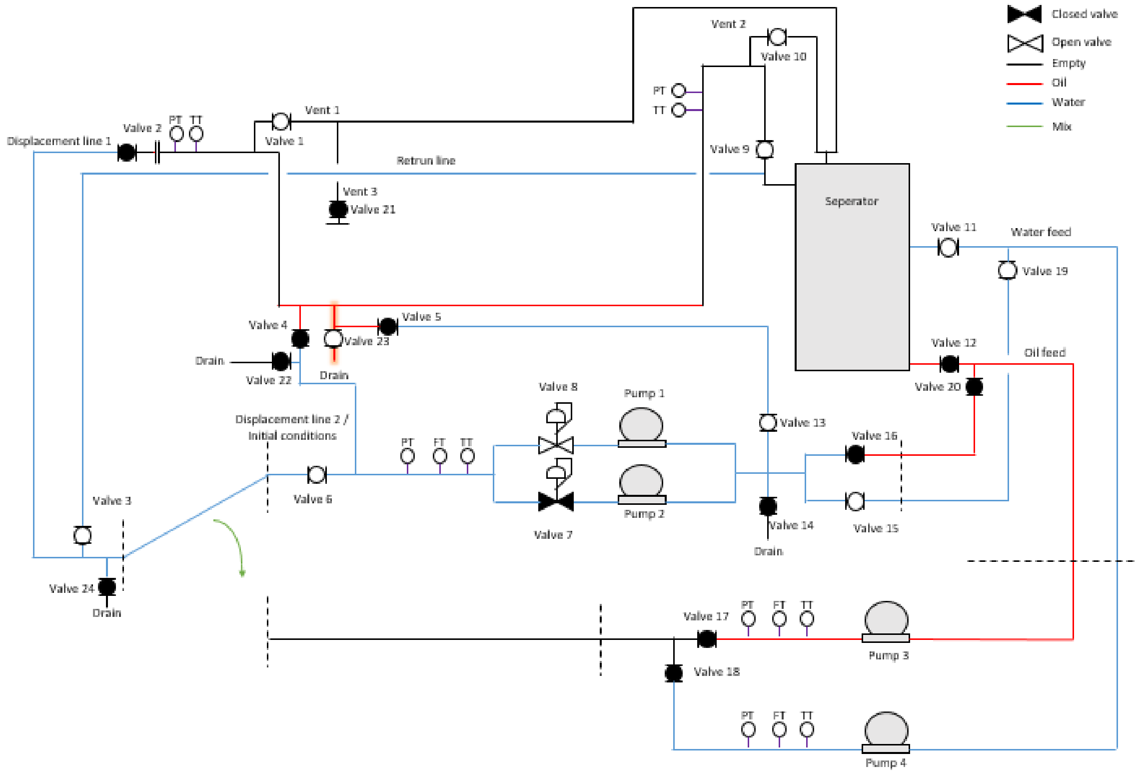

Step	Operation
19	Reestablish initial conditions
20	Repeat step 1 to 6
21	Wait until two jumper volumes has been displaced
22	Repeat step 8 to 17
23	Repeat step 1 to 6
24	Wait until three jumper volumes has been displaced
25	Repeat step 8 to 16
26	Experiment finished

3.2 Oil displacing water with low-flow pump(s)

Table 32 - Shows initial valve status

Valve	Status
Valve 3	Open
Valve 6	Open
Valve 7	(open)
Valve 8	Open
Valve 9	Open
Valve 10	Open
Valve 12	Open
Valve 16	Open
Valve 20	Open

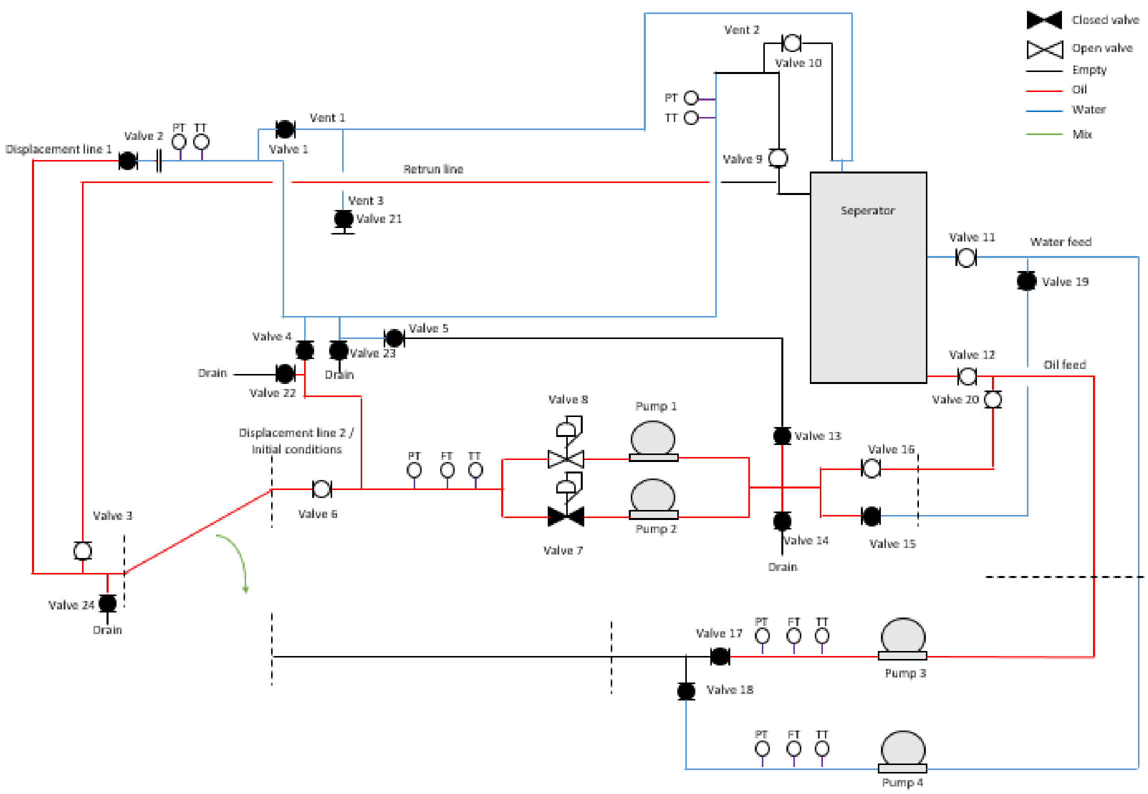

Step	Operation
1	Put valves in initial status
2	Start pump 1(2), and adjust flow to desired rate

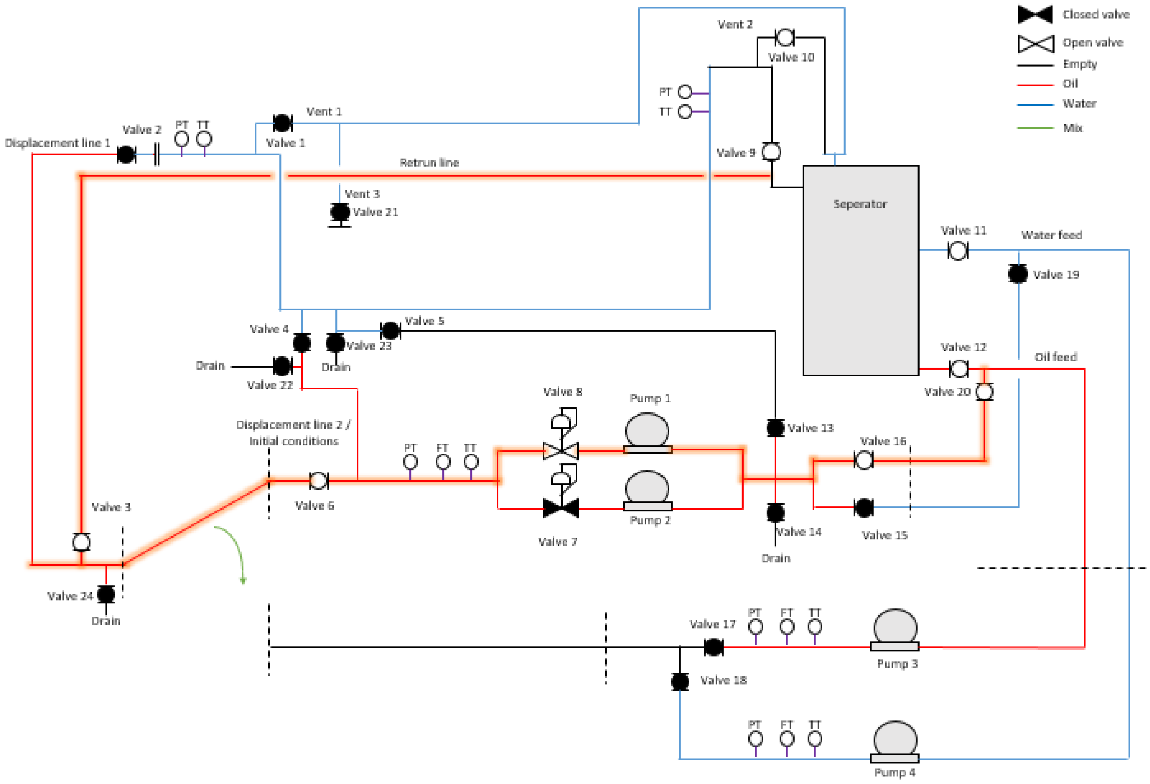

Step	Operation
3	Wait to flow stabilizes
4	Close valve 3
5	Open Valve 2
6	Monitor accumulated flow

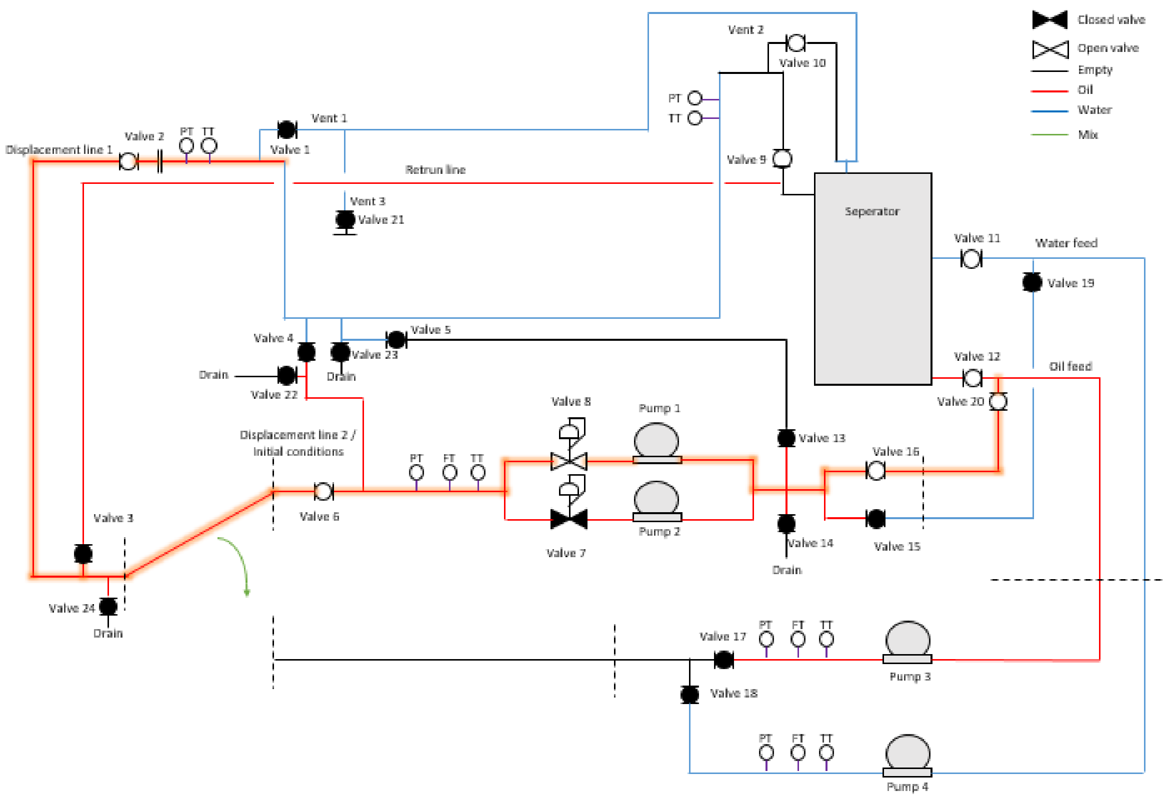

Step	Operation
7	Wait to one jumper volume has been displaced
8	Close valve 2 and stop pump
9	Close valve 16

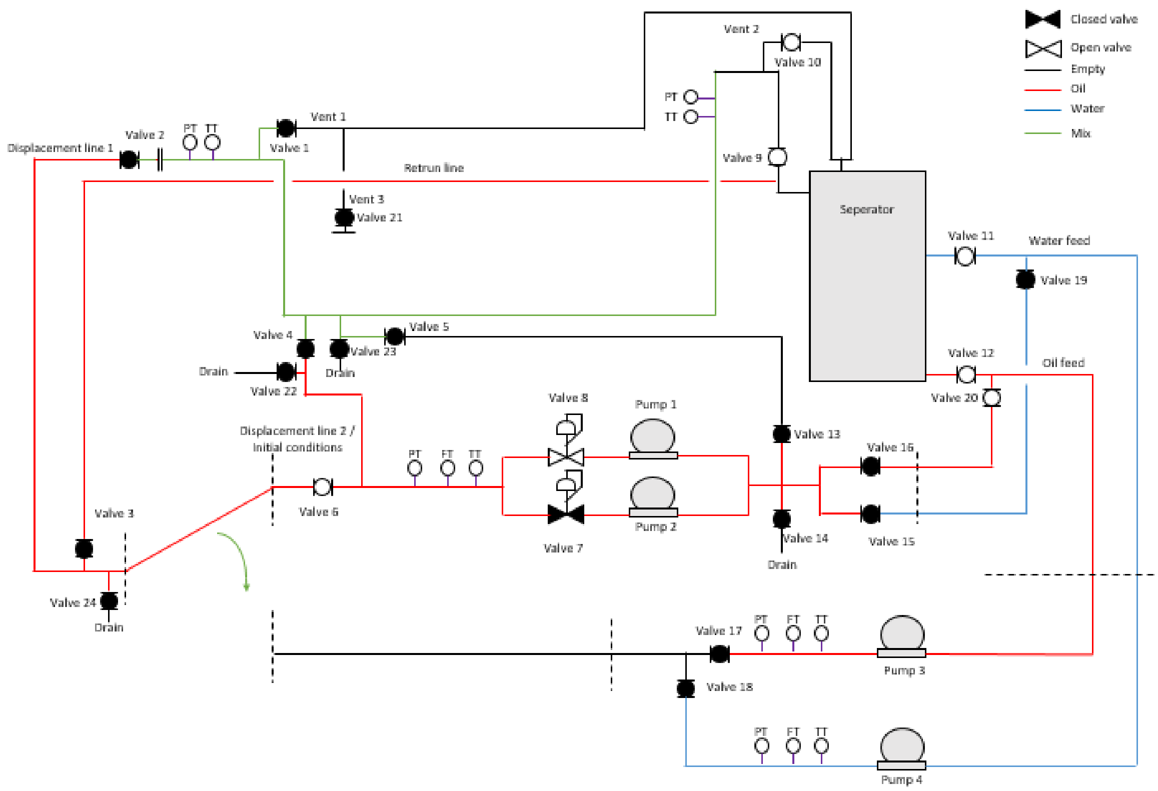

Step	Operation
9	Wait until the water and oil is completely separated
10	Open Valve 1
11	Open valve 23 and measure remaining water

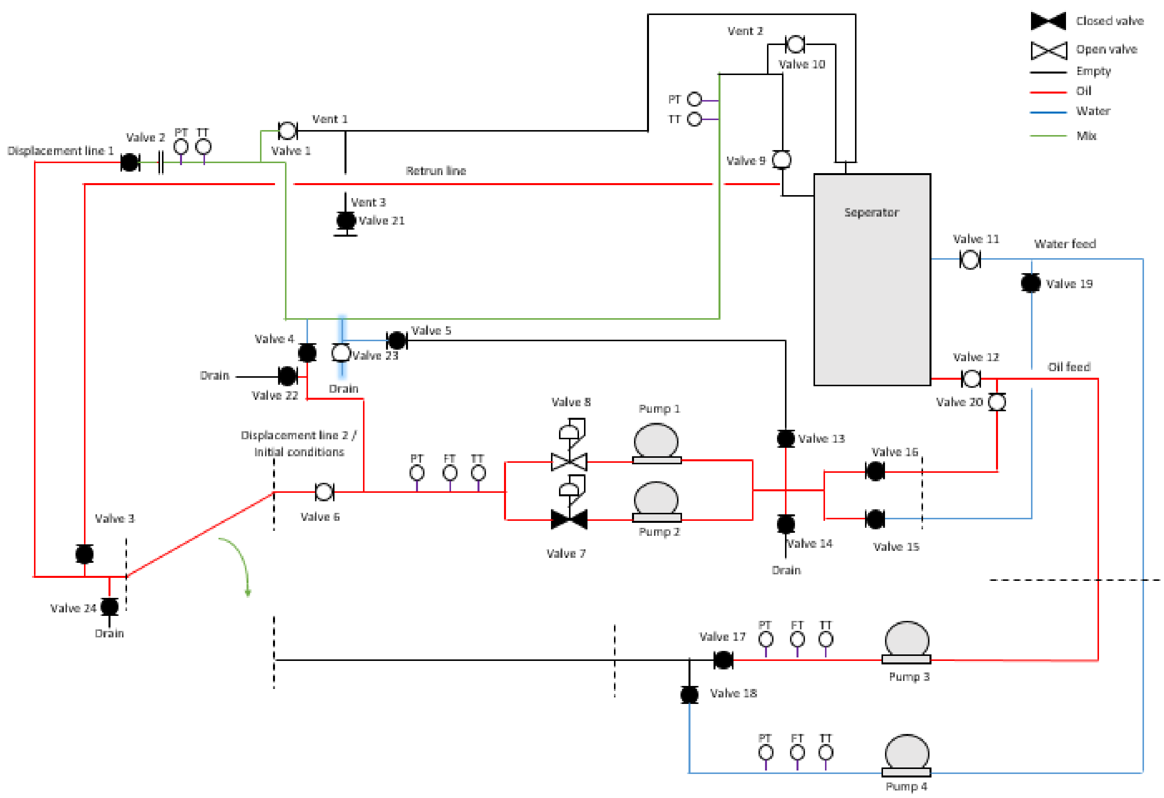

Step	Operation
12	Close valve 23
13	Open valve 5
14	Open valve 13
15	Open Valve 3
16	Start pump 1, set rate to 2 m3/h
17	Pump out remaining oil, stop pump once empty

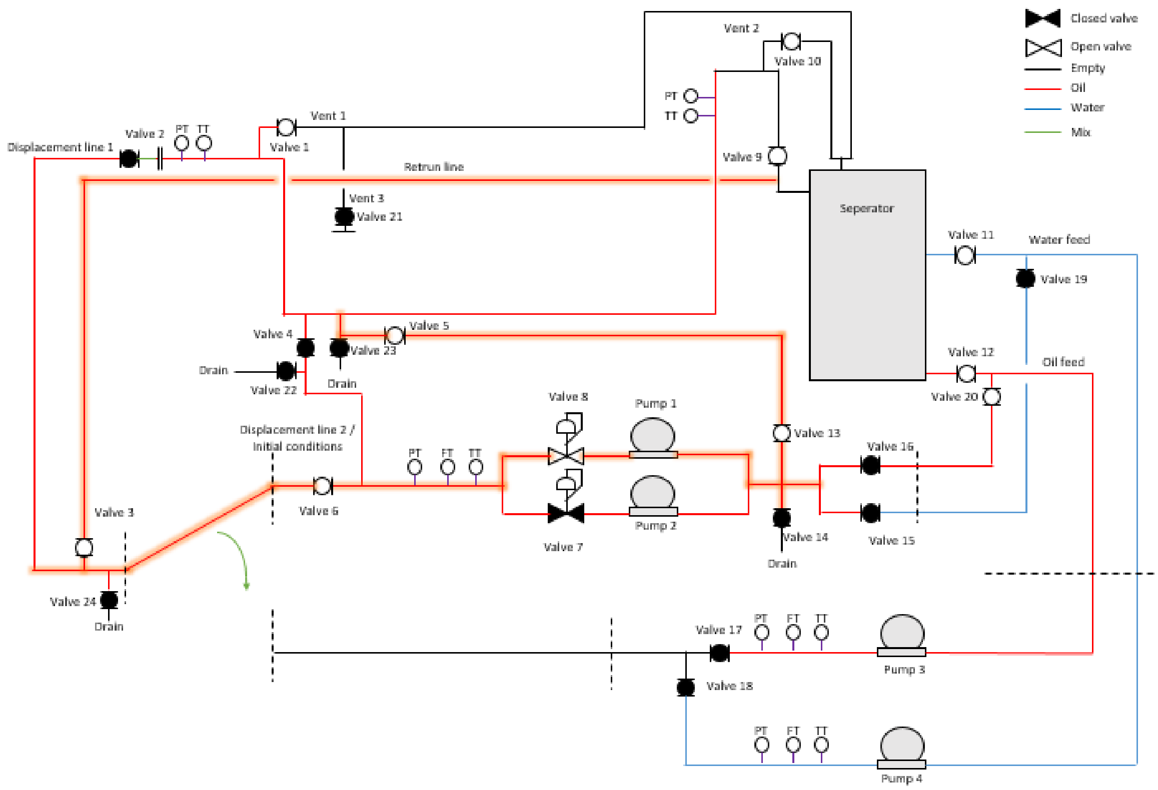

Step	Operation
18	Reestablish initial conditions
19	Repeat step 1 to 6
20	Wait until two jumper volumes has been displaced
21	Repeat step 8 to 17
22	Repeat step 1 to 6
23	Wait until three jumper volumes has been displaced
24	Repeat step 8 to 16
25	Experiment finished

3.3 Water displacing oil with high-flow pump

Table 33 - Show initial valve status

Valve	Status
Valve 3	Open

Valve 9	Open
Valve 10	Open
Valve 11	Open
Valve 18	Open

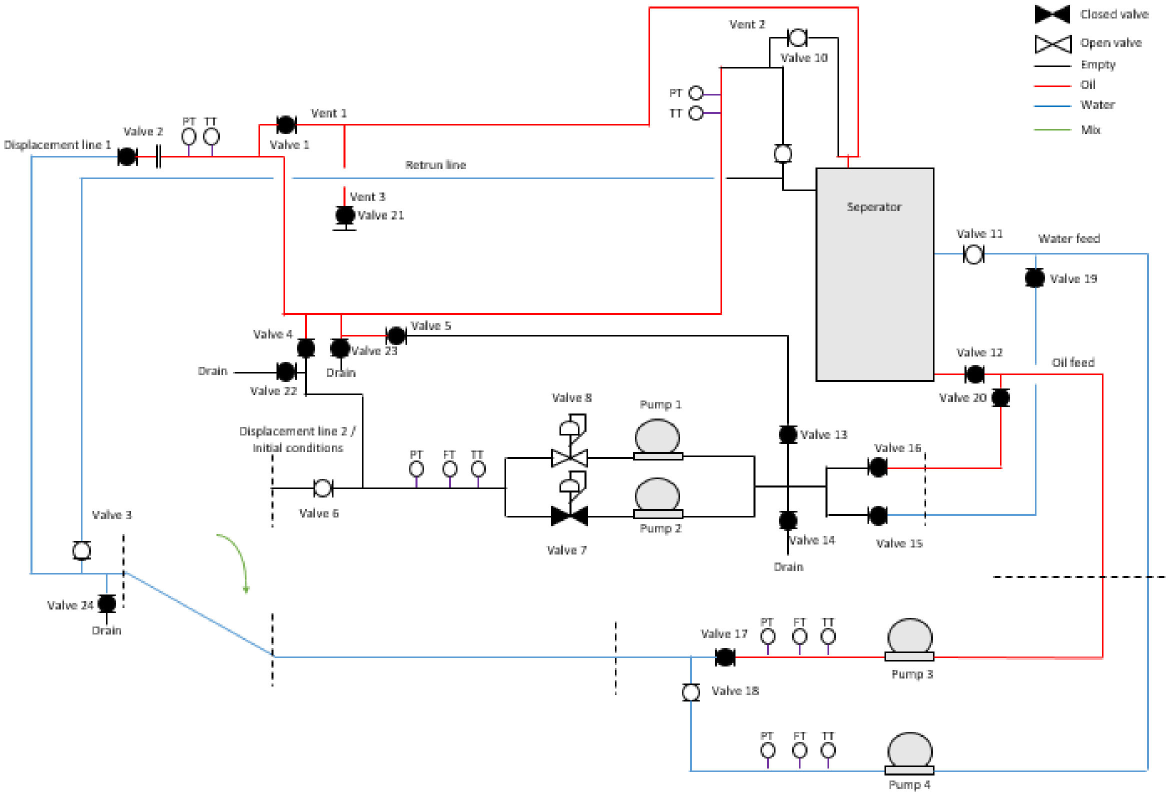

Step	Operation

1	Put valves in initial status
2	Start pump 4, and adjust flow to desired rate

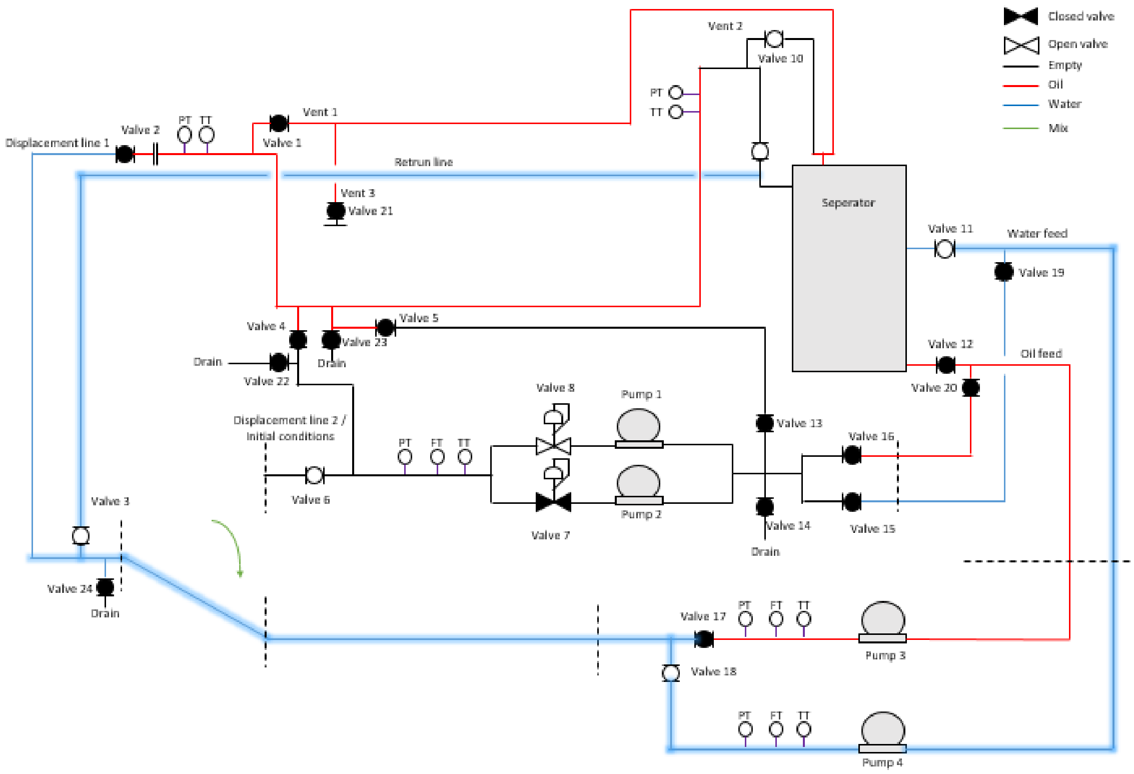

Step	Operation
3	Wait to flow stabilizes
4	Close valve 3
5	Open Valve 2
6	Monitor accumulated flow

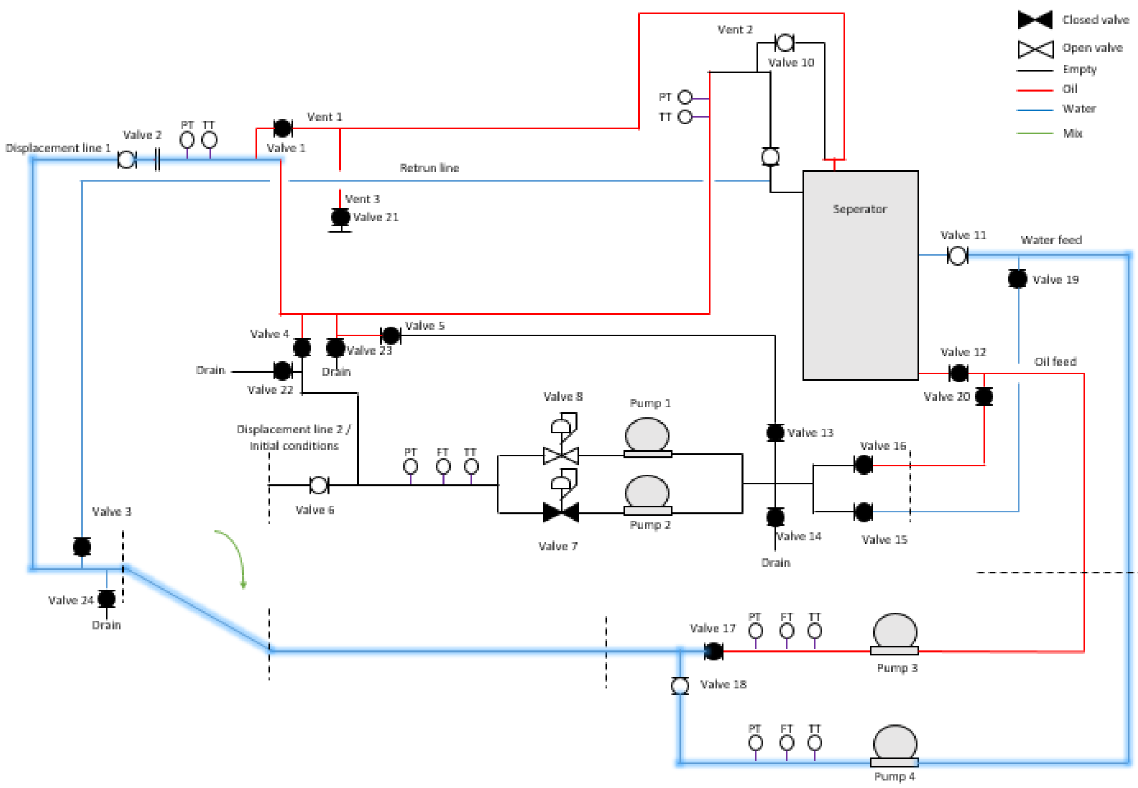

Step	Operation
7	Wait to one jumper volume has been displaced
8	Close valve 2 and stop pump
9	Close valve 18 and switch hos from high flow pump to low flow pump

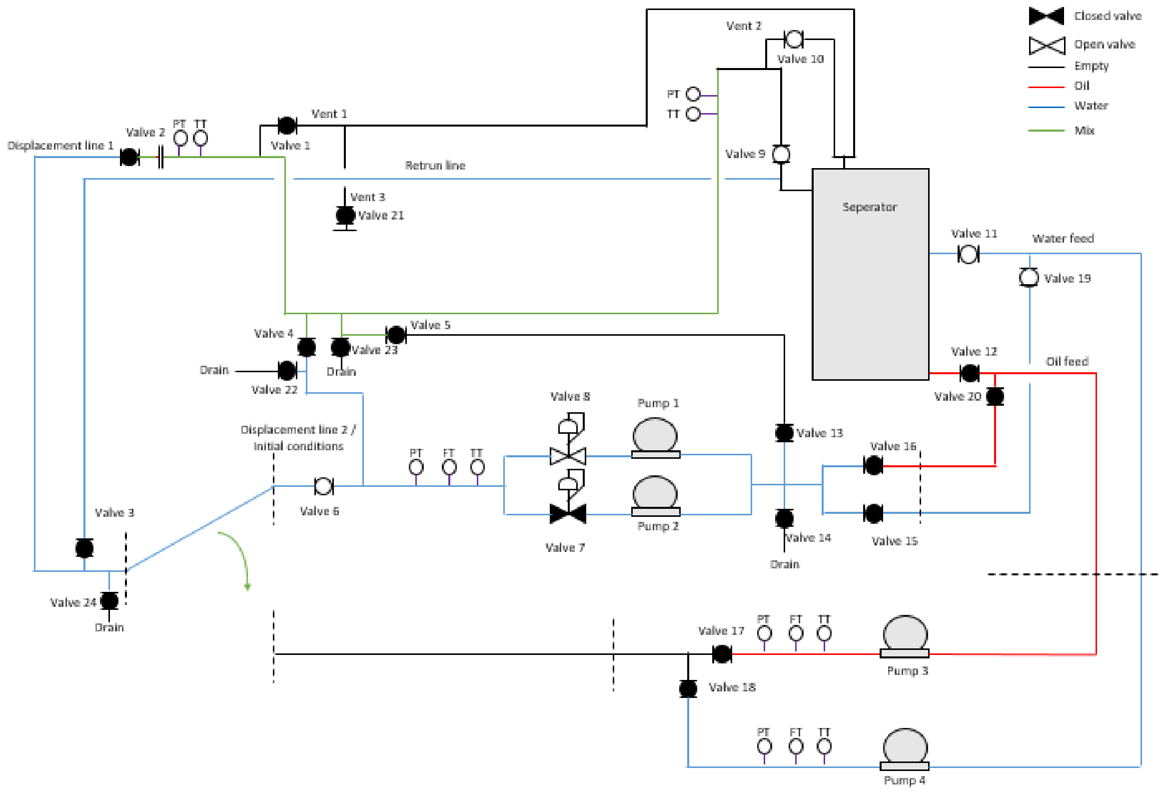

Step	Operation
10	Wait until the water and oil is completely separated
11	Ensure valve 6 is open
12	Open valve 5
13	Open valve 13
14	Open Valve 3
15	Open Valve 1
16	Start pump 1, set rate to 2 m3/h
17	Monitor remaining water in jumper

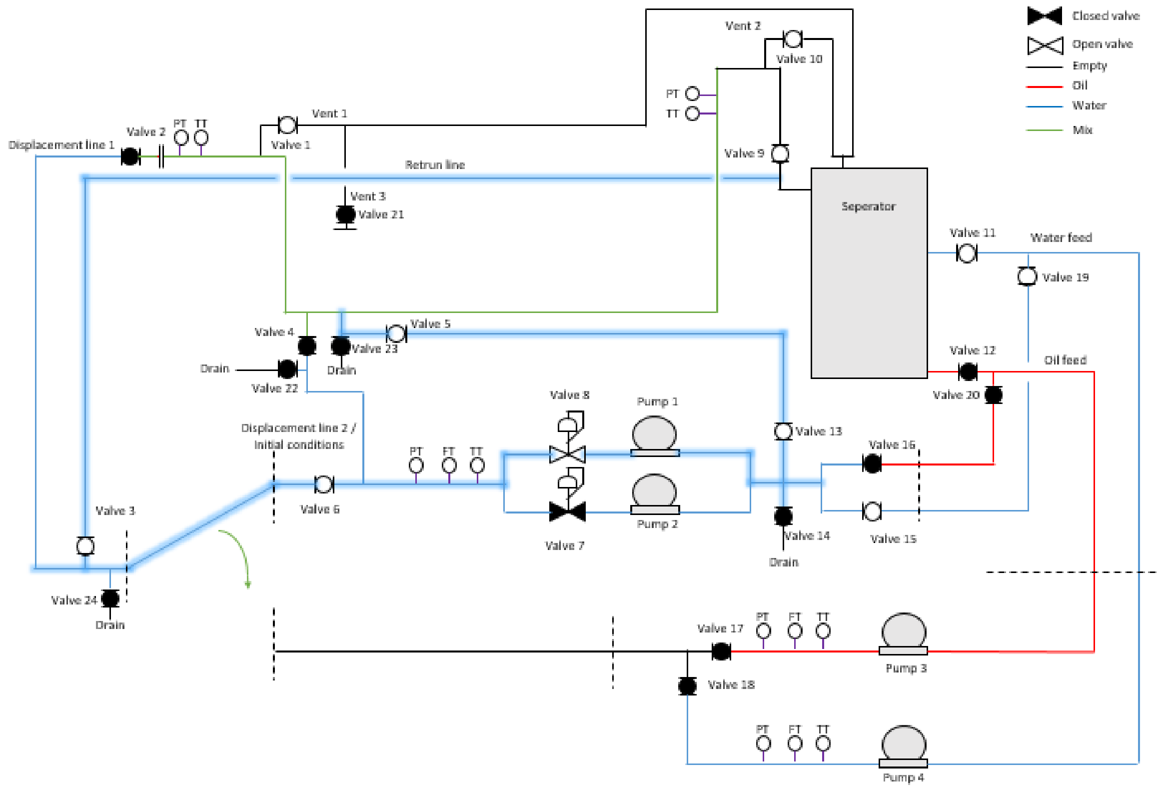

Step	Operation
18	Close valve 5 and stop pump once remaining water is low
19	Open valve 23 and measure remaining oil

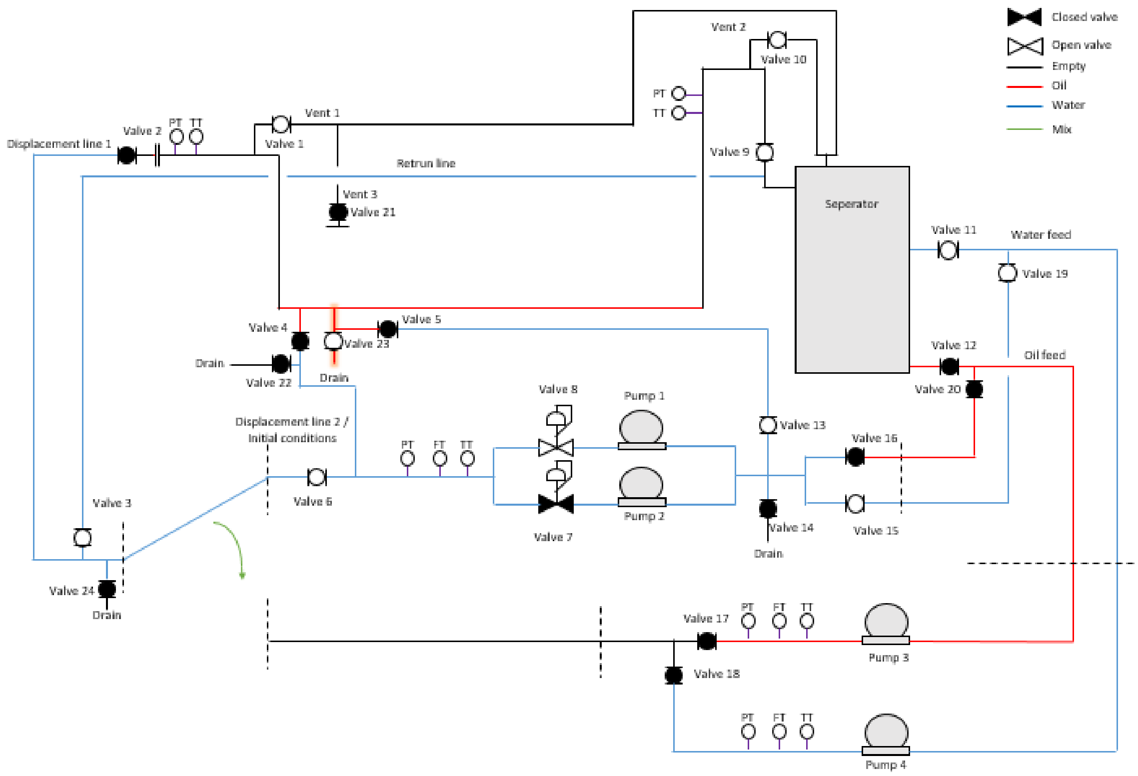

Step	Operation
20	Reestablish initial conditions
21	Repeat step 1 to 6
22	Wait until two jumper volumes has been displaced
23	Repeat step 8 to 17
24	Repeat step 1 to 6
25	Wait until three jumper volumes has been displaced
26	Repeat step 8 to 16
27	Experiment finished

3.4 Oil displacing water with low-flow pump

Table 34 - Shows initial valve status

Valve	Status
Valve 3	Open
Valve 9	Open
Valve 10	Open
Valve 12	Open
Valve 17	Open

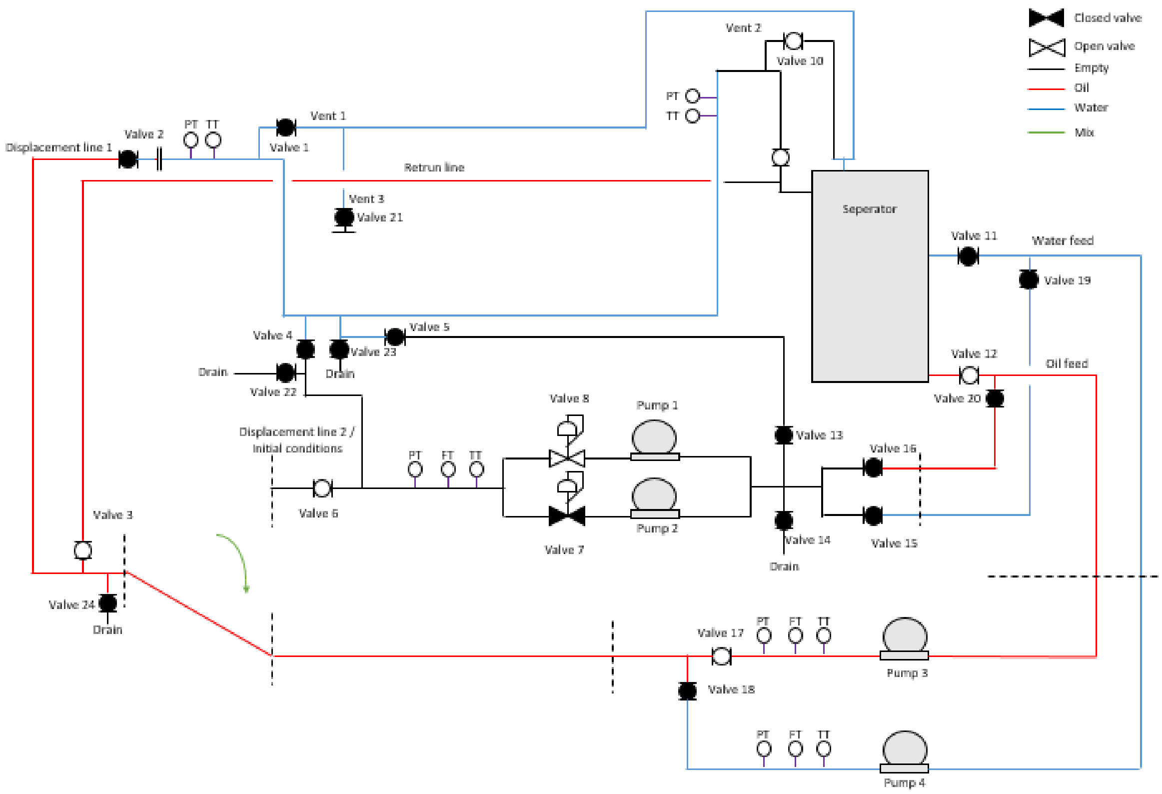

Step	Operation
1	Put valves in initial status
2	Start pump 3, and adjust flow to desired rate

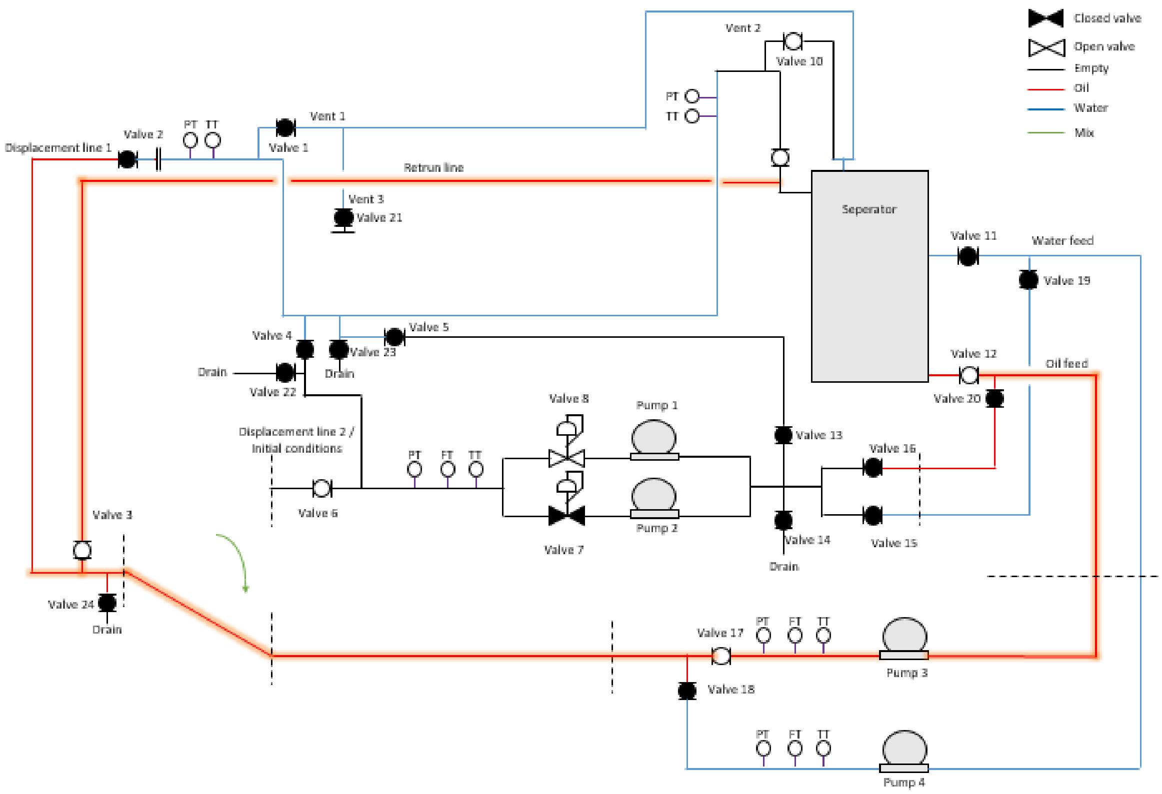

Step	Operation
3	Wait to flow stabilizes
4	Close valve 3
5	Open Valve 2
6	Monitor accumulated flow

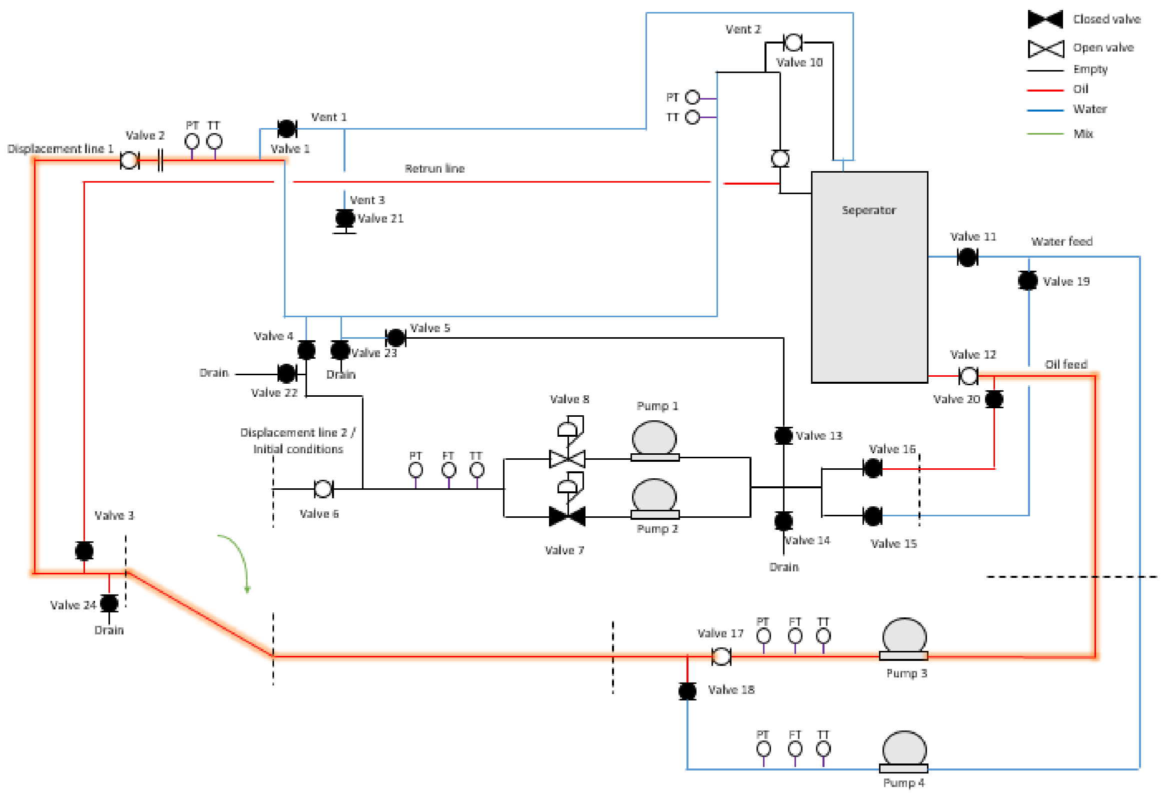

Step	Operation
7	Wait to one jumper volume has been displaced
8	Close valve 2 and stop pump
9	Close valve 17 and switch hose from high flow pump to low flow pump

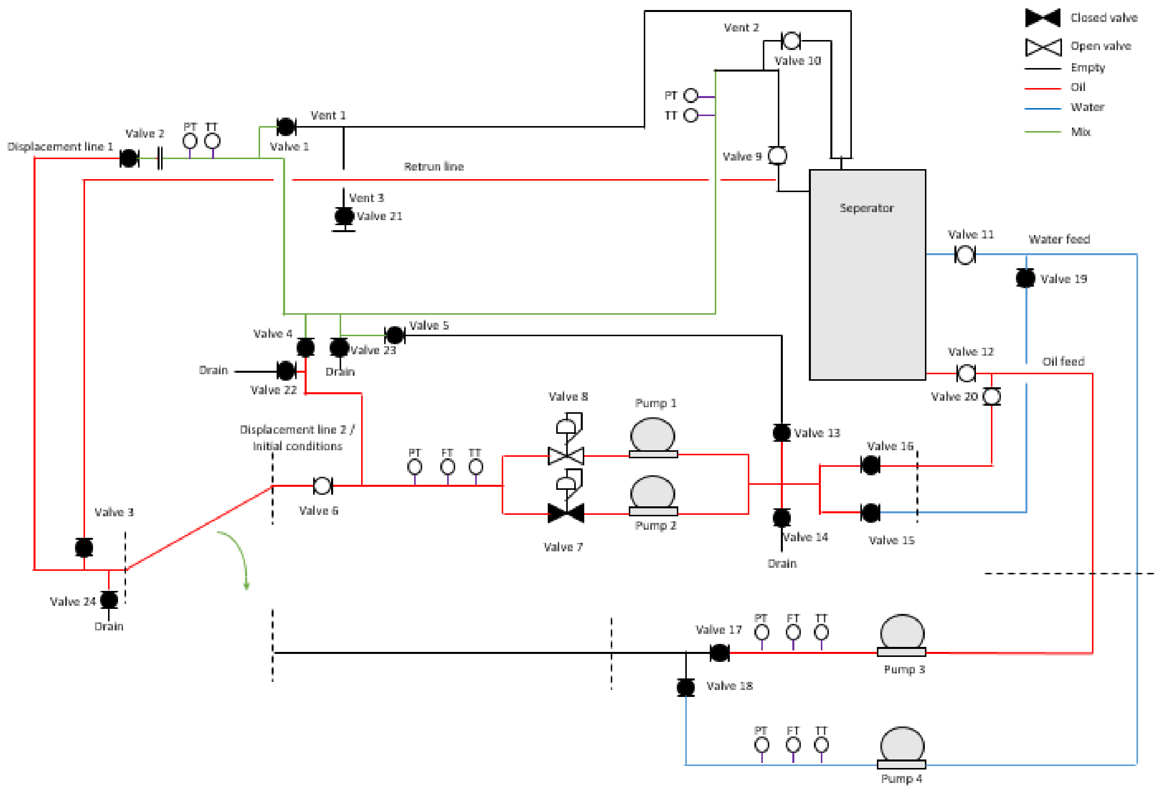

Step	Operation
9	Wait until the water and oil is completely separated
10	Open Valve 1
11	Open valve 23 and measure remaining water

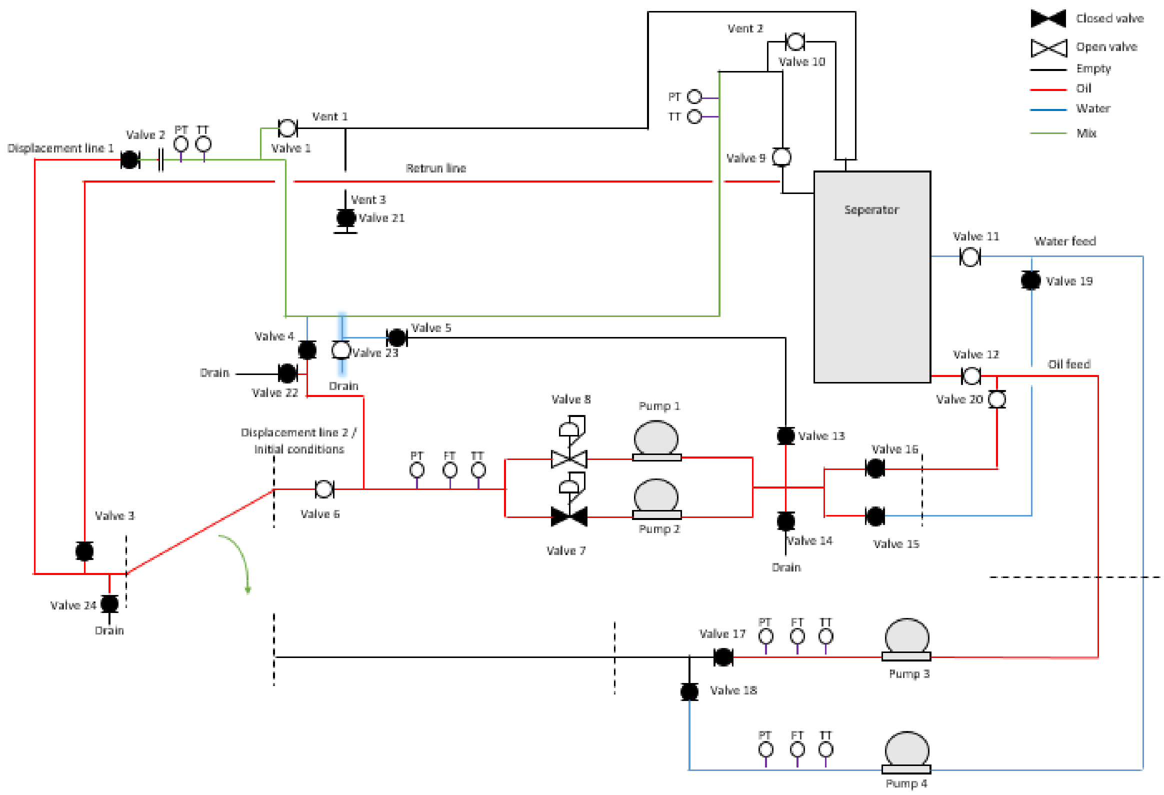

Step	Operation
12	Open valve 5
13	Open valve 13
14	Open Valve 3
15	Start pump 1, set rate to 2 m3/h
16	Pump out remaining oil, stop pump once empty

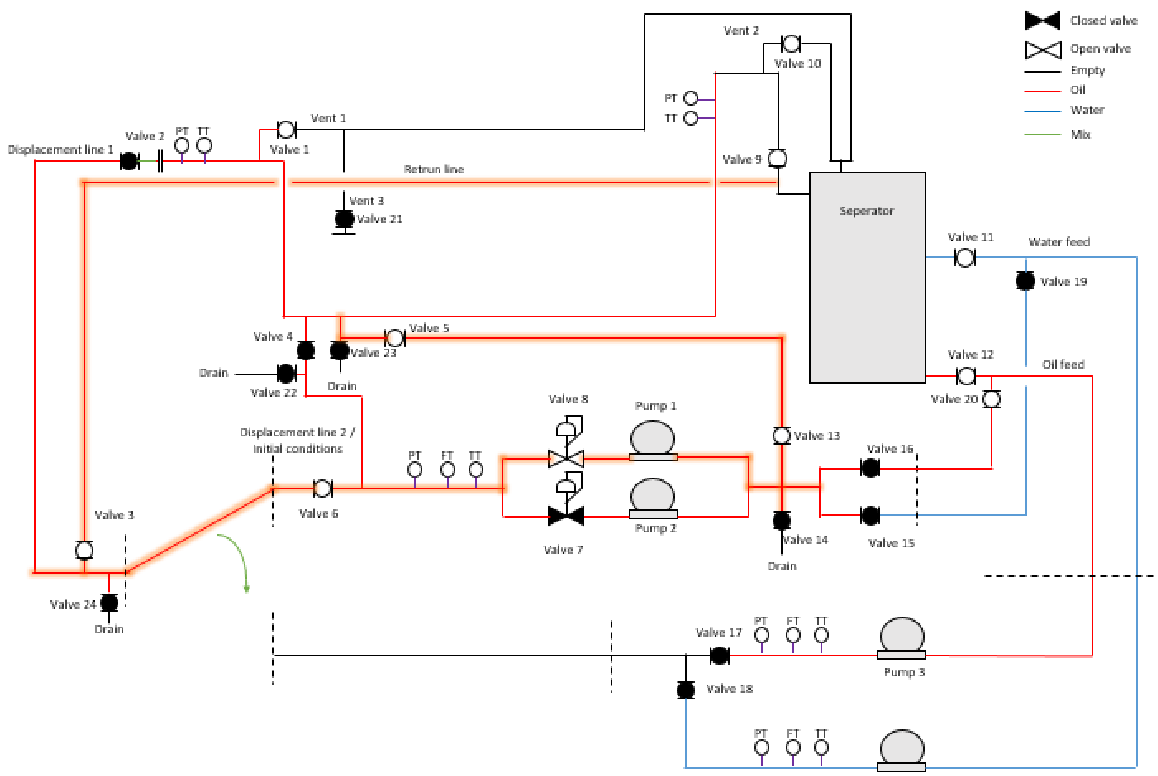

Step	Operation
17	Reestablish initial conditions
18	Repeat step 1 to 6
19	Wait until two jumper volumes has been displaced
20	Repeat step 8 to 17
21	Repeat step 1 to 6
22	Wait until three jumper volumes has been displaced
23	Repeat step 8 to 16
24	Experiment finished

Appendix B – CEL Homogenous multiphase model

Software	Parameter	Acceptable value
ICEM CFD	Quality	> 0.2
	Min/ Max Dihedral Angle	> 10° / < 170°
CFX-Solver	Orthogonality angle	> 20°
	Mesh Expansion Factor	< 20
	Aspect Ratio	< 100
CFD-POST	Edge Length Ratio	< 100
	Element Volume Ratio	< 20
	Minimum/ Maximum Face Angle	> 10° / < 170°

Appendix C – CEL Homogenous multiphase model

```
LIBRARY:
CEL:
EXPRESSIONS:
InletVelocity = 2.081289
OilVolume = VolumeInt(Oil.Volume.Fraction)@Default Domain Default
END
END
MATERIAL: Turpentine
Material Group = Constant Property Liquids
Option = Pure Substance
Thermodynamic State = Liquid
PROPERTIES:
Option = General Material
EQUATION OF STATE:
Density = 792 [kg m^-3]
Molar Mass = 158 [kg kmol^-1]
Option = Value
END
SPECIFIC HEAT CAPACITY:
Option = Value
Specific Heat Capacity = 1760 [J kg^-1 K^-1]
Specific Heat Type = Constant Pressure
END
REFERENCE STATE:
Option = Specified Point
Reference Pressure = 1 [atm]
Reference Specific Enthalpy = 0 [J/kg]
Reference Specific Entropy = 0 [J/kg/K]
Reference Temperature = 25 [C]
END
DYNAMIC VISCOSITY:
Dynamic Viscosity = 1.2989E-03 [Pa s]
Option = Value
END
THERMAL CONDUCTIVITY:
Option = Value
Thermal Conductivity = 0.136 [W m^-1 K^-1]
END
ABSORPTION COEFFICIENT:
Absorption Coefficient = 1.0 [m^-1]
Option = Value
END
```

43. SCATTERING COEFFICIENT:
44. Option = Value
45. Scattering Coefficient = 0.0 [m^-1]
46. END
47. REFRACTIVE INDEX:
48. Option = Value
49. Refractive Index = 1.0 [m m^-1]
50. END
51. THERMAL EXPANSIVITY:
52. Option = Value
53. Thermal Expansivity = 9.7E-04 [K^-1]
54. END
55. END
56. END
57. MATERIAL: Water
58. Material Description = Water (liquid)
59. Material Group = Water Data, Constant Property Liquids
60. Option = Pure Substance
61. Thermodynamic State = Liquid
62. PROPERTIES:
63. Option = General Material
64. EQUATION OF STATE:
65. Density = 997.0 [kg m^-3]
66. Molar Mass = 18.02 [kg kmol^-1]
67. Option = Value
68. END
69. SPECIFIC HEAT CAPACITY:
70. Option = Value
71. Specific Heat Capacity = 4181.7 [J kg^-1 K^-1]
72. Specific Heat Type = Constant Pressure
73. END
74. REFERENCE STATE:
75. Option = Specified Point
76. Reference Pressure = 1 [atm]
77. Reference Specific Enthalpy = 0.0 [J/kg]
78. Reference Specific Entropy = 0.0 [J/kg/K]
79. Reference Temperature = 25 [C]
80. END
81. DYNAMIC VISCOSITY:
82. Dynamic Viscosity = 8.899E-4 [kg m^-1 s^-1]
83. Option = Value
84. END
85. THERMAL CONDUCTIVITY:

86. Option = Value
87. Thermal Conductivity = 0.6069 [W m^-1 K^-1]
88. END
89. ABSORPTION COEFFICIENT:
90. Absorption Coefficient = 1.0 [m^-1]
91. Option = Value
92. END
93. SCATTERING COEFFICIENT:
94. Option = Value
95. Scattering Coefficient = 0.0 [m^-1]
96. END
97. REFRACTIVE INDEX:
98. Option = Value
99. Refractive Index = 1.0 [m m^-1]
100. END
101. THERMAL EXPANSIVITY:
102. Option = Value
103. Thermal Expansivity = 2.57E-04 [K^-1]
104. END
105. END
106. END
107. END
108. FLOW: Flow Analysis 1
109. SOLUTION UNITS:
110. Angle Units = [rad]
111. Length Units = [m]
112. Mass Units = [kg]
113. Solid Angle Units = [sr]
114. Temperature Units = [K]
115. Time Units = [s]
116. END
117. ANALYSIS TYPE:
118. Option = Transient
119. EXTERNAL SOLVER COUPLING:
120. Option = None
121. END
122. INITIAL TIME:
123. Option = Automatic with Value
124. Time = 0 [s]
125. END
126. TIME DURATION:
127. Option = Total Time
128. Total Time = 60.24636 [s]

```
END
TIME STEPS:
First Update Time = 0.0 [s]
Initial Timestep = 0.0028 [s]
Option = Adaptive
Timestep Update Frequency = 1
TIMESTEP ADAPTION:
Maximum Timestep = 0.007 [s]
Minimum Timestep = 0.002 [s]
Option = Number of Coefficient Loops
Target Maximum Coefficient Loops = 5
Target Minimum Coefficient Loops = 3
Timestep Decrease Factor = 0.8
Timestep Increase Factor = 1.06
END
END
END
DOMAIN: Default Domain
Coord Frame = Coord 0
Domain Type = Fluid
Location = SOLID
BOUNDARY: Default Domain Default
Boundary Type = WALL
Location = SOLID_1_1
BOUNDARY CONDITIONS:
MASS AND MOMENTUM:
Option = No Slip Wall
END
WALL ROUGHNESS:
Option = Smooth Wall
END
END
END
BOUNDARY: Inlet
Boundary Type = INLET
Location = INLET
BOUNDARY CONDITIONS:
FLOW REGIME:
Option = Subsonic
END
MASS AND MOMENTUM:
Normal Speed = InletVelocity [m s^-1]
Option = Normal Speed
```

```
END
TURBULENCE:
Option = Medium Intensity and Eddy Viscosity Ratio
END
END
FLUID: Oil
BOUNDARY CONDITIONS:
VOLUME FRACTION:
Option = Value
Volume Fraction = 0
END
END
END
FLUID: Water
BOUNDARY CONDITIONS:
VOLUME FRACTION:
Option = Value
Volume Fraction = 1
END
END
END
END
BOUNDARY: Outlet
Boundary Type = OUTLET
Location = OUTLET
BOUNDARY CONDITIONS:
FLOW REGIME:
Option = Subsonic
END
MASS AND MOMENTUM:
Option = Average Static Pressure
Pressure Profile Blend = 0.05
Relative Pressure = 0 [Pa]
END
PRESSURE AVERAGING:
Option = Average Over Whole Outlet
END
END
END
DOMAIN MODELS:
BUOYANCY MODEL:
Buoyancy Reference Density = 792 [kg m^-3]
Gravity X Component = 0 [m s^-2]
```

```
Gravity Y Component = -9.81 [m s^-2]
Gravity Z Component = 0 [m s^-2]
Option = Buoyant
BUOYANCY REFERENCE LOCATION:
Option = Automatic
END
END
DOMAIN MOTION:
Option = Stationary
END
MESH DEFORMATION:
Option = None
END
REFERENCE PRESSURE:
Reference Pressure = 1 [atm]
END
END
FLUID DEFINITION: Oil
Material = Turpentine
Option = Material Library
MORPHOLOGY:
Option = Continuous Fluid
END
END
FLUID DEFINITION: Water
Material = Water
Option = Material Library
MORPHOLOGY:
Option = Continuous Fluid
END
END
FLUID MODELS:
COMBUSTION MODEL:
Option = None
END
FLUID: Oil
FLUID BUOYANCY MODEL:
Option = Density Difference
END
END
FLUID: Water
FLUID BUOYANCY MODEL:
Option = Density Difference
```

```
END
END
HEAT TRANSFER MODEL:
Fluid Temperature = 25 [C]
Homogeneous Model = False
Option = Isothermal
END
THERMAL RADIATION MODEL:
Option = None
END
TURBULENCE MODEL:
Option = SST
BUOYANCY TURBULENCE:
Option = None
END
END
TURBULENT WALL FUNCTIONS:
Option = Automatic
END
END
FLUID PAIR: Oil | Water
INTERPHASE TRANSFER MODEL:
Interface Length Scale = 1. [mm]
Option = Mixture Model
END
MASS TRANSFER:
Option = None
END
SURFACE TENSION MODEL:
Option = None
END
END
MULTIPHASE MODELS:
Homogeneous Model = On
FREE SURFACE MODEL:
Option = Standard
END
END
END
INITIALISATION:
Option = Automatic
FLUID: Oil
INITIAL CONDITIONS:
```

```
VOLUME FRACTION:
Option = Automatic with Value
Volume Fraction = 1
END
END
END
FLUID: Water
INITIAL CONDITIONS:
VOLUME FRACTION:
Option = Automatic with Value
Volume Fraction = 0
END
END
END
INITIAL CONDITIONS:
Velocity Type = Cartesian
CARTESIAN VELOCITY COMPONENTS:
Option = Automatic with Value
U = 0 [m s^-1]
V = 0 [m s^-1]
W = 0 [m s^-1]
END
STATIC PRESSURE:
Option = Automatic with Value
Relative Pressure = 0 [Pa]
END
TURBULENCE INITIAL CONDITIONS:
Option = Low Intensity and Eddy Viscosity Ratio
END
END
END
OUTPUT CONTROL:
MONITOR OBJECTS:
MONITOR BALANCES:
Option = Full
END
MONITOR FORCES:
Option = Full
END
MONITOR PARTICLES:
Option = Full
END
MONITOR POINT: ResidualOil
```

```
Coord Frame = Coord 0
Expression Value = volumeInt(Velocity)@Default Domain
Option = Expression
END
MONITOR RESIDUALS:
Option = Full
END
MONITOR TOTALS:
Option = Full
END
END
RESULTS:
File Compression Level = Default
Option = Standard
END
TRANSIENT RESULTS: Transient Results 1
File Compression Level = Default
Include Mesh = No
Option = Selected Variables
Output Variables List = Density,Oil.Velocity,Oil.Volume \
Fraction,Turbulence Kinetic Energy,Water.Velocity,Water.Volume \
Fraction
OUTPUT FREQUENCY:
Option = Time Interval
Time Interval = 0.01 [s]
END
END
END
SOLVER CONTROL:
Turbulence Numerics = High Resolution
ADVECTION SCHEME:
Option = High Resolution
END
CONVERGENCE CONTROL:
Maximum Number of Coefficient Loops = 10
Minimum Number of Coefficient Loops = 2
Timescale Control = Coefficient Loops
END
CONVERGENCE CRITERIA:
Conservation Target = 0.01
Residual Target = 0.00001
Residual Type = RMS
END
```

```
TRANSIENT SCHEME:
Option = Second Order Backward Euler
TIMESTEP INITIALISATION:
Option = Automatic
END
END
END
END
COMMAND FILE:
Version = 16.2
Results Version = 17.0
END
```

Appendix D – CEL Inhomogeneous Multiphase Model

```
LIBRARY:
  CEL:
    EXPRESSIONS:
      InletVelocity = 2.081289
      OilVolume = VolumeInt(Oil.Volume.Fraction)@Default Domain Default
    END
  END
  MATERIAL: Turpentine
    Material Group = Constant Property Liquids
    Option = Pure Substance
    Thermodynamic State = Liquid
    PROPERTIES:
      Option = General Material
      EQUATION OF STATE:
        Density = 792 [kg m^-3]
        Molar Mass = 158 [kg kmol^-1]
        Option = Value
      END
      SPECIFIC HEAT CAPACITY:
        Option = Value
        Specific Heat Capacity = 1760 [J kg^-1 K^-1]
        Specific Heat Type = Constant Pressure
      END
      REFERENCE STATE:
        Option = Specified Point
        Reference Pressure = 1 [atm]
        Reference Specific Enthalpy = 0 [J/kg]
        Reference Specific Entropy = 0 [J/kg/K]
        Reference Temperature = 25 [C]
      END
      DYNAMIC VISCOSITY:
        Dynamic Viscosity = 1.2989E-03 [Pa s]
        Option = Value
      END
      THERMAL CONDUCTIVITY:
        Option = Value
        Thermal Conductivity = 0.136 [W m^-1 K^-1]
      END
      ABSORPTION COEFFICIENT:
        Absorption Coefficient = 1.0 [m^-1]
        Option = Value
      END
```

```
    SCATTERING COEFFICIENT:
      Option = Value
      Scattering Coefficient = 0.0 [m^-1]
    END
    REFRACTIVE INDEX:
      Option = Value
      Refractive Index = 1.0 [m m^-1]
    END
    THERMAL EXPANSIVITY:
      Option = Value
      Thermal Expansivity = 9.7E-04 [K^-1]
    END
  END
END
MATERIAL: Water
  Material Description = Water (liquid)
  Material Group = Water Data, Constant Property Liquids
  Option = Pure Substance
  Thermodynamic State = Liquid
  PROPERTIES:
    Option = General Material
    EQUATION OF STATE:
      Density = 997.0 [kg m^-3]
      Molar Mass = 18.02 [kg kmol^-1]
      Option = Value
    END
    SPECIFIC HEAT CAPACITY:
      Option = Value
      Specific Heat Capacity = 4181.7 [J kg^-1 K^-1]
      Specific Heat Type = Constant Pressure
    END
    REFERENCE STATE:
      Option = Specified Point
      Reference Pressure = 1 [atm]
      Reference Specific Enthalpy = 0.0 [J/kg]
      Reference Specific Entropy = 0.0 [J/kg/K]
      Reference Temperature = 25 [C]
    END
    DYNAMIC VISCOSITY:
      Dynamic Viscosity = 8.899E-4 [kg m^-1 s^-1]
      Option = Value
    END
    THERMAL CONDUCTIVITY:
```

```
    Option = Value
    Thermal Conductivity = 0.6069 [W m^-1 K^-1]
   END
   ABSORPTION COEFFICIENT:
    Absorption Coefficient = 1.0 [m^-1]
    Option = Value
   END
   SCATTERING COEFFICIENT:
    Option = Value
    Scattering Coefficient = 0.0 [m^-1]
   END
   REFRACTIVE INDEX:
    Option = Value
    Refractive Index = 1.0 [m m^-1]
   END
   THERMAL EXPANSIVITY:
    Option = Value
    Thermal Expansivity = 2.57E-04 [K^-1]
   END
  END
 END
END
FLOW: Flow Analysis 1
 SOLUTION UNITS:
  Angle Units = [rad]
  Length Units = [m]
  Mass Units = [kg]
  Solid Angle Units = [sr]
  Temperature Units = [K]
  Time Units = [s]
 END
 ANALYSIS TYPE:
  Option = Transient
  EXTERNAL SOLVER COUPLING:
   Option = None
  END
  INITIAL TIME:
   Option = Automatic with Value
   Time = 0 [s]
  END
  TIME DURATION:
   Option = Total Time
   Total Time = 90.36954 [s]
```

```
  END
  TIME STEPS:
    First Update Time = 0.0 [s]
    Initial Timestep = 0.0028 [s]
    Option = Adaptive
    Timestep Update Frequency = 1
    TIMESTEP ADAPTION:
      Maximum Timestep = 0.007 [s]
      Minimum Timestep = 0.002 [s]
      Option = Number of Coefficient Loops
      Target Maximum Coefficient Loops = 5
      Target Minimum Coefficient Loops = 3
      Timestep Decrease Factor = 0.8
      Timestep Increase Factor = 1.06
    END
  END
END
DOMAIN: Default Domain
  Coord Frame = Coord 0
  Domain Type = Fluid
  Location = SOLID
  BOUNDARY: Default Domain Default
    Boundary Type = WALL
    Location = SOLID_1_1
    BOUNDARY CONDITIONS:
      MASS AND MOMENTUM:
        Option = Fluid Dependent
      END
      WALL CONTACT MODEL:
        Option = Use Volume Fraction
      END
      WALL ROUGHNESS:
        Option = Smooth Wall
      END
    END
    FLUID: Oil
      BOUNDARY CONDITIONS:
        MASS AND MOMENTUM:
          Option = No Slip Wall
        END
      END
    END
    FLUID: Water
```

```
    BOUNDARY CONDITIONS:
      MASS AND MOMENTUM:
        Option = No Slip Wall
      END
    END
  END
END
BOUNDARY: Inlet
  Boundary Type = INLET
  Location = INLET
  BOUNDARY CONDITIONS:
    FLOW REGIME:
      Option = Subsonic
    END
    MASS AND MOMENTUM:
      Normal Speed = 1.387526192 [m s^-1]
      Option = Normal Speed
    END
    TURBULENCE:
      Option = Medium Intensity and Eddy Viscosity Ratio
    END
  END
  FLUID: Oil
    BOUNDARY CONDITIONS:
      VOLUME FRACTION:
        Option = Value
        Volume Fraction = 0
      END
    END
  END
  FLUID: Water
    BOUNDARY CONDITIONS:
      VOLUME FRACTION:
        Option = Value
        Volume Fraction = 1
      END
    END
  END
END
BOUNDARY: Outlet
  Boundary Type = OUTLET
  Location = OUTLET
  BOUNDARY CONDITIONS:
```

```
    FLOW REGIME:
      Option = Subsonic
    END
    MASS AND MOMENTUM:
      Option = Average Static Pressure
      Pressure Profile Blend = 0.05
      Relative Pressure = 0 [Pa]
    END
    PRESSURE AVERAGING:
      Option = Average Over Whole Outlet
    END
  END
END
DOMAIN MODELS:
  BUOYANCY MODEL:
    Buoyancy Reference Density = 792 [kg m^-3]
    Gravity X Component = 0 [m s^-2]
    Gravity Y Component = -9.81 [m s^-2]
    Gravity Z Component = 0 [m s^-2]
    Option = Buoyant
    BUOYANCY REFERENCE LOCATION:
      Option = Automatic
    END
  END
  DOMAIN MOTION:
    Option = Stationary
  END
  MESH DEFORMATION:
    Option = None
  END
  REFERENCE PRESSURE:
    Reference Pressure = 1 [atm]
  END
END
FLUID DEFINITION: Oil
  Material = Turpentine
  Option = Material Library
  MORPHOLOGY:
    Option = Continuous Fluid
  END
END
FLUID DEFINITION: Water
  Material = Water
```

```
    Option = Material Library
    MORPHOLOGY:
      Option = Continuous Fluid
    END
  END
  FLUID MODELS:
    COMBUSTION MODEL:
      Option = None
    END
    FLUID: Oil
      FLUID BUOYANCY MODEL:
        Option = Density Difference
      END
      TURBULENCE MODEL:
        Option = SST
        BUOYANCY TURBULENCE:
          Option = None
        END
      END
      TURBULENT WALL FUNCTIONS:
        Option = Automatic
      END
    END
    FLUID: Water
      FLUID BUOYANCY MODEL:
        Option = Density Difference
      END
      TURBULENCE MODEL:
        Option = SST
        BUOYANCY TURBULENCE:
          Option = None
        END
      END
      TURBULENT WALL FUNCTIONS:
        Option = Automatic
      END
    END
    HEAT TRANSFER MODEL:
      Fluid Temperature = 25 [C]
      Homogeneous Model = False
      Option = Isothermal
    END
    THERMAL RADIATION MODEL:
```

```
      Option = None
    END
    TURBULENCE MODEL:
      Homogeneous Model = False
      Option = Fluid Dependent
    END
  END
  FLUID PAIR: Oil | Water
    INTERPHASE TRANSFER MODEL:
      Interface Length Scale = 1. [mm]
      Option = Mixture Model
    END
    MASS TRANSFER:
      Option = None
    END
    MOMENTUM TRANSFER:
      DRAG FORCE:
        Drag Coefficient = 0.44
        Option = Drag Coefficient
      END
    END
  END
  MULTIPHASE MODELS:
    Homogeneous Model = False
    FREE SURFACE MODEL:
      Option = None
    END
  END
END
INITIALISATION:
  Option = Automatic
  FLUID: Oil
    INITIAL CONDITIONS:
      Velocity Type = Cartesian
      CARTESIAN VELOCITY COMPONENTS:
        Option = Automatic with Value
        U = 0 [m s^-1]
        V = 0 [m s^-1]
        W = 0 [m s^-1]
      END
      TURBULENCE INITIAL CONDITIONS:
        Option = Low Intensity and Eddy Viscosity Ratio
      END
```

```
      VOLUME FRACTION:
        Option = Automatic with Value
        Volume Fraction = 1
      END
    END
  END
  FLUID: Water
    INITIAL CONDITIONS:
      Velocity Type = Cartesian
      CARTESIAN VELOCITY COMPONENTS:
        Option = Automatic with Value
        U = 0 [m s^-1]
        V = 0 [m s^-1]
        W = 0 [m s^-1]
      END
      TURBULENCE INITIAL CONDITIONS:
        Option = Medium Intensity and Eddy Viscosity Ratio
      END
      VOLUME FRACTION:
        Option = Automatic with Value
        Volume Fraction = 0
      END
    END
  END
  INITIAL CONDITIONS:
    STATIC PRESSURE:
      Option = Automatic with Value
      Relative Pressure = 0 [Pa]
    END
  END
END
OUTPUT CONTROL:
  MONITOR OBJECTS:
    MONITOR BALANCES:
      Option = Full
    END
    MONITOR FORCES:
      Option = Full
    END
    MONITOR PARTICLES:
      Option = Full
    END
    MONITOR POINT: ResidualOil
```

```
      Coord Frame = Coord 0
      Expression Value = volumeInt(Velocity)@Default Domain
      Option = Expression
    END
    MONITOR RESIDUALS:
      Option = Full
    END
    MONITOR TOTALS:
      Option = Full
    END
  END
  RESULTS:
    File Compression Level = Default
    Option = Standard
  END
  TRANSIENT RESULTS: Transient Results 1
    File Compression Level = Default
    Include Mesh = No
    Option = Selected Variables
    Output Variables List = Oil.Velocity,Oil.Volume \
      Fraction,Water.Velocity,Water.Volume Fraction,Density,Oil.Turbulence \
      Kinetic Energy,Water.Turbulence Kinetic Energy
    OUTPUT FREQUENCY:
      Option = Time Interval
      Time Interval = 0.1 [s]
    END
  END
END
SOLVER CONTROL:
  Turbulence Numerics = High Resolution
  ADVECTION SCHEME:
    Option = High Resolution
  END
  CONVERGENCE CONTROL:
    Maximum Number of Coefficient Loops = 50
    Minimum Number of Coefficient Loops = 2
    Timescale Control = Coefficient Loops
  END
  CONVERGENCE CRITERIA:
    Conservation Target = 0.01
    Residual Target = 0.00001
    Residual Type = RMS
  END
```

```
    TRANSIENT SCHEME:
      Option = Second Order Backward Euler
      TIMESTEP INITIALISATION:
        Option = Automatic
      END
    END
  END
END
COMMAND FILE:
  Version = 16.2
  Results Version = 17.0
END
PARAMETERIZATION:
  INPUT FIELD: InletVelocity
    Expression Name = InletVelocity
    Method = Expression
  END
END
```

Appendix E – Running CFX on Maur HPC

1. Create .def file for simulation on your computer
2. Open CFX on your computer
3. Open command line (“Tools -> Command Line”)
4. Navigate to folder location for .def file with the following command “cd <path_to_folder>”
5. Create mesh partitions with the following command “cfx5solve –def <your_def_file.def> –double –solver-double –part-only <number of partitions> -par”
6. Upload .def and .par file to working directory on Maur
7. Use script found in “Appendix F” for local parallel or “Appendix G” for distributed parallel

Appendix F – Local parallel on Maur

```
#!/bin/bash
#
#SBATCH -J HoFull10 # sensible name for the job
#SBATCH -p IPT      # partition IPT
#SBATCH -N 1        # allocate 1 nodes for the job
#SBATCH -n 20       # 20 tasks total, same as number of mesh partitions
#SBATCH --exclusive # no other jobs on the nodes while job is running
#SBATCH -t 7-00:00:00    # upper time limit of 7 days for the job
#variables used for locating folders and running job
model='Homo'
flowrate='10'
geometry='full'
ending1='m3h.def'
ending2='m3h_001.par'
#Location of .def and .par file
cd /work/jaopstve/OilDisplacingWater/"$model"/"$geometry"/"$flowrate"
#Open the solver, allocate nodes and run solver
module load cfx/17.0
module unload rocks-openmpi
export CFX5RSH=ssh
srun hostname -s > /tmp//hosts.$SLURM_JOB_ID
nodes=`tr '\n' ',' </tmp//hosts.$SLURM_JOB_ID`
cfx5solve -def "$flowrate$ending1" -double -start-method "Intel MPI Local Parallel" -par-dist "$nodes" -solver-double -parfile-read "$flowrate$ending2"
```

Appendix G – Distributed Parallel on Maur

```
#!/bin/bash
#
#SBATCH -J HoFull10 # sensible name for the job
#SBATCH -p IPT      # partition IPT
#SBATCH -N 2        # allocate 2 nodes for the job, or more
#SBATCH -n 40       # 40 tasks total, same as number of mesh partitions each node will have n/N tasks
#SBATCH --exclusive # no other jobs on the nodes while job is running
#SBATCH -t 7-00:00:00    # upper time limit of 7 days for the job
#variables used for locating folders and running job
model='Homo'
flowrate='10'
geometry='full'
ending1='m3h.def'
ending2='m3h_001.par'
#Location of .def and .par file
cd /work/jaopstve/OilDisplacingWater/"$model"/"$geometry"/"$flowrate"
#Open the solver, allocate nodes and run solver
module load cfx/17.0
module unload rocks-openmpi
export CFX5RSH=ssh
srun hostname -s > /tmp//hosts.$SLURM_JOB_ID
nodes=`tr '\n' ',' </tmp//hosts.$SLURM_JOB_ID`
cfx5solve -def "$flowrate$ending1" -double -start-method " Intel MPI Distributed Parallel" -par-dist "$nodes" -solver-double -parfile-read "$flowrate$ending2"
```

Appendix H – Running CFD-Post in Batch Mode on Maur

```
#!/bin/bash
#
#SBATCH -J extract_results # sensible name for the job
#SBATCH -p IPT      # partition IPT or EPT
#SBATCH -N 1       # allocate 1 nodes for the job
#SBATCH -n 1      # 1 task total
#SBATCH --exclusive # no other jobs on the nodes while job is running
#SBATCH -t 7-00:00:00    # upper time limit of 7 hours for the job
#Location of .res file
cd /work/jaopstve/homo/full/30
#Open CFX and allocate nodes
module load cfx/17.0
module unload rocks-openmpi
export CFX5RSH=ssh
srun hostname -s > /tmp//hosts.$SLURM_JOB_ID
nodes=`tr '\n' ',' </tmp//hosts.$SLURM_JOB_ID`
#Run CFD-Post, .cse is the CEL/PERL script file
cfdpost -batch "/work/jaopstve/test.cse" 30m3h_002.res
```

Appendix I – PERL/CEL Script for Extracting Results

1. COMMAND FILE:
2. CFX Post Version = 17.0
3. END
4. PLANE:yzCut
5. Apply Instancing Transform = On
6. Apply Texture = Off
7. Blend Texture = On
8. Bound Radius = 0.5 [m]
9. Colour = 0.75, 0.75, 0.75
10. Colour Map = Default Colour Map
11. Colour Mode = Variable
12. Colour Scale = Linear
13. Colour Variable = Oil.Volume Fraction
14. Colour Variable Boundary Values = Hybrid
15. Culling Mode = No Culling
16. Direction 1 Bound = 1.0 [m]
17. Direction 1 Orientation = 0 [degree]
18. Direction 1 Points = 10
19. Direction 2 Bound = 1.0 [m]
20. Direction 2 Points = 10
21. Domain List = /DOMAIN GROUP:All Domains
22. Draw Faces = On
23. Draw Lines = Off
24. Instancing Transform = /DEFAULT INSTANCE TRANSFORM:Default Transform
25. Invert Plane Bound = Off
26. Lighting = On
27. Line Colour = 0, 0, 0
28. Line Colour Mode = Default
29. Line Width = 1
30. Max = 0.0
31. Min = 0.0
32. Normal = 1 , 0 , 0
33. Option = YZ Plane
34. Plane Bound = None
35. Plane Type = Slice
36. Point = 0 [m], 0 [m], 0 [m]
37. Point 1 = 0 [m], 0 [m], 0 [m]
38. Point 2 = 1 [m], 0 [m], 0 [m]
39. Point 3 = 0 [m], 1 [m], 0 [m]
40. Range = Global
41. Render Edge Angle = 0 [degree]
42. Specular Lighting = On

43. Surface Drawing = Smooth Shading
44. Texture Angle = 0
45. Texture Direction = 0 , 1 , 0
46. Texture File =
47. Texture Material = Metal
48. Texture Position = 0 , 0
49. Texture Scale = 1
50. Texture Type = Predefined
51. Tile Texture = Off
52. Transform Texture = Off
53. Transparency = 0.0
54. X = 0.0 [m]
55. Y = 0.0 [m]
56. Z = 0.0 [m]
57. OBJECT VIEW TRANSFORM:
58. Apply Reflection = Off
59. Apply Rotation = Off
60. Apply Scale = Off
61. Apply Translation = Off
62. Principal Axis = Z
63. Reflection Plane Option = XY Plane
64. Rotation Angle = 0.0 [degree]
65. Rotation Axis From = 0 [m], 0 [m], 0 [m]
66. Rotation Axis To = 0 [m], 0 [m], 0 [m]
67. Rotation Axis Type = Principal Axis
68. Scale Vector = 1 , 1 , 1
69. Translation Vector = 0 [m], 0 [m], 0 [m]
70. X = 0.0 [m]
71. Y = 0.0 [m]
72. Z = 0.0 [m]
73. END
74. END
75. # Sending visibility action from ViewUtilities
76. >show /PLANE:yzCut, view=/VIEW:View 1
77. PLANE: Bottom
78. Apply Instancing Transform = On
79. Apply Texture = Off
80. Blend Texture = On
81. Bound Radius = 0.5 [m]
82. Colour = 0.75, 0.75, 0.75
83. Colour Map = Default Colour Map
84. Colour Mode = Variable
85. Colour Scale = Linear

86. Colour Variable = Water.Volume Fraction
87. Colour Variable Boundary Values = Hybrid
88. Culling Mode = No Culling
89. Direction 1 Bound = 1.0 [m]
90. Direction 1 Orientation = 0 [degree]
91. Direction 1 Points = 10
92. Direction 2 Bound = 1.0 [m]
93. Direction 2 Points = 10
94. Domain List = /DOMAIN GROUP:All Domains
95. Draw Faces = On
96. Draw Lines = Off
97. Instancing Transform = /DEFAULT INSTANCE TRANSFORM:Default Transform
98. Invert Plane Bound = Off
99. Lighting = On
100. Line Colour = 0, 0, 0
101. Line Colour Mode = Default
102. Line Width = 1
103. Max = 0.0
104. Min = 0.0
105. Normal = 1 , 0 , 0
106. Option = XY Plane
107. Plane Bound = None
108. Plane Type = Slice
109. Point = 0 [m], 0 [m], 0 [m]
110. Point 1 = 0 [m], 0 [m], 0 [m]
111. Point 2 = 1 [m], 0 [m], 0 [m]
112. Point 3 = 0 [m], 1 [m], 0 [m]
113. Range = Global
114. Render Edge Angle = 0 [degree]
115. Specular Lighting = On
116. Surface Drawing = Smooth Shading
117. Texture Angle = 0
118. Texture Direction = 0 , 1 , 0
119. Texture File =
120. Texture Material = Metal
121. Texture Position = 0 , 0
122. Texture Scale = 1
123. Texture Type = Predefined
124. Tile Texture = Off
125. Transform Texture = Off
126. Transparency = 0.0
127. Visibility = On
128. X = 0.0 [m]

129. Y = 0.0 [m]
130. Z = 4.9816 [m]
131. OBJECT VIEW TRANSFORM:
132. Apply Reflection = Off
133. Apply Rotation = Off
134. Apply Scale = Off
135. Apply Translation = Off
136. Principal Axis = Z
137. Reflection Plane Option = XY Plane
138. Rotation Angle = 0.0 [degree]
139. Rotation Axis From = 0 [m], 0 [m], 0 [m]
140. Rotation Axis To = 0 [m], 0 [m], 0 [m]
141. Rotation Axis Type = Principal Axis
142. Scale Vector = 1 , 1 , 1
143. Translation Vector = 0 [m], 0 [m], 0 [m]
144. X = 0.0 [m]
145. Y = 0.0 [m]
146. Z = 0.0 [m]
147. END
148. END
149. >show /PLANE:Bottom, view=/VIEW:View 1
150. PLANE:BottomCut
151. Apply Instancing Transform = On
152. Apply Texture = Off
153. Blend Texture = On
154. Bound Radius = 2 [m]
155. Colour = 0.75, 0.75, 0.75
156. Colour Map = Default Colour Map
157. Colour Mode = Constant
158. Colour Scale = Linear
159. Colour Variable = Pressure
160. Colour Variable Boundary Values = Hybrid
161. Culling Mode = No Culling
162. Direction 1 Bound = 1.0 [m]
163. Direction 1 Orientation = 0 [degree]
164. Direction 1 Points = 10
165. Direction 2 Bound = 1.0 [m]
166. Direction 2 Points = 10
167. Domain List = /DOMAIN GROUP:All Domains
168. Draw Faces = On
169. Draw Lines = Off
170. Instancing Transform = /DEFAULT INSTANCE TRANSFORM:Default Transform
171. Invert Plane Bound = Off

172. Lighting = On
173. Line Colour = 0, 0, 0
174. Line Colour Mode = Default
175. Line Width = 1
176. Max = 0.0 [Pa]
177. Min = 0.0 [Pa]
178. Normal = 1 , 0 , 0
179. Option = Three Points
180. Plane Bound = Circular
181. Plane Type = Slice
182. Point = 0 [m], 0 [m], 0 [m]
183. Point 1 = -1 [m], -1.3 [m], 5.4352 [m]
184. Point 2 = 0 [m], -1.3 [m], 5.29932 [m]
185. Point 3 = 1 [m], -1.3 [m], 4.9569 [m]
186. Range = Global
187. Render Edge Angle = 0 [degree]
188. Specular Lighting = On
189. Surface Drawing = Smooth Shading
190. Texture Angle = 0
191. Texture Direction = 0 , 1 , 0
192. Texture File =
193. Texture Material = Metal
194. Texture Position = 0 , 0
195. Texture Scale = 1
196. Texture Type = Predefined
197. Tile Texture = Off
198. Transform Texture = Off
199. Transparency = 0.0
200. Visibility = On
201. X = 0.0 [m]
202. Y = 0.0 [m]
203. Z = 0.0 [m]
204. OBJECT VIEW TRANSFORM:
205. Apply Reflection = Off
206. Apply Rotation = Off
207. Apply Scale = Off
208. Apply Translation = Off
209. Principal Axis = Z
210. Reflection Plane Option = XY Plane
211. Rotation Angle = 0.0 [degree]
212. Rotation Axis From = 0 [m], 0 [m], 0 [m]
213. Rotation Axis To = 0 [m], 0 [m], 0 [m]
214. Rotation Axis Type = Principal Axis

215. Scale Vector = 1 , 1 , 1
216. Translation Vector = 0 [m], 0 [m], 0 [m]
217. X = 0.0 [m]
218. Y = 0.0 [m]
219. Z = 0.0 [m]
220. END
221. END
222. # Sending visibility action from ViewUtilities
223. >show /PLANE:topCut, view=/VIEW:View 1
224. PLANE: TopCut
225. Apply Instancing Transform = On
226. Apply Texture = Off
227. Blend Texture = On
228. Bound Radius = 2 [m]
229. Colour = 0.75, 0.75, 0.75
230. Colour Map = Default Colour Map
231. Colour Mode = Constant
232. Colour Scale = Linear
233. Colour Variable = Pressure
234. Colour Variable Boundary Values = Hybrid
235. Culling Mode = No Culling
236. Direction 1 Bound = 1.0 [m]
237. Direction 1 Orientation = 0 [degree]
238. Direction 1 Points = 10
239. Direction 2 Bound = 1.0 [m]
240. Direction 2 Points = 10
241. Domain List = /DOMAIN GROUP:All Domains
242. Draw Faces = On
243. Draw Lines = Off
244. Instancing Transform = /DEFAULT INSTANCE TRANSFORM:Default Transform
245. Invert Plane Bound = Off
246. Lighting = On
247. Line Colour = 0, 0, 0
248. Line Colour Mode = Default
249. Line Width = 1
250. Max = 0.0 [Pa]
251. Min = 0.0 [Pa]
252. Normal = 1 , 0 , 0
253. Option = Three Points
254. Plane Bound = Circular
255. Plane Type = Slice
256. Point = 0 [m], 0 [m], 0 [m]
257. Point 1 = -1 [m], -0.3 [m], 5.4352 [m]

258. Point 2 = 0 [m], -0.3 [m], 5.29932 [m]
259. Point 3 = 1 [m], -0.3 [m], 4.9569 [m]
260. Range = Global
261. Render Edge Angle = 0 [degree]
262. Specular Lighting = On
263. Surface Drawing = Smooth Shading
264. Texture Angle = 0
265. Texture Direction = 0 , 1 , 0
266. Texture File =
267. Texture Material = Metal
268. Texture Position = 0 , 0
269. Texture Scale = 1
270. Texture Type = Predefined
271. Tile Texture = Off
272. Transform Texture = Off
273. Transparency = 0.0
274. Visibility = On
275. X = 0.0 [m]
276. Y = 0.0 [m]
277. Z = 0.0 [m]
278. OBJECT VIEW TRANSFORM:
279. Apply Reflection = Off
280. Apply Rotation = Off
281. Apply Scale = Off
282. Apply Translation = Off
283. Principal Axis = Z
284. Reflection Plane Option = XY Plane
285. Rotation Angle = 0.0 [degree]
286. Rotation Axis From = 0 [m], 0 [m], 0 [m]
287. Rotation Axis To = 0 [m], 0 [m], 0 [m]
288. Rotation Axis Type = Principal Axis
289. Scale Vector = 1 , 1 , 1
290. Translation Vector = 0 [m], 0 [m], 0 [m]
291. X = 0.0 [m]
292. Y = 0.0 [m]
293. Z = 0.0 [m]
294. END
295. END
296. VIEW:View 1
297. Camera Mode = User Specified
298. CAMERA:
299. Option = Pivot Point and Quaternion
300. Pivot Point = 0, -0.6479, 2.7176

```
Scale = 0.6
Pan = 0, 0
Rotation Quaternion = 0, -0.707107, 0, 0.707107
END
END
> update

DEFAULT LEGEND:Default Legend View 1
Colour = 0, 0, 0
Font = Sans Serif
Legend Aspect = 0.07
Legend Format = %5.2f
Legend Orientation = Horizontal
Legend Position = 0.02 , 0.15
Legend Size = 0.3
Legend Ticks = 5
Legend Title = Legend
Legend Title Mode = Variable
Legend X Justification = Left
Legend Y Justification = Top
Show Legend Units = On
Text Colour Mode = Default
Text Height = 0.024
Text Rotation = 0
END
LIBRARY:
CEL:
EXPRESSIONS:
WFTopCut = areaAve(Water.Volume Fraction)@TopCut
WFBottomCut = areaAve(Water.Volume Fraction)@BottomCut
OFDomain = volumeInt(Oil.Volume Fraction)@Default Domain
WVFBottom =  ave(Water.Volume Fraction)@Bottom
END
END
END
#Get timesteps
!$timestepList = getValue("DATA READER", "Timestep List");
!@timestpes = split(/,/, $timestepList);
!$nTimesteps = @timesteps;
!$CurrentStepX = 0;
#Output files
!$OVFoutputFile = "ovfTime.csv";
!$FVoutputFile = "FrontVelocity.csv";
```

```
#Open output files
!open (OVFOut, "> $OVFoutputFile" );
!open (FVOut, "> $FVoutputFile" );
#Write headers to output files
!print OVFOut "Time;OVF\n";
!print FVOut "Time;Location;TimeStep\n";
#Variables
!$xvar = 1;
!$yvar = 1;
#Loop through the timesteps
!for $timeStep1 (@timestpes) {
#load timestep
>load timestep = $timeStep1
#Get variables
!my $WVFBottom = getExprString(WFBottomCut);
!my $WVFTop = getExprString(WFTopCut);
!my $OVFDD = getExprString(OFDomain);
!my $StepTime = getExprString(Time);
#save OVF and time
!print OVFOut "$StepTime;$OVFDD\n";
#take snapshots of each timestep // romove "#" to take snapshots each timestep
#HARDCOPY:
#  Antialiasing = On
#  Hardcopy Filename = Figure-$timeStep1
#  Hardcopy Format = png
#  Hardcopy Tolerance = 0.0001
#  Image Height = 1440
#  Image Scale = 100
#  Image Width = 2560
#  JPEG Image Quality = 100
#  Screen Capture = Off
#  Use Screen Size = Off
#  White Background = Off
#END
#>print
#Check if the flow has reach the first zx plane
!if ($xvar==1){
!if ($WVFBottom > 0.5){
!print FVOut "$StepTime;BottomCut;$timeStep1\n";
!$xvar = 0;
#take snapshot
HARDCOPY:
>Antialiasing = On
```

```
>Hardcopy Filename = Bottom-$timeStep1
>Hardcopy Format = png
>Hardcopy Tolerance = 0.0001
>Image Height = 1440
>Image Scale = 100
>Image Width = 2560
>JPEG Image Quality = 100
>Screen Capture = Off
>Use Screen Size = Off
>White Background = Off
END
>print
#check the front height
!my $WVBottomPlane = getExprString(WVFBottom);
!print FVOut "$WVBottomPlane;BottomAreaWithWater;$timeStep1\n";
!}
!}
#check if the flow has reached the second zx plane
!if ($yvar==1){
!if ($WVFTop > 0.5){
!print FVOut "$StepTime;TopCut;$timeStep1\n";
!$yvar = 0;
#take snapshot
HARDCOPY:
>Antialiasing = On
>Hardcopy Filename = Top-$timeStep1
>Hardcopy Format = png
>Hardcopy Tolerance = 0.0001
>Image Height = 1440
>Image Scale = 100
>Image Width = 2560
>JPEG Image Quality = 100
>Screen Capture = Off
>Use Screen Size = Off
>White Background = Off
END
>print
!}
!}
!}
#close output files
!close OVFOut;
!close FVOut;
```